THE UNIVERSITY
of EDINBURGH

Energy Efficiency Heterogeneous Wireless Communication Network with QoS Support

By
Ying Hou

A thesis submitted for the degree of Doctor of Philosophy.
The University of Edinburgh

September 2012
Edinburgh

Energy Efficiency Heterogeneous Wireless Communication Network with QoS Support

By
Ying Hou

A thesis submitted for the degree of Doctor of Philosophy.
The University of Edinburgh

September 2012
Edinburgh

Abstract

The overarching goal of this thesis is to investigate network architectures, and find the trade-off between low overall energy use and maintaining the level of quality of service (QoS), or even improve it. The ubiquitous wireless communications environment supports the exploration of different network architectures and techniques, the so-called heterogeneous network. Two kinds of heterogeneous architectures are considered: a combined cellular and femtocell network and a combined cellular, femtocell and Wireless Local Area Network(WLAN) network.

This thesis concludes that the investigated heterogeneous networks can significantly reduce the overall power consumption, depending on the uptake of femtocells and WLANs. Also, QoS remains high when the power consumption drops. The main energy saving is from reducing the macrocell base station embodied and operational energy. When QoS is evaluated based on the combined cellular and femtocell architecture, it is suggested that use of resource scheduling for femtocells within the macrocell is crucial since femtocell performance is affected significantly by interference when installed in a co-channel system. Additionally, the femtocell transmission power mode is investigated using either variable power level or a fixed power level. To achieve both energy efficiency and QoS, the choice of system configurations should change according to the density of the femtocell deployment. When combining deployment of femtocells with WLANs, more users are able to experience a higher QoS. Due to increasing of data traffic and smartphone usage in the future, WLANs are more important for offloading data from the macrocell, reducing power consumption and also increasing the bandwidth. The localised heterogeneous network is a promising technique for achieving power efficiency and a high QoS system.

Declaration of Originality

I hereby declare that the research recorded in this thesis and the thesis itself was composed and organised by myself in the School of Engineering at The University of Edinburgh, except where explicitly stated otherwise in the text.

Ying Hou
September 2012

Acknowledgement

First and foremost I owe my deepest gratitude to my principle supervisor, Dr. Dave Laurenson. Dr. Laurenson has supported me through my PhD program with his patience and knowledge. He was always there encouraging me and gave me advices not only for research, but also for how to represent myself. This thesis would not have been possible without his constant support. I would like to thank Professor John Thompson for his help through my study in IDCoM. Moreover, colleagues in IDCoM office, including Dr. Chaoran Du, Dr. Hongjian Sun, Dr. Jing Jang, and all of those who have helped me, are also gratefully acknowledged. I also would like to thank the people who have worked with me: Dr. Rui Wang and Mr. Stefan Videv.

Many thanks to the MVCE project that has funded my PhD study, which not only financially supported me through the last three years, but also provided valuable opportunities to work with some talented researchers and scientists from the leading companies and well known universities.

Finally, I would like to thank my parents for their constant love, guidance, support, and encouragement through my life!

Abbreviation

AAA	Authentication, Authorization and Accounting
ANDSF	Access Network Discovery and Selection Function
AODV	Ad hoc On-Demand Distance Vector
AP	Access Point
ARS	Ad-hoc Relay Station
BEM	Bandwidth Expansion Mode
BS	Base Station
BSC	Base Station Controller
BSI	Base Station Interface
BSR	Base Station Router
CapEx	Capital Expenditure
CCN	Common Core Network
CDF	Cumulative Distribution Function
CDMA	Code Division Multiple Access
CN	Correspondent Node
CW	Contention Window
DiffServ	Differentiated Services
DIFS	Distributed InterFrame Space
DSCP	DiffServ Code Point
DSDV	Destination-Sequenced Distance Vector

DSL	Digital Subscriber Line
DSMIPv6	Dual Stack Mobile IPv6
DSR	Dynamic Source Routing
DST	Destination
ERG	Energy Reduction Gain
FP	Fixed-Power scheme
GaN	Gallium Nitride
GERAN	GSM EDGE Radio Access Network
GGSN	Gateway GPRS Support Node
GPS	Global Positioning System
GPRS	General Packet Radio Service
GR	Gateway Router
GSM	Global System for Mobile Communications
HFET	Heterostructure Field Effect Transistor
HNB	Home Node B
ICIC	Inter Cell Interference Coordination
IFOM	IP Flow Mobility
IMS	IP Multimedia Subsystem
IntServ	Integrated Service
IP	Internet Protocol
L-GW	Local Gateway
LAN	Local Area Network
LBS	Location Based Service
LCA	Life-Cycle Assessment
LIPA	Local IP Access
LOS	Locator
LRM	Local Resource Manager

LTE	Long Term Evolution
MANET	Mobile Ad hoc Networking
MIP	Mobile IP
MM	Mobility Manager
MPLS	Multi-Protocol Label Switching
MSC	Mobile Switching Centre
MT	Mobile Terminal
NI	Network Interface
NS	Network Selector
OFDMA	Orthogonal Frequency-Division Multiple Access
OpEx	Operational Expenditure
P-GW	PDN Gateway
P2P	Peer-to-Peer
PC	Power-Controlled scheme
PDF	Probability Density Function
PDN	Packet Data Network
PHB	Per-Hop Behaviour
PPP	Poisson Point Process
QoS	Quality of Service
RAN	Radio Access Network
RBS	Radio Base Station
RM	Resource Manager
RNC	Radio Network Controller
RSVP	Resource ReSerVation Protocol
S-GW	Serving Gateway
SGSN	Serving GPRS Support Node
SINR	Signal to Interference plus Noise Ratio

SIPTO	Selected IP Traffic Offload
SMS	Short Message Service
SNR	Signal to Noise Ratio
SRC	Source
SIP	Session Initiation Protocol
UMA	Unlicensed Mobile Access
UMTS	Universal Mobile Telecommunications System
UNC	UMA Network Controller
VoIP	Voice over Internet Protocol
WCDMA	Wideband Code Division Multiple Access
WLAN	Wireless Local Area Network
WMM	Wireless Multimedia
WRP	Wireless Routing Protocol
WSN	Wireless Sensor Networks

Symbols

$\mathcal{A}$	single macrocell coverage
$\mathcal{A}_{\text{sys}}$	investigated system coverage
C_{AP}	femtocell AP embodied energy/s
C_{BS}	macrocell BS embodied energy/s
C_{MT}	MT embodied energy/s
$\mathcal{C}_m$	single macrocell capacity
$\mathcal{C}_f$	single femtocell capacity
d_f	distance between a femtocell user and its local femtocell
d_m	distance between a macrocell user and its local macrocell
E_b	energy per bit
$\mathbf{E}[\,]$	expectation operator
f_c	carrier frequency
$G_{\max}$	antenna boresight gain
G_β	3 dB reduction point
I_{m1}	self interference to a macrocell user (single)
I_{m2}	femtocell interference to a macrocell user (single)
I_{f1}	self interference to a femtocell user (single)
I_{f2}	macrocell interference to a femtocell user (single)
I_{f3}	neighbouring femtocell interference to a femtocell user (single)
$\tilde{I}_{m1}$	self interference to a macrocell user (multiple)
$\tilde{I}_{m2}$	neighbouring macrocells interference to a macrocell user (multiple)
$\tilde{I}_{m3}$	intra femtocells interference to a macrocell user (multiple)
$\tilde{I}_{m4}$	inter femtocells interference to a macrocell user (multiple)
$\tilde{I}_{f1}$	self interference to a femtocell user (multiple)
$\tilde{I}_{f2}$	macrocells interference to a femtocell user (multiple)
$\tilde{I}_{f3}$	intra femtocells interference to a femtocell user (multiple)

$\tilde{I}_{f4}$	inter femtocells interference to a femtocell user (multiple)
N_{AP}	number of femtocells
N_{fmax}	maximum number of users per femtocell
N_u	number of active mobile users in a BS coverage
$N_{u,f}$	number of active mobile users served by local femtocells
$N_{u,m}$	number of active mobile users served by macrocell
O_{AP}	femtocell AP operational power
$O_{\mathrm{AP},1}$	femtocell AP operational power (active)
$O_{\mathrm{AP},2}$	femtocell AP operational power (idle)
O_{BS}	macrocell BS operational power
O_{MT}	MT operational power
P_{AP}	AP power consumption (transmitting)
P_{charge}	handset charger power consumption
P_{BS}	macrocell BS transmission power
$P_{\mathrm{BS,min}}$	minimum BS transmission power
P_{fmax}	maximum femtocell transmission power
P_m	macrocell transmission power
P_{sniff}	femtocell AP low- power radio sniffer power
$\overline{P}_{\mathrm{cap},0}$	baseline system embodied energy per unit area
$\overline{P}_{\mathrm{op},0}$	baseline system operational power per unit area
$\overline{P}_{\mathrm{cap},f}$	embodied energy per unit area (a few femtocells)
$\overline{P}_{\mathrm{op},f}$	operational power per unit area (a few femtocells)
$\overline{P}_{\mathrm{cap},f'}$	embodied energy per unit area (ubiquitous femtocells)
$\overline{P}_{\mathrm{op},f'}$	operational power per unit area (ubiquitous femtocells)
PL_{fs}	free space propagation path loss model
PL_c	complex scenario propagation path loss model
PL_i	indoor propagation path loss model
PL_o	outdoor propagation path loss model
PL_{wall}	wall attenuation
R_{cell}	urban macrocell radius
R_f	femtocell radius
R_m	modelled macrocell radius
R_s	information rate per symbol
R_t	data transmission rate
SF_f	spreading factor for femtocell users

SF_m	spreading factor for macrocell users
$\mathrm{SINR}_{\mathrm{tar},f}$	target SINR for femtocell users
$\mathrm{SINR}_{\mathrm{tar},m}$	target SINR for macrocell users
$\mathcal{T}_m$	macrocell user throughput (single)
$\mathcal{T}_f$	femtocell user throughput (single)
$\tilde{\mathcal{T}}_m$	macrocell user throughput (multiple)
$\tilde{\mathcal{T}}_f$	femtocell user throughput (multiple)
u_{BS}	the number of users that each BS can suport
v_f	one femtocell's coverage area
$\mathbf{Var}[\,]$	variation operator
W	macrocell and femtocell Bandwidth
α	path loss exponent
β	a constant of proportionality
γ	lognormal random variable
$\Gamma(\,)$	gamma function
δ_{AP}	AP power consumption(not transmitting)
δ_{BS}	BS power consumption (not transmitting)
ϵ_{BS}	BS power conversion efficiency
ϵ_{char}	MT charger power conversion efficiency
ϵ_{MT}	MT handset power conversion efficiency
ρ_f	density of femtocells deployment
ρ_u	density of active mobile users
τ	femtocell switch-off threshold
ψ	fraction of customers with a femtocell access point
ω	number of wall crossed during a transmission process

List of Publications

Conference:

1. Ying Hou; David I. Laurenson. Energy Efficiency of High QoS Heterogeneous Wireless Communication Network In: *Proceedings of Vehicular Technology Conference Fall (VTC 2010-Fall), 2010 IEEE 72nd*, 6-9 Sept. 2010.

2. Ying Hou; David I. Laurenson. Analysis of Energy Consumption and QoS in Femtocell Heterogeneous Networks. In: *Proceedings of Wireless World Research Forum(WWRF), 2010 25th*, 16-18 Nov, 2010.

Contents

List of Figures

List of Tables

1

Introduction

After decades of rapid industrial development, climate change and global warming is becoming increasingly accepted as a reality. Climate change not only causes extreme weather phenomena, it may have wide influence on many industries. At the same time, energy shortage is also a rising issue world wide. Therefore, industries are looking for green solutions to save energy. Globally, the telecommunication contributes 0.1% of CO_2 emissions, and in the UK, the telecommunication contribution is around 0.3% [2].

Besides the social responsibility, telecommunication companies are also keen to find green techniques to save energy. Due to decreasing revenue per bit and increasing customer demand, improved techniques are required to reduce the transmission cost, also provide higher data rate and better Quality of Service (QoS). Therefore, energy efficiency and QoS both need to be taken into account, when a new technique is employed in the communication system.

In the telecommunication system, energy is consumed by the operator and mobile users [3]. Figure 1.1 show the components of telecommunication system energy consumption. Types of equipment include a simple phone, smart phone, WLAN access point (AP), femtocell AP and macrocell base station (BS). For each piece of equipment, energy consumption can be divided into two classes: First is operational energy, also called operational expenditure (OpEx); the other is embodied energy, also known as capital expenditure (CapEx). Operational energy is consumed during the life-time of use, such as transmission energy consumption and energy consumed for equipment maintenance, etc. Part of OpEx energy consumption, such as staff training and equipment maintenance, is not dependent on the development of wireless communication technologies. Therefore, information transmission is considered as OpEx in this thesis when drawing comparisons

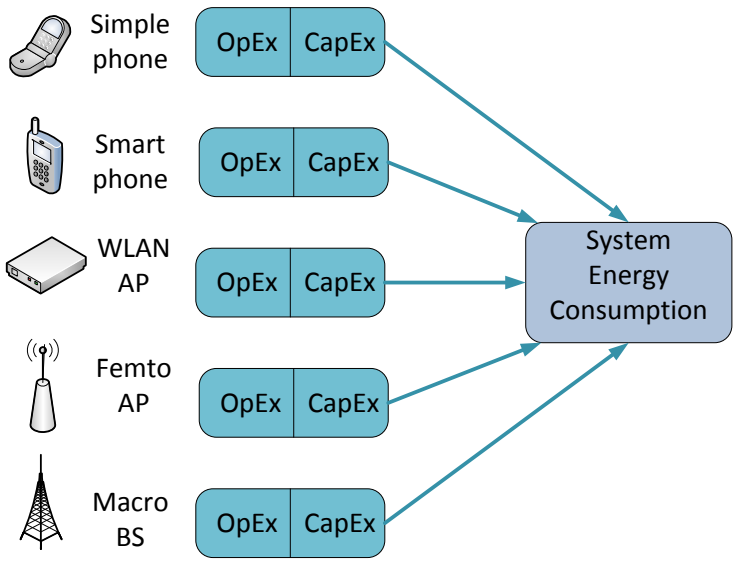

Fig. 1.1: Compositions of system energy consumption.

between different techniques. Embodied energy is defined as the energy consumed for extraction of materials, manufacture of components, transportation to site and construction of a product [4]. The embodied energy of equipment is a large proportion of the system energy consumption, which is commonly neglected in previous research [5, 6, 7]. [8] shows that the proportion of embodied energy for a macrocell base station and a mobile terminal are 32% and 76% of total energy consumed respectively. It indicates that it is essential to consider the embodied energy when evaluating an energy saving technique.

As mentioned above, the mobile user data demand has increased dramatically due to the explosive growth of mobile applications, such as watching TV programmes and online videos, surfing websites, playing Games, and using the Global Positioning System (GPS), which are shown in Figure 1.2. As well as these applications, the traditional voice and Short Message Service (SMS) services complete the mobile phone's usage. It is found that in the next a few years, the mobile data demand is expected to continuously increase with an annual rate above 100% [9], however, the use of voice service will decline [10]. Voice and data services need to be both considered in terms of QoS provision.

The relationship between energy efficiency and QoS maintenance or even

Fig. 1.2: Mobile phone usage

improvement are in conflict. It is essential to find techniques to achieve a balance between both energy efficiency and QoS. [11] introduced a scheme called Bandwidth Expansion Mode (BEM). The idea of BEM is to extend a user's bandwidth by a factor, based on the certain level of targeted throughput to adjust a higher order of modulation mode to a lower one. The energy saving is from use of a lower load, wider bandwidth, transmission power. However, it may diminish the resources available to other users. Therefore, the improvement in QoS for one user may be cancelled out by the loss of QoS for another. Some energy efficient radio techniques are presented in [12]. One is using dynamic spectrum access management to relocate users to more active spectrum or spectrum with a better propagation channel. In this case, the spectrum can be utilised efficiently, allowing radio network equipment in other bands to be partially or fully powered down. Another technique is scheduling and allocating the resource of downlink transmission from the base station, to manage traffic load. This can save transmission power of the base station. The final one is to consider energy efficient interference cancellation techniques, including distributed antenna systems and receiver interference cancellation. In this thesis, heterogenous networks are stud-

ied, by using different radio access architectures. The published research on heterogeneous networks is presented in the following section.

1.1 Historical Background and Research Objectives

One of the keywords that describe next-generation wireless communication is "seamless". The ubiquitous wireless communication environment promotes the exploration of different network architectures and techniques, the so called heterogeneous network, to enable seamless integration of various wireless access systems. A heterogeneous network is more likely to provide a better communication environment, which is able to offer a higher capacity, and greater coverage area coupled with system energy efficiency [13, 14]. Therefore, the deployment pattern, system configuration and related techniques of heterogeneous network are investigated in this thesis, with the aim of identifying an optimal scenario, taking into account the trade-off between energy efficiency and QoS. The most commonly studied heterogeneous architectures are femtocell [15, 16], WLAN [17, 18] or Ad-hoc [19, 20] combined with cellular networks.

In the macrocell-femtocell two tiered architecture, some research targets power efficiency issues, such as [5, 21]. However, the results are limited as they only address the operational energy gains. Since the embodied energy consumption accounts for a large part of overall system energy consumption, as discussed above, in this thesis a comprehensive energy consumption will be considered, including both operational and embodied energy contributions.

For the QoS performance of deploying femtocells in a traditional macrocell system, the commonly used metrics are system capacity [15, 22]and coverage [23], which focus on the system performance. However, since the femtocell is able to provide the same bandwidth as the macrocell, and supports many fewer users, the femtocell is likely to improve the QoS significantly based on each customer's point of view. Therefore, the QoS evaluation should focus on both the system and a single user's perspectives. It is also notable that, due to the limited spectrum for a cellular network, femtocells generally are deployed co-channel with macrocells [24, 25]. Thus, the performance of femtocell deployment is limited by large interference between the macrocell and femtocells. Other researchers propose a spectrum splitting scheme, which is able to locate the macrocell and femtocell in different

channels, to avoid interference [26, 27, 28].

Due to the increase of smartphone penetration, more mobile users are able to access the internet via a WLAN, by employing an 802.11 air interface. The utilisation of WLANs has grown dramatically, with statistics showing that there are nearly 13,000 and 37,000 hotspots in the UK and US respectively [29, 30]. Because WLANs are ubiquitously deployed in residences and public area, there is no extra embodied energy input to be considered, which is an advantage compared to femtocell deployment. In addition, WLANs occupy the unlicensed spectrum, which leads to a much broader bandwidth than the cellular network. For these reasons, the WLAN is another potential network for reducing power consumption and also provides a better bandwidth. Therefore, it should be considered as a means of offloading traffic from the macrocell.

Traffic offloading schemes have been analysed in several references. In [31] and [21], the benefits of femtocell deployement have been presented. They show that the QoS of indoor and outdoor users is improved. However, they did not consider the power reduction gain by using femtocells. Reference [32] focuses on an energy efficiency analysis with femtocell deployments, based on the operational energy. Some researchers focus on the offloading capabilities of WLANs [33, 34]. They point out the challenge of cooperation between the cellular network and WLANs, and present offloading algorithms from the macrocell to WLANs. There is also some research considering the cooperation between femtocells and WLANs [35, 36]. This work all shows that, with the adoption of femtocells or WLANs, a large amount of traffic can be offloaded to local networks. However, the system power consumption is not fully considered, and the QoS for each user is not evaluated. In this thesis, the comprehensive power consumption analysis and QoS evaluation will be addressed.

1.2 Thesis organisation

In this thesis, the background of heterogeneous network architectures considering both energy efficiency and QoS is presented in Chapter 2. This includes the basic concept of a heterogenous network and introduction of commonly used heterogeneous architectures. The scenarios of cellular combined with Ad-Hoc, WLAN or Femtocell are investigated specifically, since they are the network architectures studied in the following chapters. The

composition of communication system energy consumption is analysed as well, based on the two categories of embodied energy and operational energy. Finally, the QoS parameterisation and requirements for QoS in UMTS, WLAN and Ad-hoc are discussed.

A combined cellular and femtocell heterogeneous network is investigated in Chapter 3. The main techniques of femtocell deployments will be explained at the beginning. In this chapter, the first investigated scenario is a large or medium-sized city, combining both urban and rural environments, with a constant number of mobile users. After defining the simulation set and parameters, the large system simulation results are presented, including system power consumption and available bandwidth. The second investigated scenario focuses on a single urban scenario, the system performance is evaluated based on a geometric model, by using stochastic analysis methodology.

In Chapter 4, additional QoS metrics, such as system capacity and throughput per user, are considered based on a WCDMA cellular combined femtocell system. A relatively smaller urban area modelled by geometric method is applied. Also in this chapter, the system performance is evaluated based on a single macrocell scenario and a multiple macrocells scenario respectively. In this chapter, the interference between femtocells and the macrocell, and between femtocells is investigated. Several propagation models, such as large scale and small scale propagation are included for performance evaluation. Additionally, two transmission power setting schemes are proposed by considering energy efficiency, one of which is a Power-Controlled scheme, the other is a Fixed-Power scheme.

Due to the enormous growth of data traffic, with the popularity of various applications for smartphones, the current macrocell systems are becoming increasingly overloaded, and may fail to provide QoS for users. Since WLANs are already ubiquitously installed, and at the same time, the penetration of smartphones is increasing, more mobile users can be offloaded to a WLAN. Therefore, a cooperative architecture combining femtocells and WLANs is investigated in Chapter 5. The data traffic proportion of all traffic and smartphone usage is considered in the system evaluation.

Finally, conclusions and future work is drawn in Chapter 6.

1.3 Contributions

The contributions of this thesis can be listed as follows:

- For the heterogeneous femtocell network, a novel evaluation methodology is used to analyse the system level deployment. It applies practical factors, such as user capacity of a femtocell and a macrocell, and the femtocell deployment rate. An optimal heterogeneous femtocell network deployment configuration can be selected in view of different preference of the operator or user, also balancing the energy efficiency and QoS. For a cooperative network combining femtocells and WLANs, the effects of smartphone usage and data traffic are also studied, which are current and important for the evaluation.

- A stochastic geometry based model is proposed for modelling the femtocell deployment pattern, and it is utilised for analysing and evaluating the heterogeneous network performance. The proposed theoretical model results in a satisfied match for the Monte Carlo simulation results.

- A cooperative network scheme based on femtocells and WLANs is proposed. It clarifies the prerequisites and priorities of traffic offloading in different scenarios, such as when femtocell and WLAN coexist within a user's transmission area.

- A comprehensive analysis and investigation of embodied energy in evaluating system wide performance has taken place for the major components in communication system. This is commonly neglected in the previous work, yet affects the system energy consumption significantly.

- Two femtocell transmission power setting schemes are proposed, which are the Power-Controlled scheme and the Fixed-Power scheme, in order to find the trade-off between power efficiency and QoS performance.

- Since the precise data of a smartphone embodied energy is not available, three new approaches to analysing smartphone embodied energy are proposed: a price approach, a proportion approach and a CO_2 emission approach.

2

Background

This chapter is organised as follows: firstly, the different kinds of heterogeneous network architecture are introduced. Based on each scenario, a detailed analysis of system power efficiency is carried out. As well as power consumption, quality of service (QoS) as another research objective is examined in the third section. The final section of this chapter illustrates the relationships between energy efficiency and the provision of QoS.

2.1 Heterogenous Network Architectures

2.1.1 Overview of Heterogeneous Networks

Due to the rapid development of communication technologies and computer science, mobile device usage has increased in popularity and pervasiveness [9]. Customers require a more seamless usage experience, employing either unlicensed or licensed spectrum. Therefore, the next generation of wireless communications is expected to integrate a potentially large number of different heterogeneous wireless technologies, in what could be considered a huge step forward towards universal wireless access and seamless mobility [17, 37]. Under this pressure, mobiles are likely to be built as multi-mode terminals with multiple network interfaces, enabling access to different types of network.

Depending on the size of network coverage, the types of networks can be classified as Global, Macro, Micro, Pico, Femto, and Point-to-Point(P2P). As can be seen from Fig 2.1, in each category, some typical network architectures are commonly used. For instance, a satellite communication system can provide a global service, not only providing conventional communications, such as voice service for climbers in areas where the operator has coverage difficulties, but also including TV and radio, and location infor-

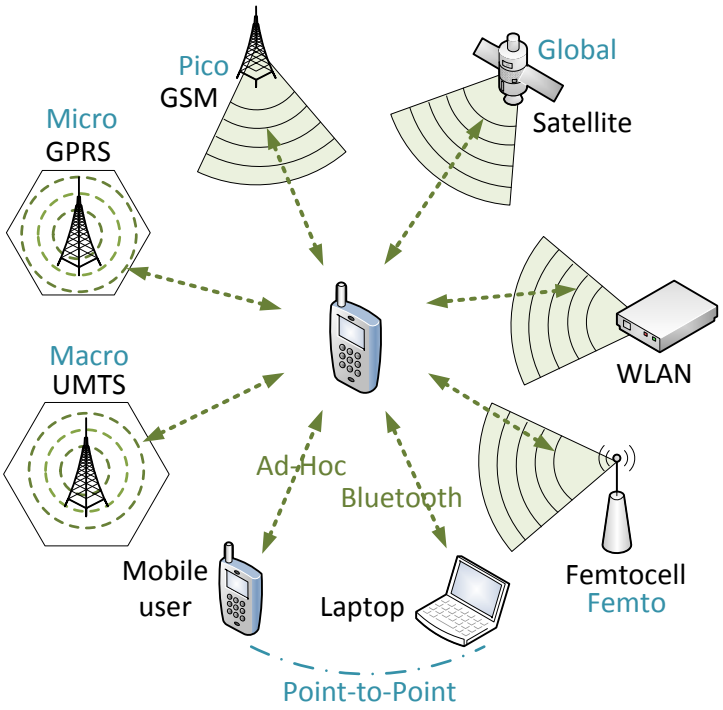

Fig. 2.1: Possible heterogeneous network architecture sketch

mation [14]. For a smaller area coverage, macro cellular is considered as a traditional mode for voice communications. Although in the 3G network the data service demand has increased dramatically, many applications are constrained in order to guarantee quality of voice service. Micro cells and picocells are typically used to extend coverage to the indoor area where outdoor signals do not reach well, or to add network capacity in areas with very dense phone usage, such as an enterprise building, train stations and shopping malls. The typical range of a macrocell coverage is 1 km to 30 km, and for a microcell and a picocell the range is 200 m to 2 km and 200 m or less respectively. Macrocells, microcells and picocells are available for most cellular technologies, including GSM, Interim Standard 95 (IS-95), UMTS and LTE. WLANs and femtocells are normally installed in homes or hotspots in cafes or restaurants. They offer better connection to meet small regions of high demand within a large cell area [15]. The coverage of a femtocell is suggested as a 100 m×100 m area [32]. Finally, as a mobile node, it can communicate with other mobile nodes directly via an Ad-Hoc

network or Bluetooth [38]. They are considered as P2P networks.

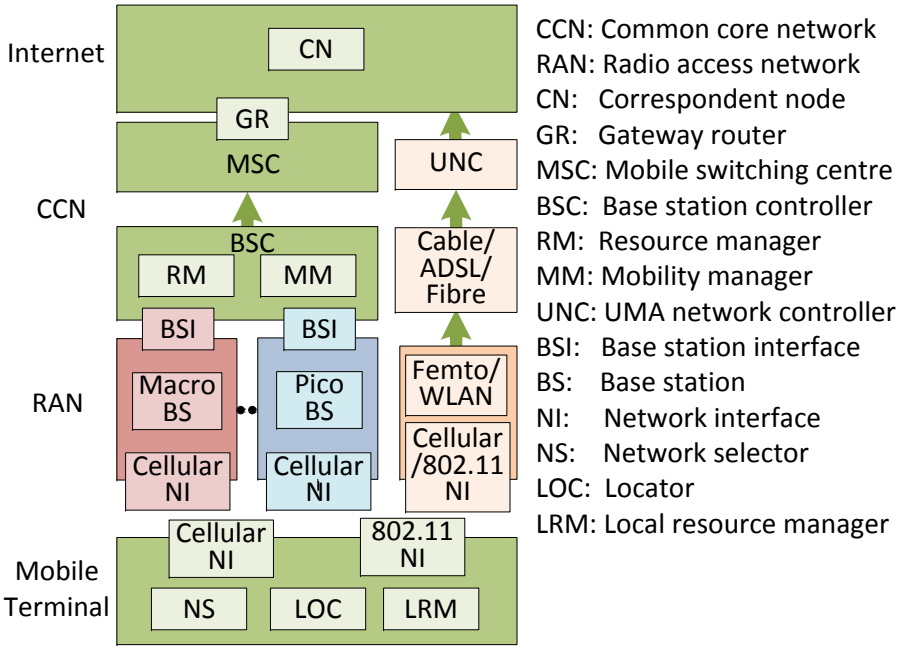

Fig. 2.2: Heterogeneous system achitecture

A multi-mode mobile terminal may be exposed to any combination of heterogeneous Radio Access Networks (RANs), which are described above. An architecture of heterogeneous networks can be seen in Fig 2.2, which is composed of four major building blocks: A mobile terminal, RANs, a Common Core Network (CCN) and an external network (or the Internet).

Within the external network, there are Correspondent Nodes (CNs) for processing and forwarding the signals from different network architectures. There are Gateway Routers (GRs) to connect the external network and the CCN. In the CCN, the Mobile Switching Centre (MSC) and Base Station Controller (BSC) are considered as important entities. The BSC performs resource management (RM) and mobility management (MM) functions, such as spectrum allocation, transmission power setting and handover decisions, during connections. The data is aggregated and passed to the MSC, which connects to the GR. The MSC is responsible for routing voice calls, SMS as well as other services, setting up and releasing the end-to-end connections, also also taking care of charging issues. Each kind of RAN is linked to the

CCN via a Base Station Interface (BSI). The Base Station (BS) is used for processing received signals and maintaining all the registration information of mobile users.

For femtocell and WLAN heterogeneous networks, the RAN unit contains not only a femtocell or WLAN, but also many of the functions of the BSC and some of the MSC. The unit is able to connect directly to the Internet, without the need for the BSC and MSC infrastructure. The traffic from a femocell or a WLAN is forwarded to an Unlicensed Mobile Access (UMA) Network Controller (UNC). UMA enables a seamless handover connection between WLANs and cellular networks [39]. The extended service includes mobile voice, data and IP Multimedia Subsystem/ Session initiation Protocol (IMS/SIP) applications. When a handset detects a WLAN, it establishes a secure IP connection through a gateway to a UNC on the carrier's network. The handover between a cellular network and a WLAN appears to the core network as if it is simply on a different base station [40]. The UNC is also used to provide a secure managed standardised interface from a femtocell to the mobile core network. [41] and [42] propose using UMA as the basis for a femtocell standard. A detailed analysis of the mechanism of a femtocell using UNC is explained in section 2.1.4. A femtocell connects with mobile user via a cellular air interface, and a WLAN uses an 802.11 interface to communicate with a mobile user.

A multi-mode mobile terminal uses different Network Interfaces (NI) to connect with different network architectures. Within a mobile terminal, there is a Network Selector (NS) to decide which network should be selected for transmission, depending on the communication environment and required QoS. A Locator (LOC) can provide the location of the mobile terminal, and a Local resource manager (LRM) can provide the local resource information, to assist the RM in the BSC.

It can be seen that all kinds of wireless communication methods can be integrated to improve coverage, capacity and QoS, to achieve a universal communication platform. The possible commonly used and investigated heterogenous networks are combining cellular with ad-hoc [5, 19, 43, 44], combining cellular with WLAN [14, 35, 45, 46, 47], and combining cellular with femtocells [28, 41, 42, 48], which combined macro, micro and P2P networks. Fig 2.3, Fig 2.4 and Fig 2.6 illustrate the communication principle of each network architecture. With the aid of these illustrations, each of the

architectures is described below. It should be pointed out that a mobile user communicates with other mobile nodes or a WLAN via an 802.11 air interface. While to connect with a femtocell, only a cellular interface is required. In some cases, a femtocell acting as an Ad-hoc Relay Station, only collects data and forwards it to a server, which is able to act as a base station with MSC and BSC functions. However in this thesis, a femtocell is considered as an independent unit, which has resource and mobility management functions that can connect to the Internet directly. Therefore, a femtocell access point is more like a WLAN access point, with a similar appearance, similar coverage area, and similar backhaul options, such as cable, ADSL and fibre.

2.1.2 Combined Cellular and Ad-hoc Architecture

In the combined cellular and ad-hoc network architecture, each Mobile Terminal (MT) is assumed to be a multi-interface device (cellular and 802.11). In Fig 2.3, if the source node is C, and C starts a new call connection to D, both customers are covered by a cellular network. This communication follows the conventional method that transmitted signals are delivered to the local Radio Base Station (RBS) first, and processed by the core network, finally they are forward to the destination node D. Some nodes may not be covered by any cellular cell, such as nodes A and E. If one of these start a call request, the following scenarios may occur by using the heterogeneous architecture, and they are distinguished from each other by different source (SRC)) and destination (DST):

- SRC=A, DST=D
  A is an external node for cellular cell, and D is a internal node. Internal mobile nodes all register their information with the local base station when they enter this area. For a simple cellular network, node A is not able to communicate with node D. When ad-hoc communication is introduced into a communication system as an aid, node A can use a Mobile Ad hoc Networking (MANET) mode to form the connection. Node A senses the nearest MT (node B) which is covered by a cellular network, and sends the message to B, using B as a relay node. Then, depending on the routing protocol, the routes after node B can be selected. For example, further relay nodes can be employed for transmitting signals from node B to the BS, or it is also possible for

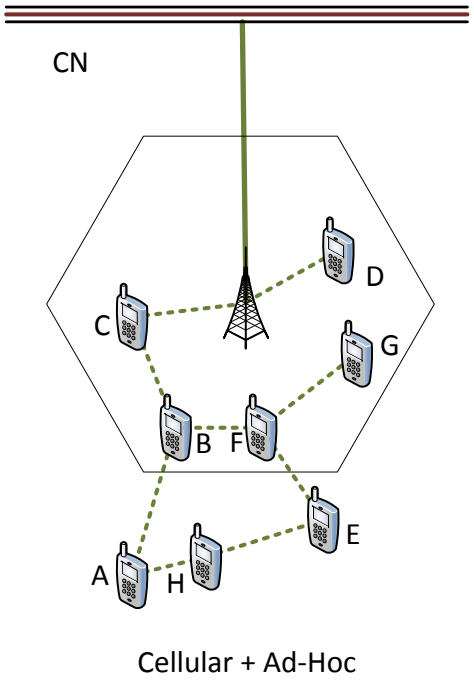

Fig. 2.3: Cellular combined Ad-hoc network communication scenario

node B to transmit to the BS directly. The BS delivers the messages to the destination D, by using the registration information of node D.

In this process, routing protocols need to be applied for maintaining the network topology in each Ad-Hoc node. They can be classified into two major categories: proactive routing protocols and reactive routing protocols. Proactive protocols continuously broadcast signals during a certain interval of time, exchanging topological information among the network nodes to maintain neighbouring node information. Some typical proactive routing protocols are Destination-Sequenced Distance Vector (DSDV) [49] and Wireless Routing Protocol (WRP) [50]. The energy consumption of maintaining the network by using a proactive routing protocol may be high, and if the network activity is low, the information about the actual topology might even not be used before the next update. On the other hand, reactive protocols only establish route(s) to the destination when the need arises. Ad Hoc On-Demand Distance Vector (AODV) [51] and Dynamic Source Routing

(DSR) [52] etc. are examples of reactive protocols. By applying any kind of routing protocol, each mobile user is able to obtain the list of the number of hops to other mobile users. Some topology control algorithms collect node information, whilst maintaining a low power consumption [20, 44, 53].

- SRC=E, DST=G
  E is an external node, similar to node A. E wants to communicate with G, which is not far away from E geographically. The customer may not know this fact, but the agile network can determine this. In this case, the message from node E is delivered between a group of MANET mode relay nodes, and finally transmitted to the destination G. It should be noted that, in this communication process the issues of identity management, security, authentication etc. need to be considered. When the applications between two mobile nodes are authenticated by password, IP address or digital certificate, such as video conferencing within a building, file sharing or short range of texting, these applications can be implemented directly between nodes, by applying Mobile IP (IP) and Authentication Authorisation and Accounting (AAA) protocols in Ad-hoc and Bluetooth networks [54, 55]. The transmission pattern is as described above, from node E to node G. However, if the application needs to be authenticated by network operators, the mobile node needs to connect to the local core network to find the registration information of the destination node. In this case, the source node E needs to use other mobile users, which are located in a cellular network, as relay stations. It then connects to the core network to communicate with node G.

- SRC=A, DST=E
  If the source node and destination node are both outside the coverage of the cellular network, they are still able to communicate with each other. Node A can transmit signals through relay nodes using the MANET mode, regardless of whether these nodes are external or internal to the cellular cell. However, the feasible connections are limited to short range of data transmission, where the security and authentication issues can be solved by MIP and AAA protocols of Ad-hoc networks.

The main mechanism of cellular combined ad-hoc architecture is presented as detailed above. The benefits of an integrated cellular and ad-hoc architecture are: reduced congestion probability by diverting the data traffic load from the BS to the mobile handset or relay node. The less congestion that occurs, the lower the resend rate, therefore, more transmission power is saved. Additionally, more transmission power reduction results from shorter transmission distance between hops. Furthermore, with certain connections, the whole communication process can avoid the participation of the RBSs, and further reduce transmission power in the RBSs. This architecture will also provide greater network coverage by using the ad-hoc extension. However, the benefits are only for data services, due to the latency between ARS nodes. In the end, since an 802.11b interface can provide much higher data rate in MANET mode compared to a cellular network, it is able to support more applications which require higher data rate, such as multimedia, for mobile users.

The drawbacks of this architecture are notable as well, and illustrated below. First of all, latency is the biggest issue. This is because the multihop mechanism is considered as the core technique of this heterogeneous network, hence the handovers between nodes and relay stations occur frequently, which is likely to cause significant delay and is unacceptable for voice services. The multihop mechanism also increases the protocol complexity dramatically [56]. Next, this architecture is seriously limited by MT mobility. Cellphone users have high mobility and the topology structure is changing all the time. Therefore, it may be difficult or complicated to implement and manage the MANET routing protocols efficiently or successfully when the MT is moving at high speed. Finally, all types of ad-hoc combined cellular networks require hardware investment, either in dual-mode MT hardware upgrades as well as possible relay infrastructure installation, which results in extra hardware investment.

In reality, the integrated cellular and ad-hoc network may potentially raise some practical issues. As the system requires each user to carry a dual-mode MT, it may have a negative influence on the customer's willingness to upgrade their cellphone. Beyond this there are still some issues about how to authorize the right for one MT to use another MT as a relay node, how to prevent a malicious attack, and also if the relay node user is willing to let other users occupy his local resource and consume his local battery energy

or not.

Considering the above advantages and disadvantages, many researchers have been working on variations of this architecture. For instance, in [57], the MT is distinct from relay stations. A number of Ad-hoc Relay Stations (ARSs) are deployed by the network operator and equipped with two interfaces. Therefore, the MT do not need to be updated. It also avoids many issues caused by considering a normal node as a relay station. However, the installation of ARSs still needs to be included in the whole system cost, and the density of ARSs allocation is also a complicated issue that is related to the system cost and user demand distribution. In order to combat the mutable topology structure, a new mechanism has been introduced so that each MT keeps two buffer cache tables. One is for its own location information, and another is for a multihop routing table, including its neighbor's topology information [58]. Each MT sends its own location information frequently, regardless of whether this node is idle or active. Hence the optimal routing can be structured in a short time, and the delay due to multihop handovers can be conquered efficiently. Whilst each MT keeps sending its location information even if its state is idle for most of the time, lots of extra power is consumed to improve the network performance and also the high quality of service provision.

On the basis of the above, it can be seen that the research tends to overcome the drawbacks originating from this architecture by exploring new routing protocols. These new routing protocols improve some aspects of QoS support for this integrated architecture, such as providing a more secure arrangement for users and latency reduction. However, a lot of sacrifices are necessary in order to achieve these targets, as they require a large amount of infrastructure upgrading and investment. Therefore, there is a potential conflict between energy efficiency and QoS provision.

2.1.3 Combined Cellular and WLAN Architecture

As ad-hoc is considered as a mode of a WLAN architecture with no infrastructure, as defined in the IEEE standard 802.11, another mode of WLAN, with infrastructure [59], is illustrated below. In order to distinguish this from the ad-hoc heterogeneous architecture, the infrastructure WLAN heterogeneous network is also referred to in this thesis as a combined cellular and WLAN architecture.

The same scenario as that shown in Fig 2.3 is used to analyse the routing strategies in this architecture. The same number of MTs and the same locations of these MTs are assumed. In this architecture, a certain number of Access Points (APs) are additionally located randomly, as Fig 2.4 shows.

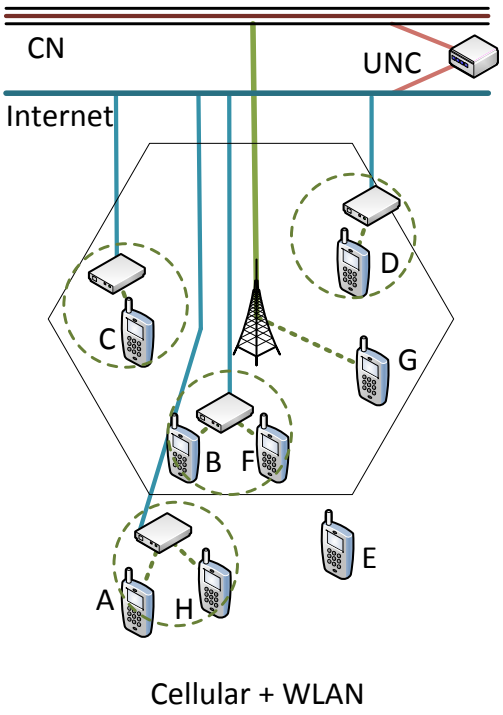

Fig. 2.4: Cellular combined WLAN network communication scenario

Currently, one of the most studied examples of this architecture is the basis of the Unlicensed Mobile Access (UMA) standard as a part of 3GPP, which defines a technique for integrating Wi-Fi (WLAN) access and GSM (cellular). The switch unit between the Internet and the mobile communication core network is called the UMA Network Controller (UNC), which can be seen in Figure 2.5. The UMA technology enables seamless handover between cellular and short range communication technologies, that provides IP based secured connection making voice over WLAN possible. This architecture requires a dual-mode cellphone for implementation. At present, a couple of manufacturers have launched this kind of handset.

In the UMA system, the MT starts in a cellular mode, and executes the

normal cellular power-up sequence. Then, it might switch to another mode, based on the users preference setting or the operator's configuration [60]. There are four possible operation modes for selection.

- GERAN-only: GERAN represents for GSM Edge Radio Access Network. In this mode, the MT stays in the GSM mode, and never switches to the UMA mode. For example, the node G in Figure. 2.4 is not covered by a WLAN, the operation mode can be manually set as GERAN-only by the user, or automatically set by the operator. This move can reduce energy consumption, because the MT does not need to send signals to detect the environment if there is an available UMA network.

- GERAN-preferred: In this mode, the MT stays in the GSM mode, as long as the connection with GSM is available. Otherwise the MT searches for WLAN coverage. If it is detected, the service is switched to the UMA mode. At any time, if a GSM service becomes available, the service is switched back to the GSM mode. This mode can be applied to the mobile users, who are normally active in a certain region with strong cellular signal strength.

- UMAN-preferred: At any time, the MT uses an 802.11 connection if a WLAN is in range. Otherwise the MT attempts to connect with a cellular network if it is available. This operation mode can be used for an enterprise scenario where the cellular service can not fulfill the demands of a dense population within an area, or for some residences which may be located at the edge of a cellular network with poor connection and coverage, such as node B and F in Figure. 2.4.

- UMAN-only: In this operation mode, the MT uses only the 802.11 connection. This operation mode can be used for nodes A and H, which may be not covered by any cellular network for a long time, but have service from the local WLAN. They are able to save signaling power compared to UMAN-preferred mode.

This mechanism is also suitable for an UTRAN system. When a MT selects an operating mode that needs to connect with the UMA network, the end-to-end chain and QoS provision need to be considered. Since voice

service requires the highest QoS, it is taken as an example to explain QoS provision in UMA network.

First the signal is transmitted from handset to a WLAN AP for the uplink. QoS over Wi-Fi is achieved by implementing Wi-Fi Alliance Wireless Multi Media (WMM) certification. For a voice service, the highest level of QoS, WMM 'voice', is utilised. Handsets must queue all voice frames as 'voice', and usually signaling frames are similarly tagged. When the voice signal is sent to a WLAN AP, it is given priority to traffic tagged (according to 802.1d) at level 6 (voice) or 7 (network control). Then the voice traffic transmits over the Internet via the operator's gateway. The public Internet is not generally priority-aware, however, given sufficient bandwidth on the access link, VoIP over the Internet can be successfully accomplished. After the gateway, the signal is delivered to the operator core network, where schemes can be implemented to handle VoIP traffic. In the downlink, it is likely that packets will lose their QoS tags as they traverse the Internet. Therefore it is important that packets are re-tagged as soon as possible after entry to the local WLAN network.

Figure. 2.4 also shows that, node E is not covered by any network. In this architecture, node E is not able to communicate with any of the nodes, which is an unfavourable condition for a certain users. In this respect, the cellular combined ad-hoc architecture is better than the cellular combined WLAN architecture, although the former one may consume more power. Therefore, there is a trend to combine these two architectures. Hence node E is able to communicate with other nodes through multihop routing, and the flexibility of the network is improved enormously. However, the routing protocol then become a complicated issue.

The UMA structure is one of the studied combined cellular and WLAN networks. It is able to provide a satisfactory voice service based on a sufficient Internet resource. However, without using the UMA scheme, the QoS of voice services can not be guaranteed in this heterogeneous network.

Besides the UMA structure, the 3GPP is also working on the data offloading specifications for the cellular combined WLAN heterogeneous network [61, 62]. The methodology is called IP Flow Mobility (IFOM), and is studied in Chapter 5.

2.1.4 Combined Cellular and Femtocell Architecture

A Femtocell is also known as an Access Point Station, and it provides broadband network services for indoor clients in a limited small area. In 2004 and 2005, more and more companies or institutions paid more attention to this technolgy, and the femtocell is now widely recognised. By 2007, femtocells had become mainstream and had been promoted worldwide.

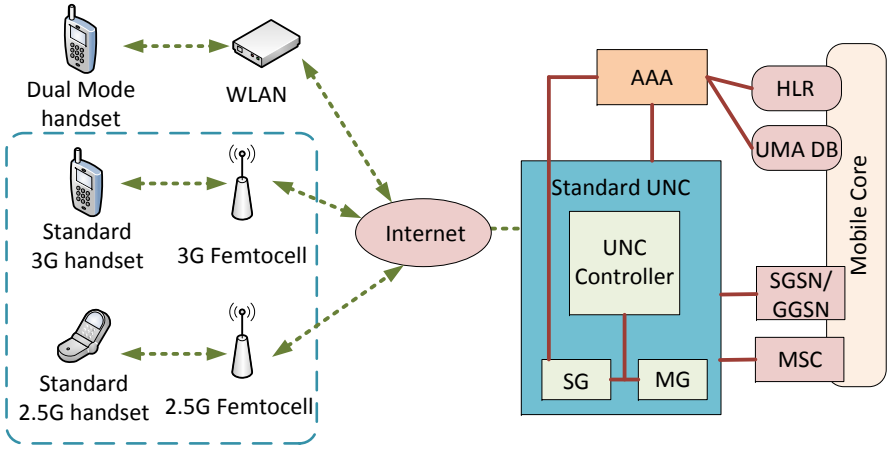

Fig. 2.5: Utilisation of UMA infrastructure in femtocell network

A Femtocell can be considered as a small cell within a cellular network. A MT does not need to be a dual-mode handset to communicate with the femtocell, since the femtocell AP provides the same communication channel and the same air interface as a cellular network. If a number of femtocell networks are located in a macrocell network, the network will then be a hierarchical network. However, as the femtocell networks are using the same channel as the macrocell network, and are also located in the macrocell area, RF interference may occur between the macrocell and the femtocell, or between femtocells [63]. This is a significant issue in the combined cellular and femtocell architecture, and also a research "hot topic".

Femtocells also can be considered as a technique derived from UMA. These two architectures are based on the Voice over Internet Protocol (VoIP) technique, and APs from both networks are connected to a Digital Subscriber Line (DSL) or a cable modem. It can be seen from Fig 2.5 that,

a femtocell network can reuse the existing UMA infrastructure as an alternative to installing a new Base Station Router (BSR). For instance, the UMA protocol provides the connection to the mobile core, tunneling the Iu protocol. The existing security and media gateways, Authentication, Authorization and Accounting (AAA) protocol, transport and device management of the UMA are all utilised by the femtocell network, which contributes to a significant power saving.

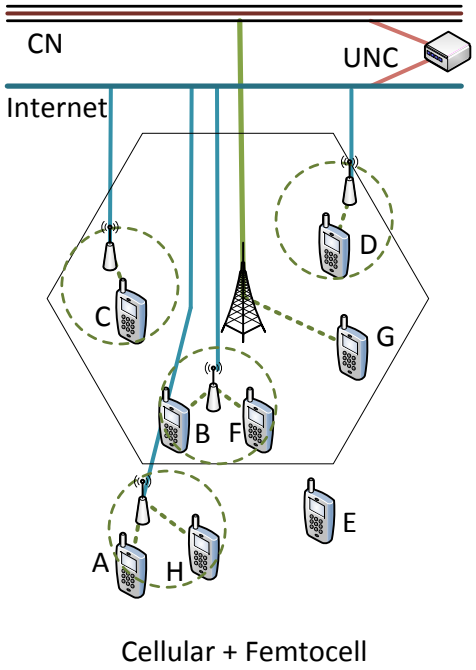

Fig. 2.6: Cellular combined Femtocell network communication scenario

It can be seen from Fig 2.6 and Fig 2.4, that the communications scenarios in femtocell heterogeneous network are similar to a WLAN heterogeneous network. Each node that is covered by a femtocell can communicate with the nodes either covered by a cellular network or a femtocell network. On the other hand, if one node is not covered by any type of network, it is not able to implement any communication.

The integrated cellular and femtocell network has a similar routing algorithm to a UMA protocol. However, there are some differences in certain scenarios. For example, the authorisation of public access to the local fem-

tocell network should be given by the femtocell owner, and the owner has the priority to occupy this femtocell network, which is the same for a UMA network. If each guest node can be authorised to access each AP, then the femtocell and WLAN can both accomplish the connection through a similar routing. Whereas, when an AP owner is not willing, or not able (due to reaching the maximum number of users) to authorise public access for a temporary user, this user cannot get a connection in the femtocell network. In addition, the local femtocell introduces a strong interference to this user, and shields this user for getting service from the macrocell. But it will not happen in a WLAN heterogeneous network, since the WLAN AP use different channels to the cellular network. It illustrates two potential access methods for femtocell configurations: one is open access, allowing any mobile subscriber to use any femtocell; the other is close access, providing service restrictedly to specifically registered users. Some researchers propose that the operator should encourage the femtocell owner to choose open access by offering some compensation measures, such as offering cheaper calls at home [48]. Generally speaking, the integrated cellular and femtocell network may be relevant for more practical issues, such as authentication, authorisation and accounting. If these issues cannot be solved properly, it may dramatically affect the performance of the whole architecture.

Along with the development of Long Term Evolution (LTE) standards specifications, the data offload mechanisms between local femtocell and macrocells are defined for the LTE network architectures since Release 8 by 3GPP, which are Local IP Access (LIPA) [64] and Selected IP Traffic Offload (SIPTO) [65]. The detailed study of these mechanisms are introduced in Chapter 5.

2.2 System Power Consumption

In order to explore new power saving techniques, the whole system power consumption needs to be analysed in detail, which is the aim of this section.

The power of a heterogeneous wireless communication system is primarily made up of the following components: Base Stations (BS), Access Points (AP) (from WLAN or femtocell) and the customers' Mobile Terminals (MT). For each piece of equipment, their power consumption comprises embodied energy and operational energy. Since different architectures contains different components, each architecture scenario is analysed, based on embodied

energy and operational energy respectively.

The embodied energy is defined as the total primary energy consumed in the work of making a product. It aims to express the sum of total energy needed for a product's life cycle, including extraction, transport, manufacturing, etc. One example of this is a detailed inventory database of a large number of building materials' embodied energy, provided by the University of Bath [66]. For a certain product, the embodied energy can also be considered as capital expenditure, which can be abbreviated as CapEx.

Operational Energy, also called Operational Expenditure (OpEx), is the energy consumed during the equipment's use phase in a telecommunication system, including the core network, data centre maintaining, signal transmission and processing at each item of equipment, together with equipment repairing, etc. It is another essential constituent part of the system energy consumption model. Considering that the operational energy consumption at the core network varies, based on the different network architectures and standards, it may not make a significant contribution into the system. Therefore, only the typical network equipment energy consumptions are taken into account, i.e. BS, AP and MT. Additionally, the energy consumed for equipment maintenance and repair varies significantly due to various reasons, such as the differences in labour force and transportation, which is difficult to quantify. The expenditure in these areas has a direct effect on the system energy consumption performance. As it is not possible to fully quantify expenditure in this area, it is assumed that the maintenance and repair costs are lower for femtocells than macrocells. Assuming that this is the case, equipment maintenance and repair energy consumption are not considered in this thesis.

The system backhaul power consumption is not included in this thesis. This is for two reasons: for the BS, the backhaul power consumption largely depends on the structure of the cellular system, and the adoption of the femtocell technique will not have much effect on the backhauls power consumption; for the femtocells and WLANs, considering that the commonly used backhaul of the femtocell is DSL or cable, which has already been ubiquitously installed, the additional backhaul energy is limited to the operational energy of the broadband supplier.

2.2.1 Base Station

The Base station (BS) contributes significant energy consumption in a communication system [67]. There are two ways to decrease energy consumption of the BS: one is minimising the energy consumption of a single BS; the other is minimising over a number of BS sites.

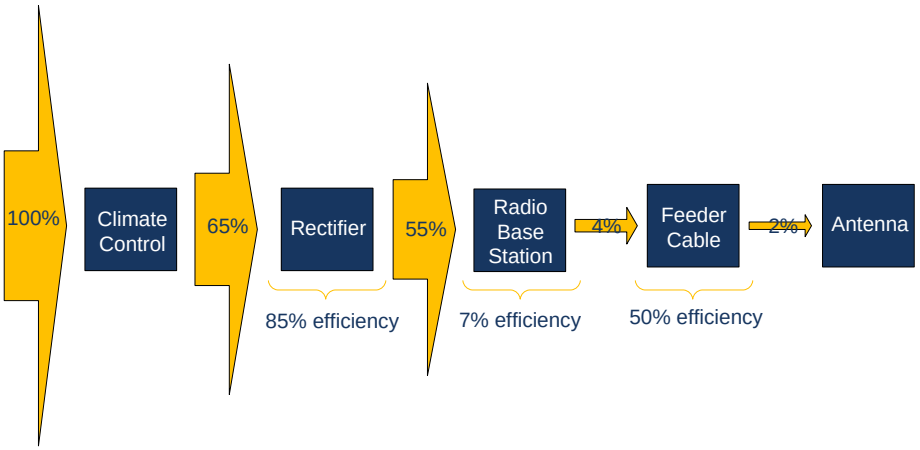

Fig. 2.7: Base station efficiency

For a single BS energy efficiency analysis, Fig. 2.7 [68] indicates each entity's energy efficiency. The cooling system is only 65% efficient. This suggests that BSs should be built in an outdoor environment to decrease the cooling and/or heating energy consumption.

The most significant component contributing to energy consumption is the power amplifier in the Radio Base Station. The main technique for improving power amplifier efficiency is to use different methods of linearization, or use DSP methods to decrease the required linear area. [69] proposes a a high-performance Gallium nitride (GaN) heterostructure field-effect transistors (HFETs) to achieve good linearity and high-efficiency performance, since GaN HFETs are able to provide higher voltage operation and high power density at microwave frequencies. The results show that the efficiency can be improved by more than 50% [69].

The energy loss in the feeder cable is 50%. In order to decease the energy loss, it is suggested that the RF transmitter is located close to the antenna, reducing the distance of transmission. Finally, research has concentrated

on antenna techniques, such as using smart antennas [70], to improve the directional antenna gain. [71] proposed a multiple beam adaptive antenna, which is able to cancel the co-channel interference and also be aware of energy efficiency.

One other method of reducing energy consumption from BSs is to minimise the number of BS sites. First, sleep mode schemes are proposed based on communication traffic patterns. Some BS sites are switched to sleep mode, operational energy consumption can be saved. Some BS sleep mode mechanisms are proposed in [72, 73, 74]. Other research has investigated the impact of the deployment of small, low power networks alongside the conventional macrocell network with full traffic load, such as the use of microcells and femtocells. [75, 76] and [77] investigate the deployment of micro base stations within a macrocell. When considering only operational energy the more microcells deployed within a macrocell, the higher the power consumption. However, the spectral efficiency increases along with the deployment of microcells. These papers claimed that there is little point in deploying smaller networks within a macrocell, if viewed only from the operational energy consumption perspective. However, as mentioned before, embodied energy of equipment contributes a significant proportion of system energy consumption. It should not be neglected in any analysis when techniques or deployment strategies are proposed in order to reduce the system energy. Therefore, base station embodied energy analysis is carried out as follows.

There are two sources relating to a Base Station's embodied energy and operational energy. One is David Lister's presentation, who is research manager from Vodafone, " An Operator's view on Green Radio" [8] presented at the ICC conference on 18th June 2009. The other presentation is from a researcher of Alcatel-lucent, Francis Mullany, "OPERA-Net: Optimising Power Efficiency in Mobile Radio Networks" [78], presented at the Mobile VCEs Education day on 30th April 2009.

In Lister's presentation, some information can be obtained as follows:

- Power/Energy demand per radio site 2–3 kW ($\sim$ 22,000 kWh/year)
- The majority of radio site power/energy demand is consumed by Radio equipment and Cooling

The annual budget, for both the base station's embodied and operational energy consumption is approximately 80 GJ (22,000 kWh $\times$ 3600). The

equivalent power consumption of the base station is approximately 2.5 kW (22,000 kWh/24/365).

In Mullany's presentation, the following two items can be derived:

- 3 billion subscribers' annual energy consumption: $\sim$ 2 TWh
- 4 million BTS/NodeB annual energy consumption: $\sim$ 60 TWh

Since it has not been clarified whether these figures are for operational energy or embodied energy, we can estimate them from the first item: 3 billion subscribers' annual energy consumption is $\sim$ 2 TWh. Therefore, for one mobile terminal, the average power consumption is 76 mW, which is a reasonable value for a mobile terminal's operational power, and is significantly lower than a mobile terminal's embodied energy (as will be discussed in section 2.2.3). Hence, we consider that item two refers to the base station's operational energy as well. The operational power of the base station can be calculated, and the power consumption value is around 1.5 kW.

Summing up the above two references, the overall power consumption of the base station is approximately 2.5 kW, and the operational power consumption of the base station is about 1.5 kW. Therefore, the approximate value for the base station's embodied power is around 1 kW. We assume that the lifetime of the base station is 10 years (the majority of a base station's components' lifetime is about 10 years, such as the high-power amplifiers, oscillators, etc [79].), therefore, the lifetime embodied energy of the base station is $\sim$300 GJ.

2.2.2 Access Point

For a Femtocell Access point, the operational power consumption is given in picoChip CTO, Dr Doug Pulley's presentation, "Femtocells: Trends in Power Consumption & Scalability" [1]:

- Current WCDMA HSDPA Femtocell power consumption: 6.05 W
- Next Generation WCDMA HSPA Femtocell power consumption: 5.05 W

[1] Mobile VCE Green Radio, Education Day, 30 April 2009

- Future 10 MHz LTE Femtocell: 8.75 W
- Future Dual-Mode LTE/HSPA+ Picocell: 13.25 W

Therefore, in my simulation, the value of 6 W is adopted as the operational power consumption of the access point.

On the other hand, the data of the access point's embodied energy is difficult to derive. It is not available from any references. The industrial partners in the Mobile VCE have pointed that an access point's embodied energy should be similar to that of a mobile terminal [8]. Hence, this has been added to the simulation parameters used in Chapter 3.

2.2.3 Mobile Terminal

Simple Phone Embodied Energy

A technical report [80] from Nokia has provided significant detail and analysis of a mobile phone's Life Cycle Assessment (LCA). From this report, the following details about the mobile phone's embodied energy can be found:

- For both mobile phone types (type B and type C [2])the components manufacture phase accounted for the biggest part with an energy consumption of 126-130 MJ.
- The raw material extraction and processing accounted for 25-40 MJ depending on the product type.
- The assembly line contribution to the environmental impact was 11MJ and landfill's only 0.005-0.007 MJ.
- The contribution of the transport was about 10% (if the transport of components to the assembly plant and the transportation of phones to the first customer are added).

The relevant data can be seen in Fig 2.8.

Since the new definition of embodied energy from [66] has excluded the transportation expenses, to sum up the previous 3 items, for the type C products, the embodied energy is 162 MJ for average 2 year lifetime. This means that, the mobile terminal's embodied power is 2.6 W.

[2]Type B: Nokia's products between 1992-1994; Type C: Nokia's products between 1995-1996.

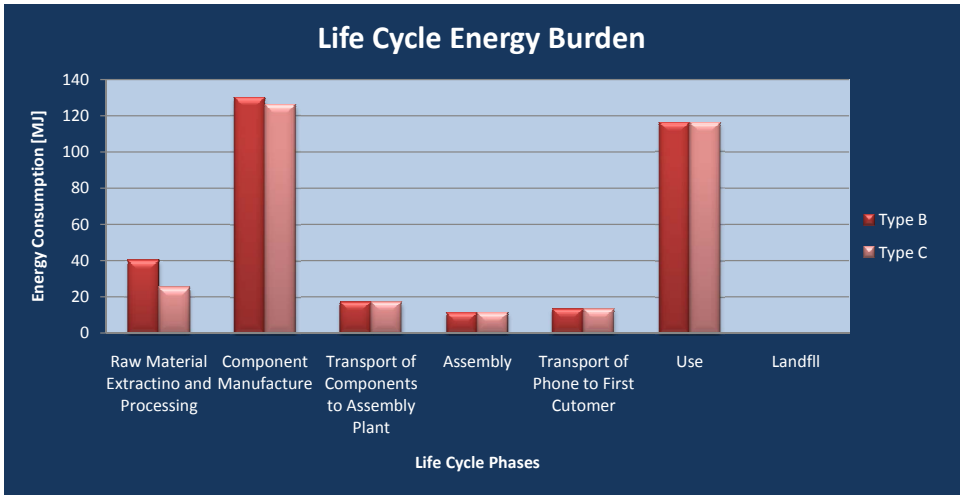

Fig. 2.8: Mobile Terminal's Life Cycle Energy Burden [80]

Smartphone Embodied Energy

Currently the smartphone is experiencing a significant rise in uptake with the development of 3G communication networks and a wide applications base for smartphones. The popularity of smartphones also enables use of WLANs as part of a combined cellular network. Customers can switch their services to a local WLAN for a better QoS, also potentially gaining from low cost and low power consumption. In order to analyse the power consumption of a combined WLAN and cellular network system, the smartphone is an essential component. Thus, the embodied energy of a smartphone is required for this part of the investigation. However, due to the diversity of smartphones from each manufactor, and also the protection of commercially sensitive information, no typical values of embodied energy of smartphones are published. Therefore, three different approaches are used to estimate it, and aim to find a reasonable or typical value for further system performance evaluation.

Price Approach

This approach assumes a relationship between the smartphone handset's price and it's embodied energy. A simple 2G phone is valued around £40, and the cheapest smartphone is around £80, i.e. double the cost of a simple phone. (This information is from the Carphone Warehouse website [81], the

handsets are sim-free, and are end of line, thus have no contract costs associated with the handset and have already recovered any advertising cost).The data of a simple phone's embodied energy is 162 MJ with an average 2 years of use [80]. Comparing a smartphone with a simple phone based on embodied energy, the extra cost is mainly from the dual-mode transceiver with two sets of function chips and interfaces for both cellular and WLAN networks, and a larger or higher technical touch screen for a better users experience of multiple applications. Based on this analysis, since the transportation and advertising costs are excluded from the prices, the embodied energy of a typical smartphone is at least twice that of a simple phone. Therefore, it leads to a value of 324 MJ embodied energy for a smartphone. If its lifetime is also 2 years, then spreading the 324 MJ embodied energy over this time, the smartphone's embodied energy per second is achieved.

$$324 \times 10^6(\mathrm{J})/2/365/24/3600 = 5.2(\mathrm{W}) \tag{2.1}$$

Proportion Approach

It is shown in [82] that during a mobile phone's life time, 20% of energy consumption is from operational energy, 80% is from embodied energy. The operational power consumption from the heaviest user to the lightest user ranges from 1 W to 40 mW. By using the proportion approach, the embodied energy per second should be 4 times of the operational power. Hence, the embodied energy per second is from 4 W to 0.16 W. Over a 2 year span of smartphone usage, then the smartphone's embodied energy ranges from 252.3 MJ to 10 MJ. This approach lacks certainty, since it results in a wide range of values, and is also based on an enormous diversity of user behaviour.

Therefore, by using the proportional approach, and considering the heaviest mobile user, the smartphone's embodied energy is 252.3 MJ, and 4 W for the embodied energy per second over a 2-year lifetime.

CO_2 Emission Approach

The energy consumption is closely linked to CO_2 emissions. A lot of handset manufacturers are also using this as an indicator of their product's energy consumption. In the following, manufacturer's product CO_2 emissions are listed for analysis.

Nokia [83]

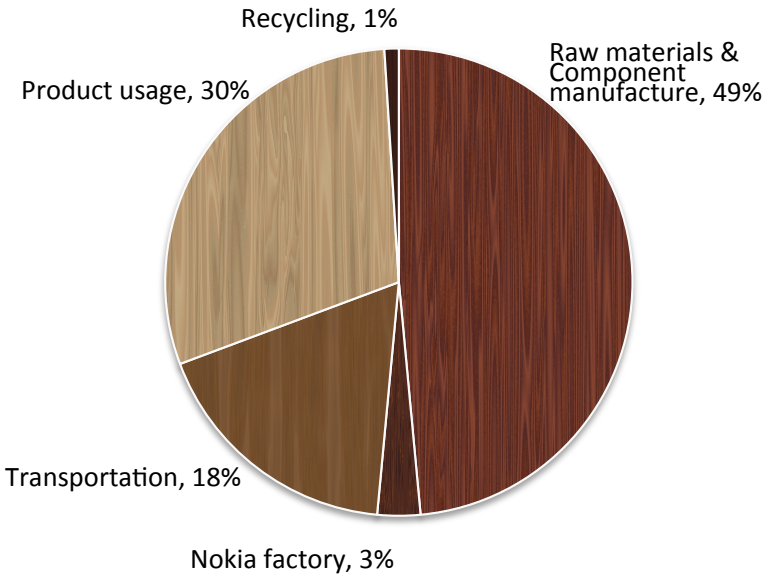

Fig. 2.9: A typical Nokia handset life cycle assessment of energy use [83]

Fig 2.9 shows a typical Nokia mobile device's energy consumption during its life cycle. The total energy consumption is 270 MJ, equal to 17.5 kg CO_2 emissions. Within this life cycle, only Raw materials and Component manufacture are considered as embodied energy, which is 49% of the total energy consumption. Therefore, the embodied energy of a typical Nokia handset is 132.2 MJ with 8.575 kg CO_2 emissions. In the reference, it is not stated whether the handset is a basic model or a smartphone, however this value is lower than an expected smartphone's.

Sony-Ericsson [84]

Fig 2.10 gives a typical Sony-Ericsson handset life cycle energy use assessment in each subcategory. The CO_2 emissions of the full life cycle is 23.8 kg, in which raw material extraction, component manufacture, and phone assembly, testing and warehousing are included in the embodied energy definition. These three elements account for 66% of the entire life cycle energy use. This leads to the conclusion that, the embodied energy of a Sony-Ericsson mobile results in 15.7 kg of CO_2 emissions, which is equivalent to 242 MJ energy consumption. The document does not state whether

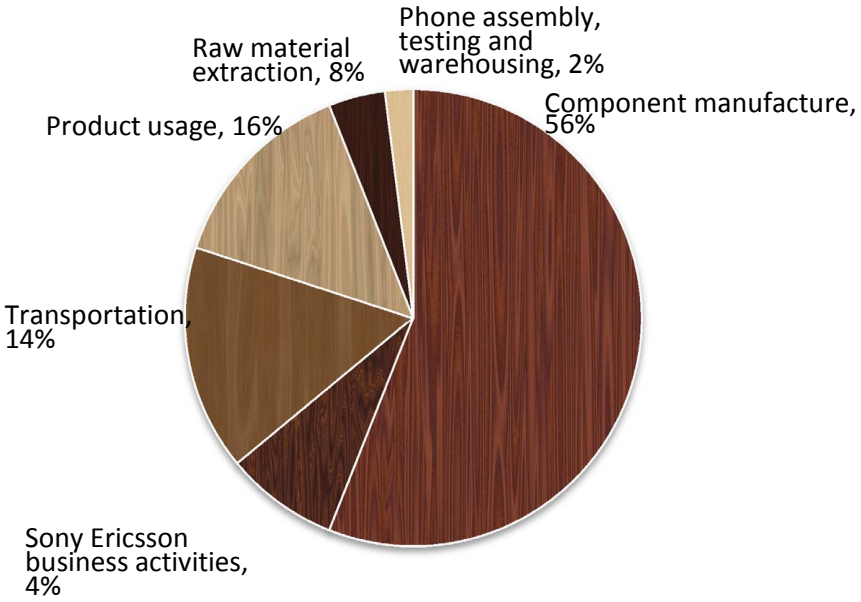

Fig. 2.10: A typical Sony-Ericsson handset life cycle assessment of energy use [84]

this is a smartphone or not, however it is based on the products of 2009, when smartphones were already quite extensively used. Therefore, we consider this figure approximates that of a smartphone.

iPhone 3G [85] and iPhone 4 [86]

iPhone series products are considered as one of the most popular smartphones. This section gives a detailed analysis of the iPhone 3G and iPhone 4 energy consumption during the lifetime. Fig 2.11 and 2.12 show the energy use of the iPhone 3G and iPhone 4 respectively. For iPhone 3G, 45% of the total 55 kg CO_2 emissions are from production, and lead to 24.75 kg CO_2 emissions and 381.6 MJ energy consumption of embodied energy. Similarly, the iPhone 4 has 57% of the total 45 kg CO_2 emissions for embodied energy consumption. Converting 25.65 kg CO_2 emissions to energy is 395.4 MJ, which is similar to the iPhone 3G. Considering the iPhone series products are designed beyond a standard smartphone, we consider this value is higher than the expected embodied energy of a typical smartphone.

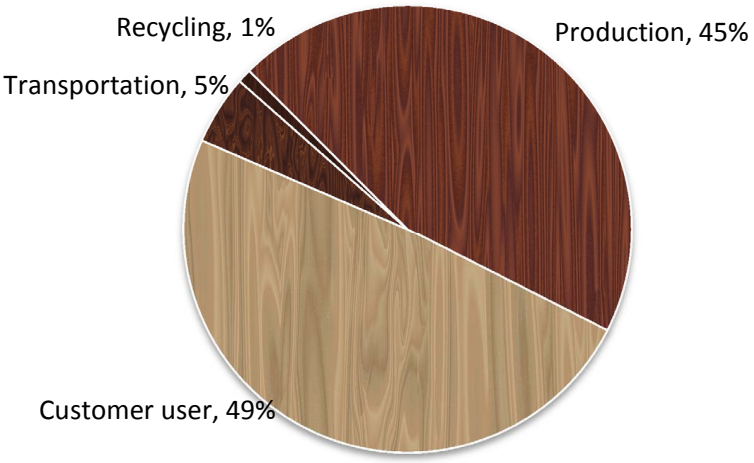

Fig. 2.11: iPhone 3G life cycle assessment of energy use [85]

The detailed summary of energy consumption analysis and comparisons of the above products are listed in Table 2.1.

Table 2.1: CO2 Emission and Embodied Energy Lookup table

Brands	CO_2e(kg)	Lifetime Embodied Energy (MJ)	Embodied Energy per second (W)
Nokia	8.575	132.2	2.1
Sony-Ericsson	15.7	242	3.8
iPhone 3G	24.75	381.6	6.1
iPhone 4	25.65	395.4	6.3

In this section, some well-known brands handsets are compared based on the embodied energy analysis. Among these brands, Nokia and Sony-Ericsson provide typical values, but did not specify whether they related to a 2G phone or a smartphone. On the other hand, the iPhone provides a much higher value, since they target a high-expense market. Hence, this analysis results in a reasonable embodied energy range for smartphone. A typical smartphone's embodied energy is greater than 242 MJ (Sony-Ericsson) and

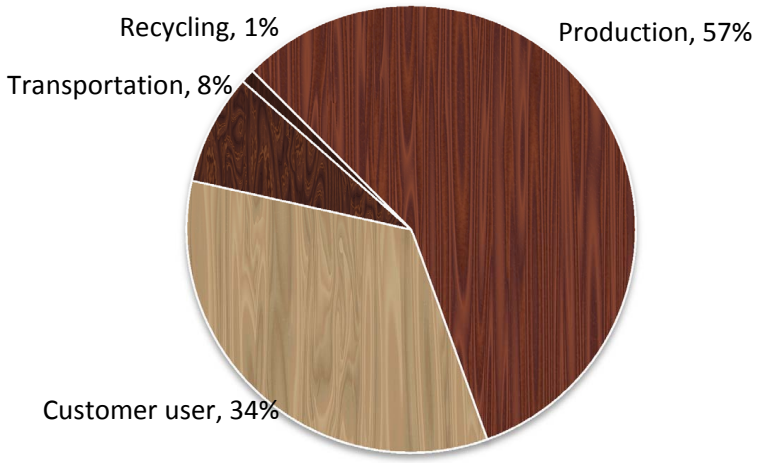

Fig. 2.12: iPhone 4 life cycle assessment of energy use [86]

smaller than 381.6 MJ (iPhone 3G), which also gives a range of the embodied energy per second 3.8 W- 6.1 W.

Table 2.2: Smartphone Embodied Energy Summary by Using Different Approaches

Approaches	Lifetime Embodied Energy (MJ)	Embodied Energy per second (W)
Price	324	5.2
Proportion	252.3	4
CO_2emission	242∼381.6	3.8∼6.1

Combining all the three approaches, the derived embodied energy data of smartphones are summarised in Table 2.2. It can be seen that, all the approaches result in a range of embodied energy: from 3.8 W to 6.1 W per second. Considering the price approach is based on the cheapest smartphone analysis, and also the value is the average value from the CO_2 emissions approach, 324 MJ and 5.2 W will be taken as the assumptions for the smartphone lifetime embodied energy and lifetime-expanded embodied

energy respectively.

Cell Phone Operational Power

Next the mobile terminal's operational energy is considered. From section 2.2.1, it has been calculated that the average operational power per user is 76 mW. However in the simulation, the mobile terminal's operational energy will change dramatically based on different transmission data rates and transmission distances, since the mobile will transfer its service from macrocell to local femtocell. Therefore, it is more reasonable to calculate operational power by using the following equation [87], which shows the MT energy, required to send a bit of information from one end to another:

$$E_b = \beta \times d^{\alpha} \tag{2.2}$$

where β is a constant of proportionality, with the value 0.2 $\text{fJm}^{-\alpha}$, d is the distance between the transmitter and the receiver, α is the path loss exponent. For an urban scenario this value is in the range of $2.7 \sim 3.5$ [88].

Hence, the MT's operational power can be calculated as follows:

$$O_{\text{MT}} = \frac{E_b \times R_t}{\varepsilon} + P_{\text{charger}} \tag{2.3}$$

in this equation, R_t represents the data transmission rate, ε is the efficiency of the MT, and P_{charger} is the MT's charger power consumption.

It shows that in the calculation of transmission power, the efficiency of the mobile terminal is considered as well. First of all, referring back to the base station's efficiency, Fig. 2.7 is investigated. For a mobile terminal, except for climate control and the feeder cable, the mobile terminal has a similar structure to the base station. Therefore, after the rectifier's 85% efficiency and the transceiver's 7% efficiency, the whole mobile terminal's efficiency is around 6%. So, in order to obtain the input power of a mobile terminal, the transmission power should be divided by 6% efficiency, which is the operational power of a mobile terminal.

Additionally, in reference [80], it has been mentioned that, over the lifetime of use the total energy consumption is 116 MJ, including 101 MJ energy consumed by the charger standby. Therefore, the mobile charger contribution cannot be ignored. However, the value of 101 MJ is questioned. Since the life time is 2 years, then the charger power consumption is 1.6 W. Ac-

cording to Nokia's Charger Energy Rating [89] the power consumption range for a charger is from 0.5 W to 0.03 W. For Nokia's products, the power consumption of the charger can be seen in Table 2.3. Therefore, the charger standby power consumption is 0.3 W which is more typical. The charger will also consume less power than when a mobile is plugged in. This assumes that the mobile charger is not always plugged in, but that people sometimes forget to pull the plug out after charging. Hence, it is assumed that during the daytime (12 hours), there are 6 hours in which charger is plugged in. This power should be added into the mobile operational power consumption.

Table 2.3: Nokia Charger Energy Rating

Nokia charger model	Charger energy rating	No-load power consumption
AC-8, AC-10	★★★★★	< 0.03W
AC-3	★★★★	<0.15W
AC-6	★★★★	< 0.15W
AC-4	★★★	< 0.3W
AC-5	★★★	< 0.3W

2.3 Quality of Service

System power reduction is the dominant motivation of this project. However, the customer is generally happier to keep the current service experience or improve QoS regardless of whether or not green techniques are employed. Ultimately, the objective of this project is to achieve a green telecommunication system without compromising QoS. Hence, as the energy efficiency is analysed in the previous section, the QoS metrics are detailed below.

2.3.1 QoS Metrics

Quality of Service (QoS) is something experienced by the user, and is also judged by the user. However, from a technical viewpoint, with the question of how to measure the QoS of a system, certain parameters are introduced to evaluate the system's QoS.

First of all, the system bandwidth is considered as the most conventional QoS parameter. However, measuring the bandwidth is relatively complex [90]. As the data transmission is in the form of packets or chunks, the

bandwidth value is not constant. Hence, the overall average bandwidth is normally used as the assessment metric. For certain other applications, the peak bandwidth is also significant. The bandwidth calculation depends on the operator and the type of network. For instance, as O2 is one of the companies who have the largest licensed spectrum [91], it is more able to provide a wider bandwidth for users. Universal Mobile Telecommunications System (UMTS) supports a maximum theoretical data transfer rate of 45 Mbps [92]. Theoretically, the capacity for WLAN and Ad-Hoc networks are significantly greater than that of the cellular network. This is primarily due to lower interference from neighbouring access points due to a much lower radio range. This is an advantage for WLAN and Ad-Hoc heterogeneous networks.

The next important parameter is the system capacity. It refers to the information rate that can be transmitted over a given bandwidth in a specific communication system. This parameter can be considered as an indicator if it's worth to increase the available bandwidth [59]. It can be affected by many factors, such as co-channel interference, noise, attenuation caused by long distances, fading caused by shadowing and multipath, as well as Doppler shifts. Therefore, the system capacity can be improved by applying interference avoidance techniques, OFDM and MIMO techniques, which can eliminate the interference effects, and combat multipath fading.

The final parameter that is considered in this thesis is throughput per user. The throughput is considered as an important criterion in the evaluation of system QoS [93, 94]. In this thesis, the throughput is examined with respect to each user. Smaller sized networks may provide a similar bandwidth or spectrum efficiency, however, they support many fewer users compared to a macro network. From each user's point of view, smaller sized networks may have the advantage of providing better QoS. The evaluation of QoS is based on user's experience, hence, it is fair to compare each user's performance.

2.3.2 QoS in UMTS, WLAN and Ad Hoc

In traditional telecommunication networks, QoS support is provided in the system as an inherent element. By contrast, the Internet provides a Best-Effort service. This circumstance brings about a conflict for UMTS systems. On the one hand, a UMTS system needs to provide a service that is as stable as the traditional telecommunication networks; on the other hand, the

UMTS system relies on the Internet to accomplish the service although it may provide an unstable quality of service, and there is no mature technique with the Internet that can ensure QoS.

UMTS defines four Traffic Classes [95]. These are Conversational Class, Streaming Class, Interactive Class and Background Class. Conversational Class applications, such as voice communication or video conferencing, require the highest transmission priority and a guaranteed bit rate because of a high real-time requirement. Conversational class communication requires a stringent limit of delay, of not more than 100 ms [95]. For Streaming Class applications, e.g. multimedia streaming, they do not need a real-time communication service. Therefore, their transmission priority is lower, and their delay tolerance value is 300 ms, which is greater than Conversational Class. Streaming Class still requires a guaranteed bit rate to ensure continuous multimedia streaming. Interactive Class, including Web browsing or gaming applications, is closer to the Best-effort service. It does not require either a real-time service, or a guaranteed bit rate. The last class is the Background Class, which does not need any bit rate guarantee, or any QoS, and support services such as messaging or email. Table 2.4 provides the relevant parameters and standard values of all four UMTS Traffic Classes.

Table 2.4: Range of QoS parameter values for UMTS Traffic Classes[90]

Parameters (unit)	Conversational Class	Streaming Class	Interactive Class	Background Class
Maximum bit rate (kbps)	up to 16,000	up to 16,000	up to 16,000	up to 16,000
Transfer Delay (ms)	100	300		
Guaranteed bit rate (kbps)	up to 16,000	up to 16,000		
Traffic handling priority			1,2,3	

Considering the end-to-end QoS for WLAN and Ad Hoc, note that the 802.11e standard only defines QoS provision in the link layer [90], it needs to be combined with the network layer IP-based QoS mechanism, which is generally based on Best-effort service.

2.4 Summary

In this chapter, three topics are covered: firstly, three types of heterogeneous network architectures are introduced and analysed from their advantages and disadvantages respectively; secondly, based on different network components, power consumption parameters are proposed; finally, based on different network types, QoS evaluation criteria are defined.

Considering the different heterogeneous network architectures, they all have power saving potential. However, they also all appear to have certain drawbacks. The combined cellular and ad-hoc network tends to divert the communication traffic from a base station by employing relay nodes, therefore the power saving is mainly from a reduction in base station power. A relay node can be a common relay station or a dual-mode mobile device. However, this architecture experiences a serious latency problem that results notably in authorisation and safety issues. The combined cellular and WLAN network architecture reduces the base station's power consumption by employing access points, which avoid the societal issues raised in the first heterogeneous architecture. However, it requires a large hardware investment for dual-mode mobile devices for successful implementation. Additionally, it is only able to offload the data traffic from a cellular network. Finally, the combined cellular and femtocell network architecture has similar benefits to the previous architecture. Also it does not require mobile handset updating, since the femtocell access point is utilising the same bandwidth as a cellular system.

The system energy reduction is from both OpEx and CapEx, including the consumption from the operators and mobile users. Another consideration is that the system energy consumption consists of three parts, which are from the BS, AP (both femtocell and WLAN), and MT. A comprehensive analysis is proposed based on the aforementioned aspects. Note that three factors are used to obtain a reasonable value for smartphone embodied energy, which are price, proportion and CO_2 emission approaches.

Quality of Service (QoS) is the other consideration in this thesis. The chosen parameters to evaluate QoS are average transmission bandwidth, system capacity, and available throughput per user. Across the different types of network architectures, cellular network has the highest communication quality requirements, including real-time service and high priority connec-

tion. By contrast, an ad-hoc or a WLAN network, which uses IP based communication, only afford best effort service. The gap between different QoS provision is a challenge for the heterogeneous techniques.

3

Combined Femtocell and Cellular Network Architecture: System Power Consumption analysis

As previously mentioned a ubiquitous heterogeneous network is more likely to provide a better communication environment, which is able to offer a higher capacity and greater coverage area coupled with system energy efficiency. Some research targets heterogeneous networks which are proved to be power efficient such as [5]. In this chapter, however, a comprehensive power consumption analysis is presented, based on a combined cellular and femtocell wireless network architecture. The power reduction is considered in terms of operational energy and embodied energy from the operator and mobile users point of view. A novel power consumption model is adopted in the simulation in order to compare different scenarios.

The sections are organised as follows: the first section describes the concept of deploying femtocells within a macrocell; different scenarios with different densities of femtocells deployment are illustrated. The second section examines the power consumption of a large scale communication network with femtocells. It includes both urban and rural environment analysis. The following section utilises a normalised small scale urban area for the investigation. The work in this section is based on a geometric model and stochastic analysis. The final section is the conclusion of this chapter.

3.1 Femtocell Heterogenous Networks Overview

A femtocell can be considered as a small cellular base station, which is installed by random customers. It has a much lower power consumption than a macrocell base station and can provide a relatively high bandwidth. Fem-

tocell research is becoming popular due to these reasons. This section will outline combined femtocell and cellular schemes. The benefits and drawbacks of femtocell deployment will be investigated.

3.1.1 When few femtocells are deployed

Figure 3.1 shows the current cellular communication network. Each macrocell is able to support a certain number of active mobile users. In this example, 10 active users are assumed to be covered by one macrocell. In Figure 3.1(a), another 5 active users are out of service, which are coloured in green. When femtocells are introduced into the system, whilst only a few femtocells are employed in homes, it is assumed that the users near femtocells handover their service to the local femtocell. This move brings multiple benefits, as can be seen from Figure 3.1(b): mobile users avoid a long distance communication to a macrocell, thus transmission power is saved; fewer users in a macrocell can lead to a cell size increase, meaning the users, which were out of service previously, may be able to be covered by a macrocell; alternatively, if the out-of-service user is close enough to an active femtocell, it can get served from that femtocell. Therefore, femtocell adoption has the advantages of, achieving lower power consumption, and increasing the system's coverage.

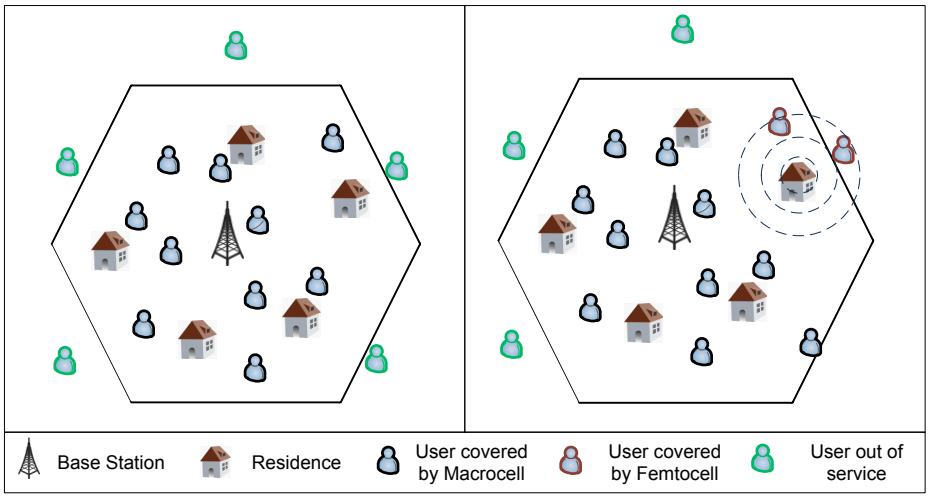

Fig. 3.1: A sketch of initial benefits of femtocell deployment: (a) No femtocells are installed. (b) A few femtocells are installed.

3.1.2 When an appropriate number of femtocells are deployed

Within a certain range, an increase in femtocell adoption is able to reduce the system power consumption, and also provide a relatively high QoS. Figure 3.2(a) depicts that, along with the increase of femtocells, the area of macrocell coverage can be further enlarged, and may result in a number of redundant base stations that can be switched off completely. For example, in Figure 3.2(a), the shaded base station can be switched off, since all active users are served by other base stations. In some cases, femtocell deployment may avoid a new base station installation, which leads to a massive energy saving in embodied energy.

3.1.3 When femtocells are over deployed

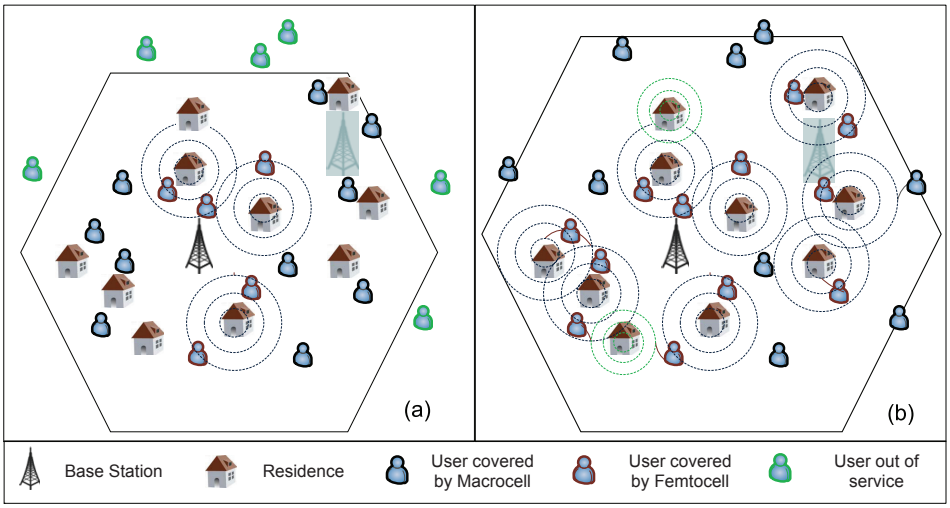

Fig. 3.2: A sketch showing the comparison of femtocell that are properly used, and over used: (a) An appropriate number of femtocells are installed. (b) Femtocells are over installed

Excessive femtocell adoption results in more redundant femtocells which will be switched to sleep mode. In the Figure 3.2(b), the small green rings represent the femtocells in sleep mode. When femtocells are over deployed, the embodied energy of a femtocell access point is not negligible. This will introduce unnecessary embodied energy, and increase the system power consumption again. On the other hand, over deployed femtocells cannot

improve the QoS in advance, as redundant femtocells are switched to sleep mode.

In light of the above, femtocells are able to provide a higher QoS, larger coverage area, and also reduce the macrocell system power consumption. However, how many femtocells should be deployed, what the optimal configuration for femtocells is, and how to know the performance of a specific femtocell deployment, are important questions that will be answered by the following sections.

Femtocell deployment is investigated in two scenarios. The first scenario considers a combined rural and urban area, where a mathematical model is proposed to represent a commuting scenario as described in [32]. A more complete system power consumption analysis is presented compared with [32]. This part of the work presents a large scale analysis. Furthermore, the femtocell deployment is analysed in an urban area, since the femtocell technique may be more beneficial for the scenario with a high density of residence and mobile usage. This part of the work is based on a geometric stochastic model, that provides an expected system power consumption based on a normalised scenario.

3.2 Combination of Rural and Urban Scenario

In this section, the effects of femtocell deployment on the current cellular network is investigated in a large scale environment including both a rural and urban scenario.

3.2.1 Simulation Set Up

In order to obtain some more realistic simulation results and to be able to compare with other published work, an accurate simulation scenario is required. One method to achieve this is to regenerate some simulations based on published references, that have used practical measured data in their work. [32] is utilised in this chapter for deriving an accurate simulation scenario.

The simulation parameters used in [32], are shown in Table 3.2.1.

The other assumptions are:

1. The user demand for the the scenario under investigation is based on measurements of voice traffic, extrapolated to the different operator market shares considered.

2. Simulated operator market share is 40%.
3. The home distribution is equivalent to the user distribution for evening demand.
4. Each femtocell access point has a power consumption of P_{femto}=15 W.
5. Each macrocell base station has a power consumption P_{macro}=2.7 kW.

Based on the above assumptions, the system energy consumption per annum (=8760 hours) can be written as

$$E_{\text{network}} = (n_{\text{macro}}P_{\text{macro}} + n_{\text{femto}}P_{\text{femto}})8760h \tag{3.1}$$

Parameter	Value
Scenario	10 km × 10 km
Population	200,000
Number of Homes	65,000
Proportion of Mobile Phone Users	95%
Average Usage of Cell Phone	37 hours per month[1]
User Demand Distribution	normal
Home Density Distribution	uniform
BS Bandwidth	5 MHz
Femtocell AP Coverage	100 m × 100 m
Operator Market Share	40%

Table 3.1: Reference Simulation Parameters

The simulation result from [32] is shown in Figure 3.3.

Since the reference simulation is based on measurements of voice traffic, and this data is not publicly available, the only way to regenerate the simulation result is to use a mathematical model to estimate the user demand distribution and home distribution.

It is assumed that normally mobile users use their mobile phones during the day time, and away from home (otherwise they may prefer to use a landline). When people are outside, they are more likely to be in the city centre (for working or for entertainment). Hence the user demand distribution can be seen as a 2-D normal distribution, and the peak point is the city centre, which is shown in Figure 3.4.

[1] the usage is assumed to be 740 minutes per user per month with an average call duration of 3 minutes

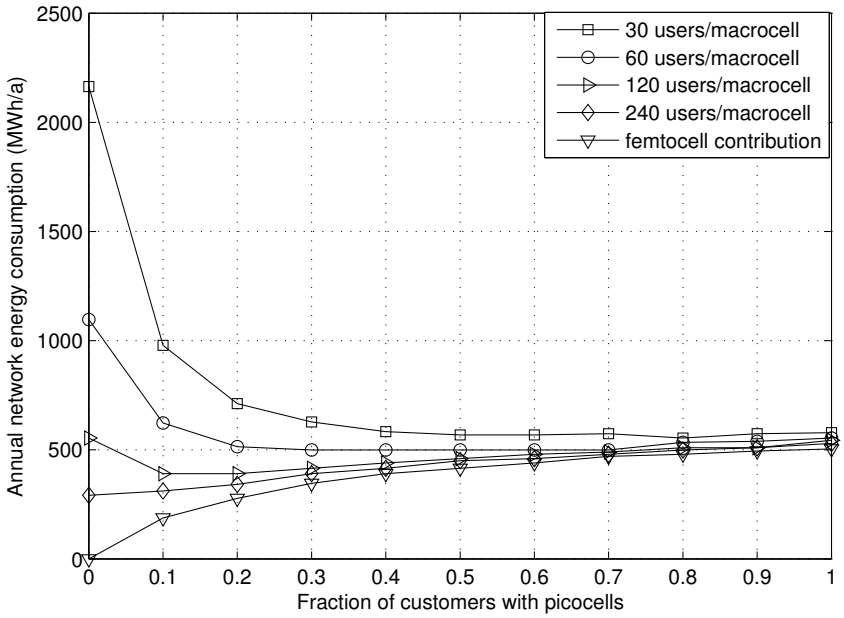

Fig. 3.3: Annual energy consumption of the network for an operator with 40% market share with different number of supported users per macrocell [32]

Considering the residence location, few people locate their home in the city centre, and also people don't like to live far away from the city centre for convenience. Hence, the home distribution can be considered as two or more 2-D normal distributions surrounding the city centre. 5 different home distribution models are simulated, and parameters are adjusted to provide a good match to the reference results. In the end, one home distribution model, which is composed of three normal distributions, produced the closest simulation results to the reference [32]. This home distribution is exhibited in Figure 3.5.

Figure 3.4 and 3.5 are plotted based on multivariate normal distribution, with 2-dimensional random vector $\mathbf{a} = [X, Y]$. The vector $\mathbf{a}$ represents the location of users or residences, which have $\mathbf{a} \sim \mathcal{N}(\boldsymbol{\mu}, \boldsymbol{\Sigma})$. Since X and Y are independent from each other, therefore, $\mathbf{a}$ also can be considered as 2-dimensional Gaussian distribution. The Probability Density Function

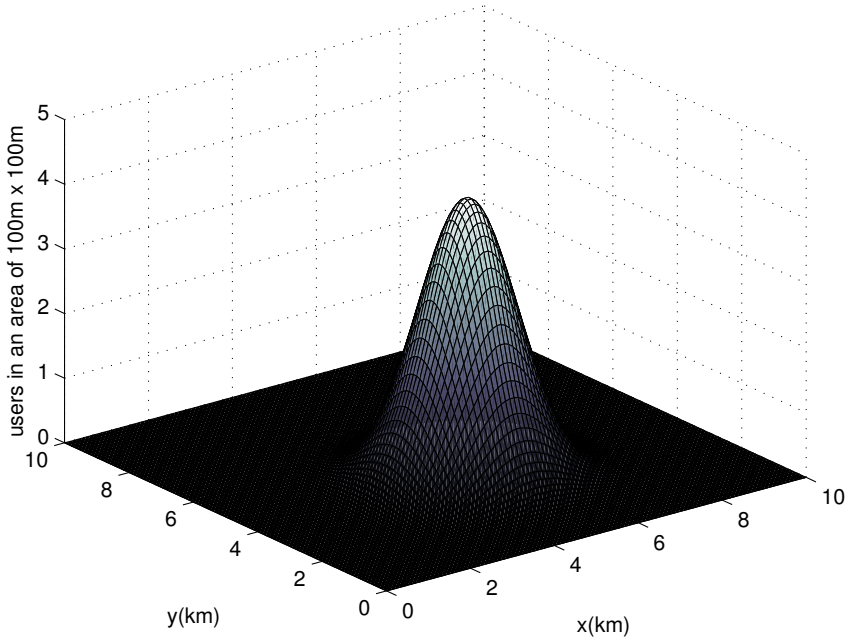

Fig. 3.4: User demand scenario for an operator with 40% market share

(PDF) of **a** can be expressed as:

$$f(x,y) = \frac{1}{2\pi\sigma_x\sigma_y} \exp\left(-\left(\frac{(x-\mu_x)^2}{2\sigma_x^2} + \frac{(y-\mu_y)^2}{2\sigma_y^2}\right)\right) \tag{3.2}$$

where μ_x and μ_y are the expected value of X and Y respectively, and σ_x and σ_y are the standard deviations. Hence, $\boldsymbol{\mu}$ and $\boldsymbol{\Sigma}$ can be obtained:

$$\boldsymbol{\mu} = \begin{pmatrix} \mu_x \\ \mu_y \end{pmatrix} \; ; \qquad \boldsymbol{\Sigma} = \begin{pmatrix} \sigma_x^2 & 0 \\ 0 & \sigma_y^2 \end{pmatrix} \tag{3.3}$$

The parameters applied in the simulation are listed in Table 3.2. The notation “0” for user distribution, and “1, 2, 3” for residences distributions.

Figure 3.6 shows the femtocell coverage results from reference [32] and the theoretical results on the mathematical models. For the femtocell coverage, the proposed model achieved similar results to the reference using real

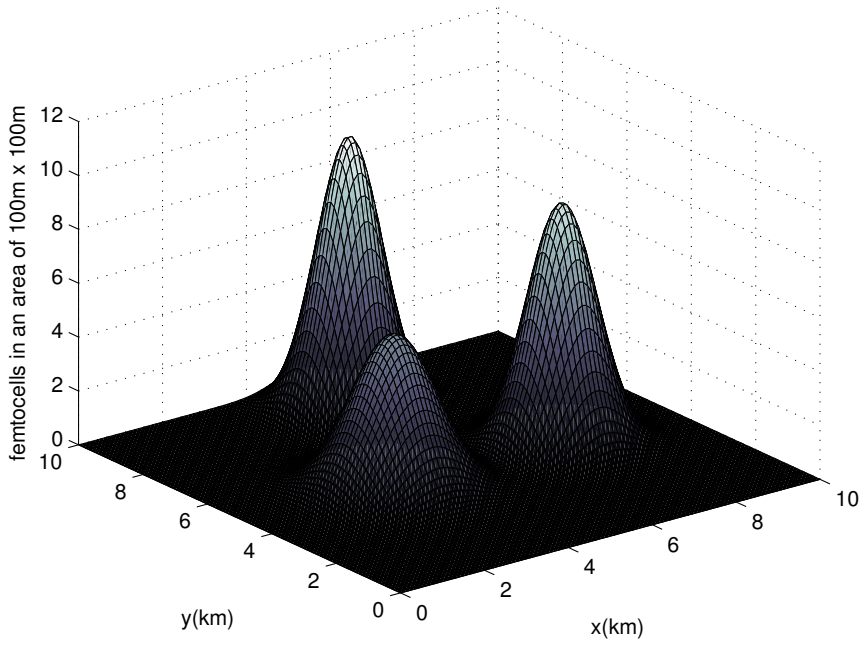

Fig. 3.5: A possible home distribution scenario

Table 3.2: 2-dimensional Gaussian Distribution Parameter

μ_{x0}	5	μ_{y0}	4	σ^2_{x0}	0.9	σ^2_{y0}	0.9
μ_{x1}	3	μ_{y1}	4.5	σ^2_{x1}	0.7	σ^2_{y1}	0.7
μ_{x2}	7	μ_{y2}	5	σ^2_{x2}	0.45	σ^2_{y2}	0.45
μ_{x3}	5	μ_{y3}	8	σ^2_{x3}	0.4	σ^2_{y3}	0.4

measurement data. Therefore, the proposed simulation scenario model is used for further simulations.

The system level analysis is based on the approximate model described above. The assumptions adopt the parameters which are from [32](Table 3.2.1), except for two that need to be modified.

Firstly, the value of the operator market share needs to be changed from 40% to 30%. In the UK, the top three communication operators' market share are: O_2 27.8%, Vodafone 25.86%, Orange 22.0% respectively [96]. Hence, 30% market share is more reasonable in the UK's situation.

Secondly, the simulation scenario model is based on 12 hours of day

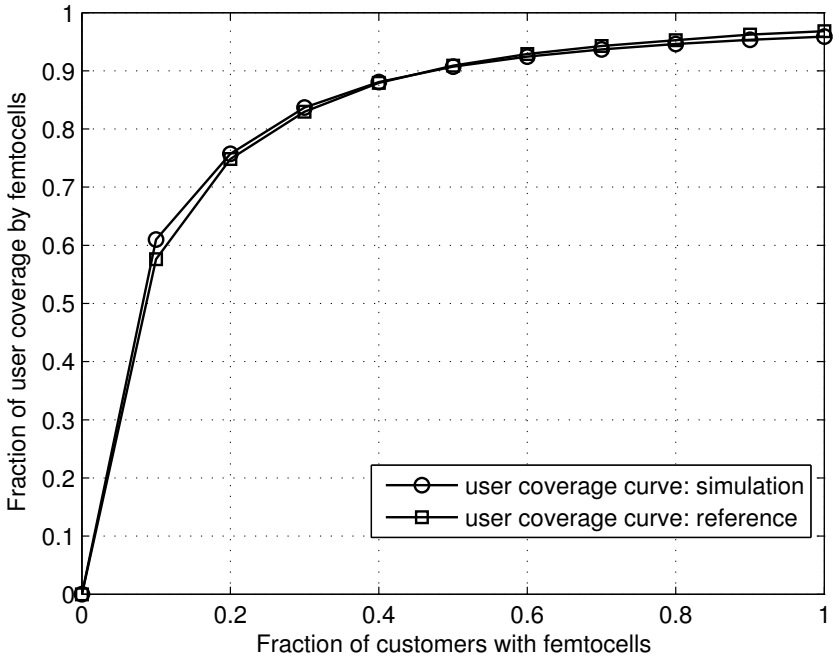

Fig. 3.6: Comparison of user coverage for 40% operator market share between reference and proposed model

communications (only voice service considered), and the average user has 0.5 hours cell phone usage per day [97]. Therefore, each mobile user's probability of being active is 0.5/12.

Based on the previous analysis, the system model and parameter assumptions can be summarised as follows:

The scenario area is 10 km×10 km, with a population of 200,000, of which 95% are mobile users. There are 65,000 homes located in this area. During the daytime, these active users' positions follow a normal distribution, and the peak point can be considered as the city centre. The distribution of femtocell access points has multiple peaks corresponding to residence distribution, with each concentration being normally distributed. In the UMTS system, each BS has three sectors, each with a bandwidth of 5 MHz. Therefore, for the highest requested data rate of 500 kbps, one BS can provide service for a maximum of 30 users. At lower data rates, more users can be supported. Each femtocell AP can provide service to a maximum of 8 users,

within a 100m×100m coverage. It is assumed that the market share of an operator is 30%. The parameters are enumerated in Table 3.3

Table 3.3: Simulation Parameters

Parameter	Value
Scenario	10 km × 10 km
Population	200,000
Number of Homes	65,000
Proportion of Mobile Phone Users	95%
Average Usage of Cell Phone	0.5 h/day [97]
User Demand Distribution	normal
Home Density Distribution	normal
BS Bandwidth	5 MHz
Femtocell AP Coverage	100 m × 100 m
Operator Market Share	30%
Minimun Capacity of Macrocell	30%

In the previous chapter, each component's operational power consumption and embodied energy have been presented, and explained. Based on the above assumptions, the power consumption for each user can be written as:

$$P_{\text{user}} = \sum_{i} \frac{n_i \times (C_i + O_i)}{n_{\text{user}}} \quad (i \in \{\text{BS}, \text{AP}, \text{MT}\}) \tag{3.4}$$

where BS, AP and MT represent the base station, access point and mobile terminal respectively. For instance, n_{BS} is the number of base stations in this system, and C_{AP} gives the embodied energy per second of a femtocell access point. The power consumption data for each equipment is listed in Table 3.4. $n_{\text{AP}}$is given by $n_{\text{homes}} \times \varphi \times 30\%$, where φ is the fraction of customers with a femtocell access point. n_{BS} is defined as $n_{\text{active\_user}}/u_{\text{BS}}$, with $n_{\text{active\_user}}$ being the remaining users who are not covered by any femtocells, and u_{BS} the number of users that each BS can support.

As mentioned in section 2.2, the MT's operational energy is not a constant value, it may change dramatically based on different transmission data rates and transmission distances, since the mobile will transfer its service from a long distance macrocell to a local femtocell. Therefore, Equation (2.3) is applied for the calculation of MT's operational energy:

$$O_{\text{MT}} = \frac{\beta \times d^{\alpha} \times R_t}{\varepsilon} + P_{\text{charger}} \tag{3.5}$$

Table 3.4: Cross Reference Table of Embodied Energy and Operational Power of each entity.

Facilities and Equipment	Life Time (years)	Lifetime Embodied Energy	Embodied Energy per sec(W)	Operational Power(W)
BS	∼10 years	∼300 GJ	∼1000 W (C_{BS})	∼1500 W (O_{BS})
Femtocell AP	∼5 years	162 MJ	∼ 1W (C_{AP})	6 W (O_{AP})
MT	∼2 years	162 MJ	2.6 W (C_{MT})	—

3.2.2 System Power Consumption

In this section, the power consumption results are presented. When femtocells are introduced, more wireless connections are transferred from macrocells to local femtocells, thus fewer base stations are required. At this point, there could be 2 scenarios: First, although theoretically fewer sites are required, the number of sites stays the same. Therefore, the femtocell techniques only reduce the operational power of the base stations, and the embodied energy of the base stations remain the same. Since the number of base stations stays the same, this scenario is called "Constant System". Second, the number of mobile customers has been increasing in the last 10 years, and there is no sign of this stopping [96]. In the extreme case, all new mobile customers get wireless service from femtocells. Therefore, extra base station installation will be avoided. It can be also considered that the base station's embodied energy and operational energy will be reduced as old base stations are not replaced. This scenario is called "Newly installed System".

Variable number of users per macrocell

In this section, it is assumed the capacity of a macrocell is variable, based on different QoS requirements and data rates. The investigated maximum number of active users per macrocell is set to one of 30, 60, 120 and 240.

In the constant system, the number of customers and BSs are fixed. Therefore, for the macrocells with different numbers of supported users, the numbers of required BSs are different. For example, in one system if each BS can support 30 users on average, then 79 BSs are required in this system; and if each cell can support 60 users on average, then only 40 BSs are required.

This means that when more users can be supported in a single cell, less BSs are required, reducing BS embodied energy. Figure 3.7 illustrates this point.

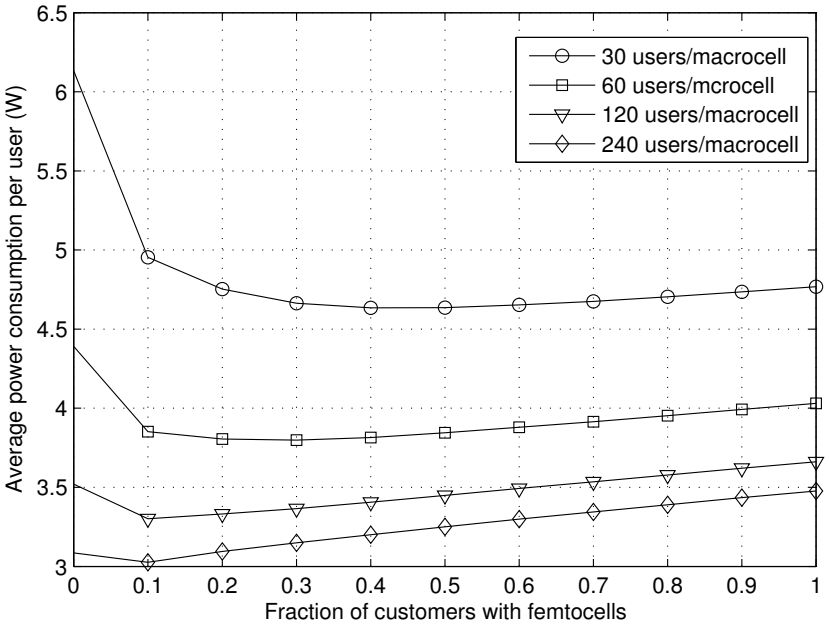

Fig. 3.7: Average power consumption per user for an operator with 30% market share with different number of supported users per macrocell in the constant system

Figure 3.7 also shows that, in the cases of each macrocell supporting 30, 60, 120 or 240 users, the system power consumption per user decreases when the fraction of femtocell owners increases up to a certain point, and then average power consumption grows with more femtocell installations.

On the other hand, in a newly installed system, if the number of BSs is reduced as femtocell installation increases, both the embodied and operational energy of the BS are reduced. The simulation result can be seen in Figure 3.8. It has some similar conclusions to Figure 3.7, in that a lower embodied energy of the AP results in an increased potential of power saving by deploying femtocells.

In practice, the communication system's performance will be between the constant system and the newly installed system. That means that as the number of users will continue to rise in the future, then a femtocell

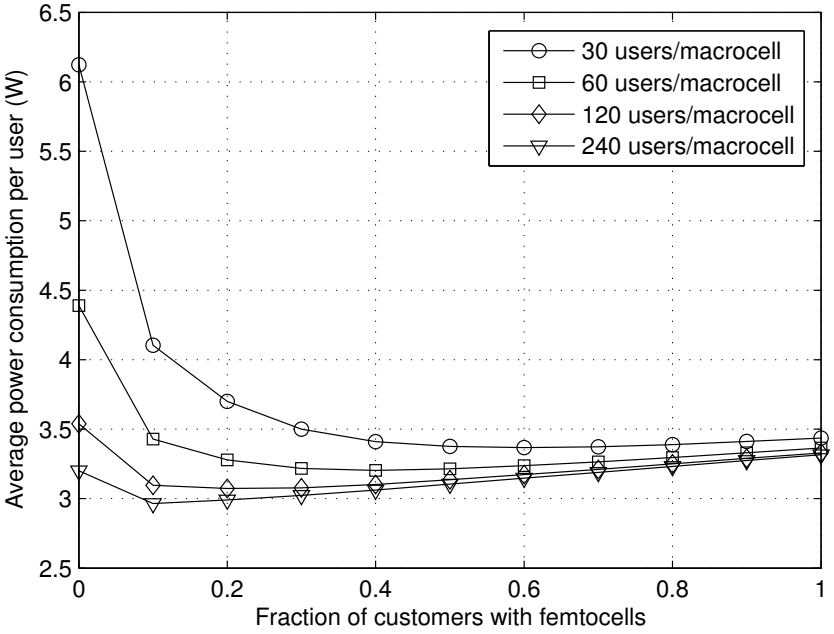

Fig. 3.8: Average power consumption per user for an operator with 30% market share with different numbers of supported users per macrocell in a newly installed system

implementation will avoid some extra BS installation; however, the number of mobile users may not track femtocell deployment, as in the newly installed system. When comparing Figure 3.7 and Figure 3.8, two conclusions can be drawn: firstly, as the number of users increase, higher power reduction ratio can be achieved. For instance, assume the macrocell has a capacity of 30 users, in the constant system (Figure 3.7), the highest power reduction ratio of the macrocell is 15%, and in the developing system (Figure 3.8) this figure is 29%. Secondly, when the number of users increases, the system with macrocells supporting fewer users tends to have more power saving potential. For example, for the 30 users macrocell, from the constant system to the developing system, the highest power reduction has been increased from 15% to 29%. However, for a 240 user macrocell, the highest power reduction ranges from 3.3% to 10%.

Fixed number of users per macrocell

The previous section's analysis focused on the different macrocell systems with different levels of mobile user. In order to develop a more specific analysis of the UK's communication system, the following conditions are considered. The number of active mobile user connections in the UK is 126.1 per 100 population [96] at the end of 2008. The UK's resident population is 60,975,000, as obtained from the National Statistics website. Therefore, the number of mobile phone subscriptions is approximately 76,900,000 in the UK. Assuming that each mobile is used for 30 minutes during a day time period of 12 hours [97], the number of simultaneous mobile users in the UK is 3,200,000. Note that at the start of 2009 there were approximately 51,300 base station sites in the UK. Hence, on average, each base station provides services for around 60 users at the same time. The next section is developed based on this assumption. Although the UK's situation is adopted as an example for the evaluation, a more generic conclusion is given in this section's summary.

Figure 3.9 and Figure 3.10 distinguish each component of power consumption contribution per user from the previous results, based on the constant system and the newly installed system respectively. It can be seen that the system's power consumption per user comes from the base station (BS), the femtocell access point (AP) and the mobile terminal (MT). For each component, the power consumption is composed of both lifetime embodied power and operational power consumption.

Figure 3.9 shows the constant system's power consumption composition. The BS's embodied energy contribution per user is constant, which is expected since the number of BSs is constant. However, as the number of users with femtocells grows, the operational power consumed by BSs decreases dramatically. At the same time, both the femtocell access point's embodied energy and operational power consumption contribution rise, since more femtocells are installed and more embodied and operational energy is introduced into the system. Nevertheless, the increased amount of power consumed by the femtocells is less than the power saving of the BS. Therefore, the overall power consumption is reduced when compared with no femtocell implementation. For mobile terminals, as the main power contribution is from embodied energy, which is 2.6 W per user, the increasing number of femtocells has a minor impact on the MT's power consumption.

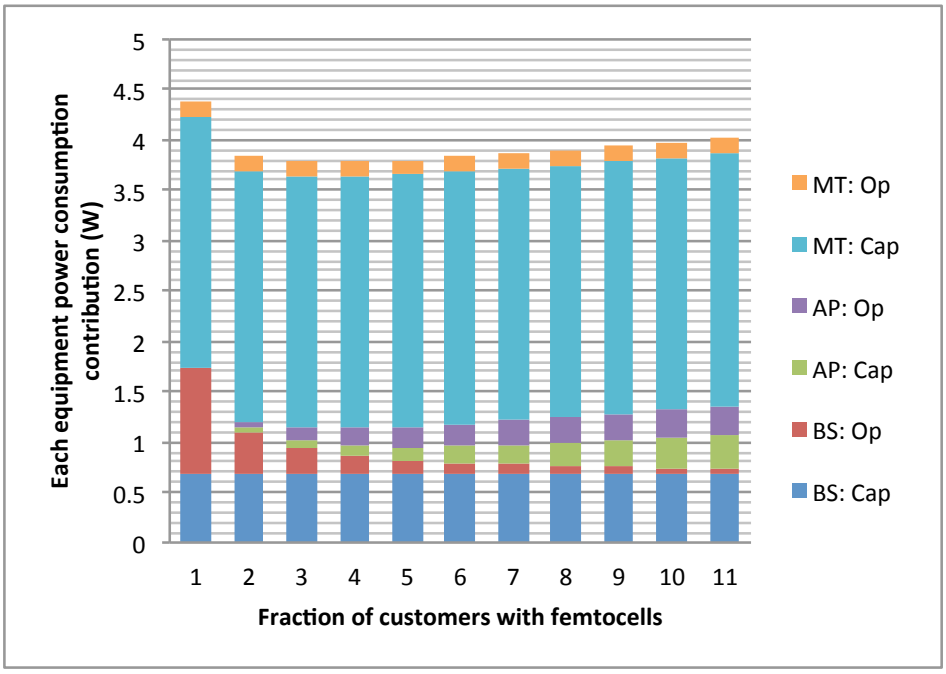

Fig. 3.9: Power consumption of each network component per user in the constant system when different fraction of users operate femtocells

It can also be seen in Figure 3.9 that when the femtocell installation rate is 30%, the constant system obtains the lowest power consumption level. The Energy Reduction Gain (ERG) can be calculated as follows:

$$ERG = \frac{P_0 - P_1}{P_0} = 1 - \frac{P_1}{P_0} \tag{3.6}$$

where P_0 is the original system power consumption prior to the femtocell architecture being employed; and P_1 represents the system power consumption at the lowest point on the curve. Hence, the power reduction ratio with 30% customers installing a femtocell is 13.7%.

Figure 3.10 shows the developing system's power consumption composition. The AP and MT have similar trends to the constant system. However, in the developing system, when the number of mobile users is increasing, and the requirement for extra BSs is avoided since the increased mobile users obtain the communication service from a local femtocell. Hence, from the whole system's point of view, the power consumption contribution of

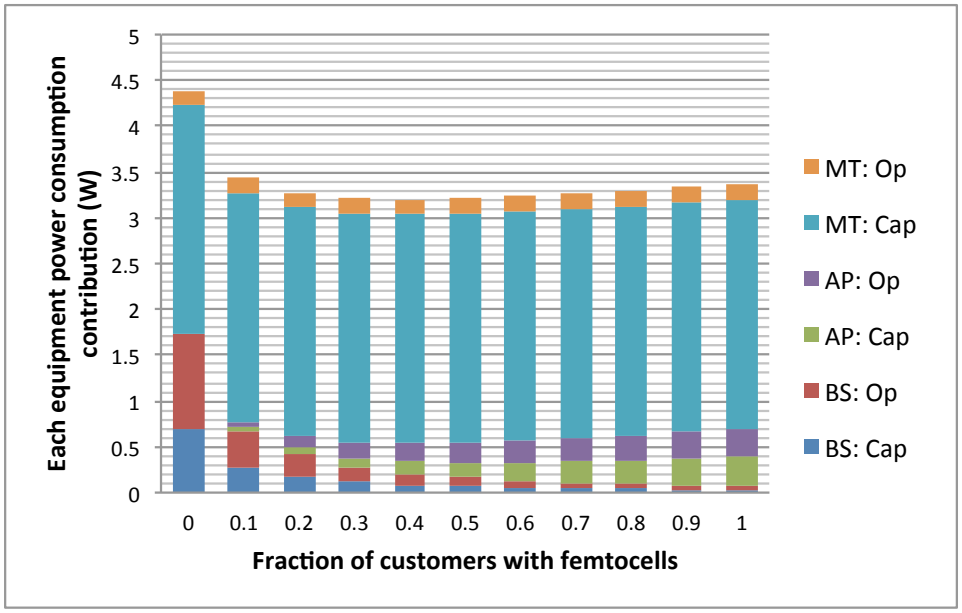

Fig. 3.10: Power consumption of each network component per user in the developing system when different fraction of users operate femtocells

the BS's embodied energy per user decreases. Therefore, the developing system is likely to achieve a higher power reduction ratio. By employing Equation (3.6), the developing system power ratio is 27.3% when 40% of customers are using the femtocell service.

Comparing Figure 3.9 and Figure 3.10, there are three conclusions that can be drawn: first of all, the most notable difference between these two system is the different values of BS embodied energy contribution. Second, the developing system has a higher power saving potential, and achieves a higher power reduction ratio. Finally, the constant system achieves the lowest power consumption per user point at an installation factor of 30%, and the point for a newly installed system is at 40%.

In the previous simulations, each femtocell AP can support a maximum of 8 users. However, in real life, femtocell APs with different capacities are available. Moreover, the capacity of femtocells can impact on both the system power consumption and the QoS . In this section, femtocells able to support 4, 8, 12 or 16 users will be studied. The system power consumption comparisons with these scenarios are implemented. Since the wireless communication system is in the rapid developing phase, the developing scenario

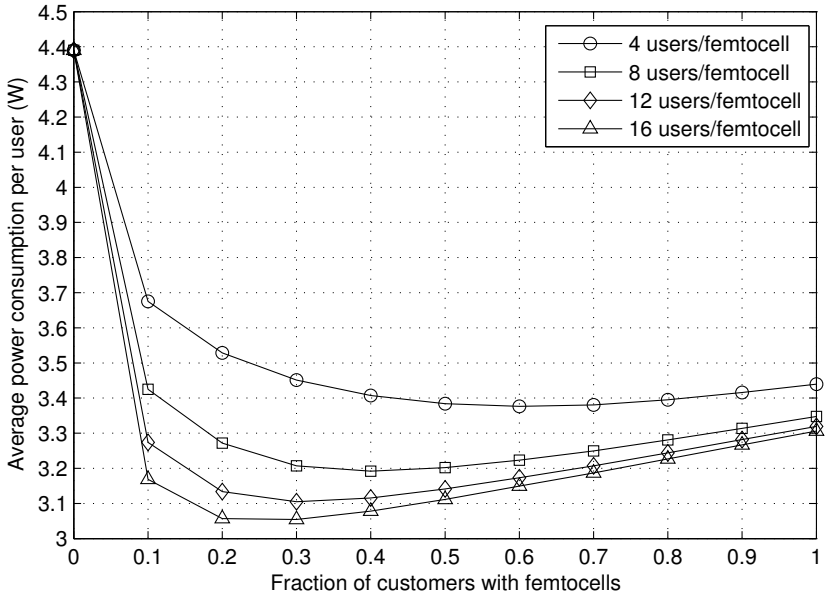

Fig. 3.11: Average power consumption per user for the different capacities of femtocells in the newly installed system

is taken for analysis in this section.

Figure 3.11 shows the system power consumption per user curves with different femtocell capacities. It can be seen that, as the number of users per femtocell increases, more power can be saved. The power saving can be viewed from two approaches. First, if one femtocell has a lower capacity, for instance each femtocell can only support a maximum of 4 users, and there are more than 4 users requiring the communication service, the local femtocell cannot fulfil all the demands of the users, and the additional users still need to connect with a macrocell. Therefore, the long distance transmission between a user and a macrocell leads to a high power consumption. On the other hand, if each femtocell can offer services to a larger number of users, the neighbouring femtocell is not required since one femtocell can cover all the active users in this area. Hence, the neighbouring femtocell can be switched into sleep mode, and more operational power has been saved.

It should be mentioned that, Figure 3.11 (even along with Figure 3.7, 3.8) shows a potential for system power consumption to be modelled and analysed with a convex function. However, these results are based on specific

distributions of users and homes, which was generated to achieve a good match for a real city scenario. Therefore, this figure refers to one scenario of users, and it is difficult to generalise it using an analytical framework.

Based on Figure 3.11, indifference curves are produced in Figure 3.12. Each curve represents a different power consumption level. These curves show the tradeoff between the femtocell capacity and the fraction of femtocells. For example, if there is a strict requirement for power consumption, e.g. 3.2 W per user, this target can be achieved by implementing a 20% femtocell installation with a 10 user capacity per femtocell, or a 30% femtocell installation with a 8 user capacity per femtocell.

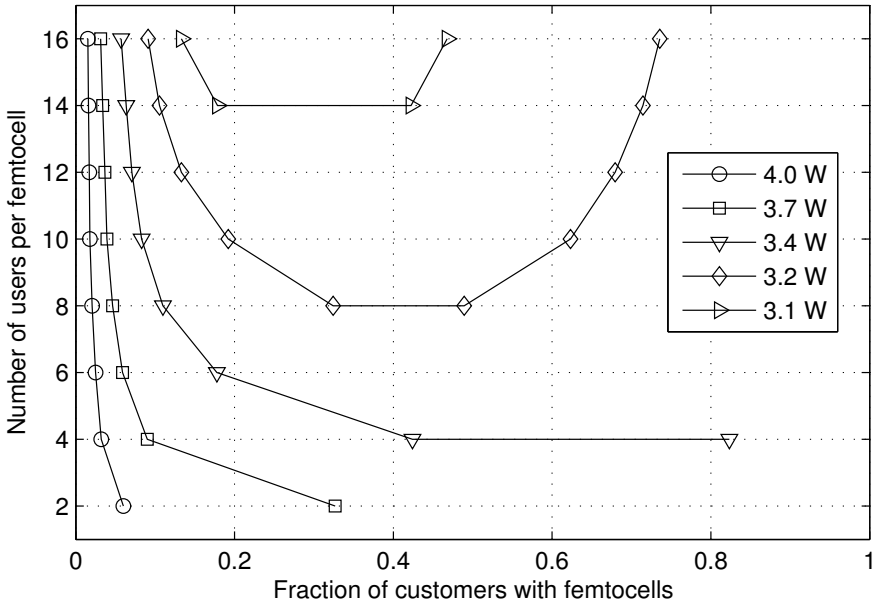

Fig. 3.12: The average power consumption indifference curves for the tradeoff between femtocell's installation and femtocell's capacity in the developing system

The indifference curve figure can be considered as an executive guide. One possible usage is with regard to the future implementation decision: a certain power consumption level is given, and the combinations of different femtocell installation rates and different femtocell capacities will provide a couple of options for the system implementation.

3.2.3 System Transmission Bandwidth

After analysing the system's power consumption, QoS is another very important issue that needs to be considered. The system bandwidth is considered as the most conventional QoS parameter. However, the bandwidth measure is relatively complex [90]. As the data transmission is in the form of packets or chunks, the bandwidth value is not constant. Hence, the overall average bandwidth is normally used as the bandwidth parameter. Therefore, in this section, the average transmission bandwidth of a user is simulated, based on variable and fixed number of users per macrocell respectively.

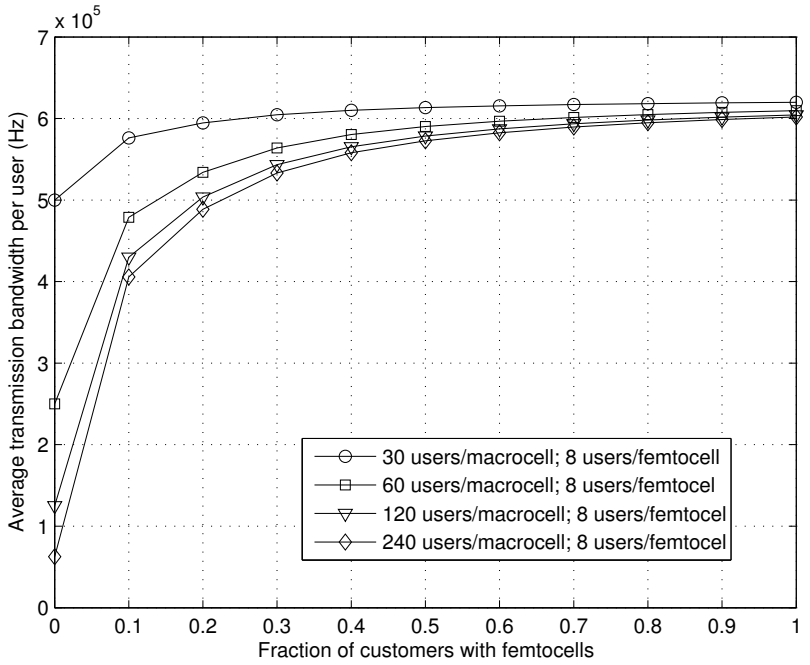

Fig. 3.13: Average power consumption per user for the different capacities of femtocells in the developing system

Variable number of user per macrocell

Assuming that for four different levels of BS support, each macrocell can provide voice/data services to 30; 60; 120 and 240 users respectively. It is assumed that each femtocell can offer communication service for up to 8 users. It can be seen from Figure 3.13 that, when there are no femtocells, the four different levels of macrocells can provide maximum average

transmission bandwidth of 500 kHz; 250 kHz; 125 kHz and 62.5 kHz. As femtocell installation increases, the transmission bandwidth per user rises as well. This is because more femtocells will cause more mobile users to transfer their connections from the macrocell to the local femtocell, and each user can obtain 625 kHz in a femtocell. When the fraction of femtocell utilisation is close to 100%, then almost all mobile users are covered by femtocells. Therefore, the average transmission bandwidth is near 625 kHz.

In Figure 3.13, it is also notable that when 20% of customers have femtocell service, for four different levels of BS support, the bit rate has been increased to 595 kHz, 534 kHz, 504 kHz and 489 kHz. It means the data rate increases by a factor of 19%, 114%, 303% and 682% respectively. Hence, the macrocell with a larger number of users has a higher potential of average transmission bandwidth.

Fixed number of users per macrocell

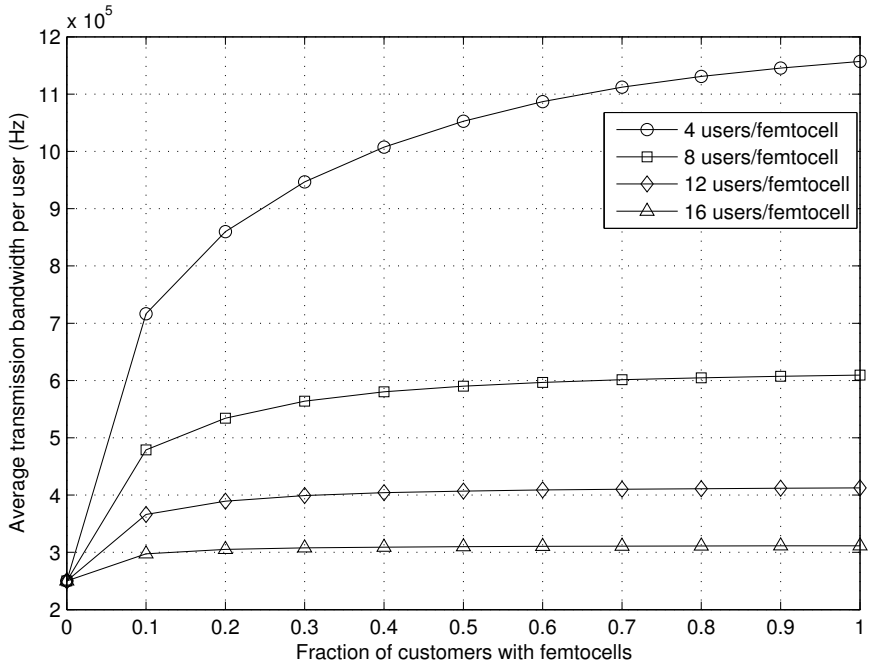

Fig. 3.14: Average transmission bandwidth per user for the different capacities of femtocells

In this section, the number of users in a macrocell is constant (60 users/mac-

rocell), and the femtocell's capacity is variable.

Figure 3.14 depicts the different transmission bandwidth levels caused by the different femtocell capacities. It is assumed that they are all UMTS femtocells, each femtocell can offer 5 MHz bandwidth in total [119]. Hence, if one femtocell can support 4 users, then each user is allocated 1.25 MHz bandwidth. By the same token, for 8 users a femtocell can offer 625 kHz bandwidth for each user, etc. Therefore, along with the increase of femtocell utilisation, the fewer users that each femtocell has to support, the higher the average transmission bandwidth the system can achieve.

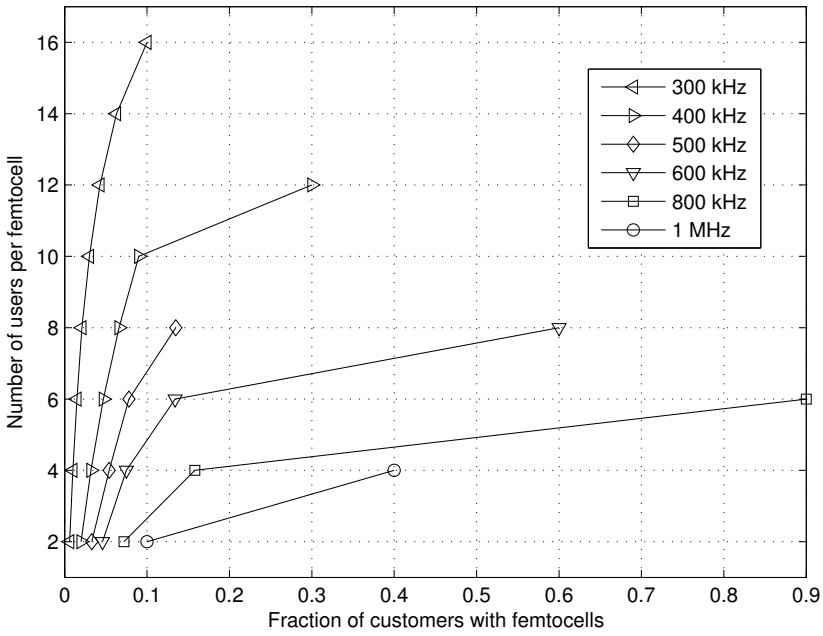

Fig. 3.15: The average transmission bandwidth indifference curves for the trade-off between femtocell's installation and femtocell's capacity

Based on Figure 3.14, the indifference curves of the average transmission bandwidth can be plotted, as shown in Figure 3.15. The bandwidth indifference curves can be used along with power consumption indifference curves, in Figure 3.12. There is an example when describing Figure 3.12 that, a femtocell with a capacity of 10 users with a femtocell deployment rate of 20% has the same system power consumption as a femtocell with a capacity of 8 users with a 30% deployment rate. Considering these two

points in Figure 3.13. The previous system can provide 400 kHz bandwidth for each user on average. However, the second system can provide 500 kHz bandwidth on average. It means that two or more systems with the same system power consumption offer different bandwidths; on the other hand, for a certain bandwidth provision, the system may operate at different power consumption levels. From the customer's point of view, QoS is the main priority, hence, they will prefer a certain level of bandwidth provision. From the operator's point of view, they may care more about the expense of power consumption, hence, based on a certain QoS provision, a more power efficient system will be selected, based on both power consumption and bandwidth indifference curves.

3.2.4 Cooperative Analysis of Power Efficiency and Bandwidth

In the previous two sections, the system power consumption and the average transmission bandwidth are investigated using indifference curves.

Figure 3.12 and Figure 3.15 shows the simulation results. In these figures, each curve represents a certain power consumption level or QoS level. Figure 3.12 and Figure 3.15 provide figures for balancing these two requirements. For instance, if the power consumption is limited to 3.2 W per person as a maximum, different combinations of femtocell densities and femtocell adoption rates are possible. Based on these combinations, the offered bandwidth is different. When one femtocell can support a maximum of 16 users and 10% of customers have femtocell APs, the power consumption per person is 3.2 W (Figure 3.12), and the average transmission bandwidth is 300 kHz (Figure 3.15). Comparatively speaking, note that a system with 8 user femtocells and 30% femtocell uptake, this combination still achieves a 3.2 W power consumption level, however, the transmission rate is greater than the previous case, and is around 500 kHz. This shows that, based on a certain power consumption or a certain level of QoS requirement, the optimal deployment strategy strongly relies on the operator market share, femtocell uptake and the capacity of femtocells. The femtocell technique can be used for both power efficiency and QoS upgrading, if appropriate planing is implemented.

3.3 Urban Scenario

In this section, an urban scenario is taken into consideration, that has a high density of mobile users and residences. The femtocell deployment scenarios are placed into three categories: the original macrocell cellular network, before the femtocell technique is introduced into the system, is called the baseline system, for comparison purposes with the following two scenarios; when the femtocell technique is adopted, and few femtocells are deployed is the second scenario; the final scenario describes when the femtocell technique is mature, and femtocells are ubiquitously used. The system power consumption is analysed based on these three scenarios respectively.

3.3.1 Baseline System

In the baseline system, it is assumed that in a macrocell coverage, N_u active users are uniformly distributed within this area. The embodied energy per unit area for this scenario can be calculated by:

$$\overline{P}_{\text{cap},0} = \frac{C_{\text{BS}} + N_u \cdot C_{\text{MT}}}{\mathcal{A}} \tag{3.7}$$

where C_{BS} and C_{MT} are the single macrocell base station (BS) and mobile terminal (MT) embodied energy respectively. $\mathcal{A}$ is the single macrocell coverage. By using a hexagon shape to model the macrocell coverage, and assuming the radius is R_{BS}, the coverage area can be obtained:

$$\mathcal{A} = \frac{3\sqrt{3}}{2} R_{\text{BS}}^2 \tag{3.8}$$

Correspondingly, the operational energy per unit area can be obtained as:

$$\overline{P}_{\text{op},0} = \frac{O_{\text{BS}} + \sum_{i=1}^{N_u} O_{\text{MT},i}}{\mathcal{A}} \tag{3.9}$$

The operational energy consumption of a macrocell base station can be classified by two modes: one is active mode, when a macrocell BS is transmitting; the other one is idle mode, when a macrocell BS is not transmitting. The equation is given as:

$$O_{\text{BS}} = \begin{cases} P_{\text{BS}}/\epsilon_{\text{BS}} + \delta_{\text{BS}}, & \text{BS transmitting} \\ \delta_{\text{BS}}, & \text{BS not transmitting} \end{cases} \tag{3.10}$$

For the active mode, the BS power consumption consists of transmission power, divided by the power conversion efficiency, which is denoted as ϵ_{BS}, accounting for the power amplifier efficiency, feeder loss and extra loss related to cooling etc; and other power consumption δ_{BS}, which is independent of the transmission function of a BS, including circuit power for signal processing, battery backup, etc. When a macrocell BS is switched to an idle mode, the BS only consumes the δ_{BS}, keeping parts of the BS running, in order to wake the BS to an active mode as soon as it is necessary.

Since the active users are uniformly distributed, the aggregation of all users' transmission power can be approximated by the expected value of an active user multiplied by the number of active users in this area. Therefore, (3.9) can be substituted as:

$$\overline{P}_{\mathrm{op},0} = \frac{O_{\mathrm{BS}} + N_u \cdot \mathbf{E}[O_{\mathrm{MT},i}]}{\mathcal{A}} \tag{3.11}$$

where $\mathbf{E}[O_{\mathrm{MT},i}]$ is given by:

$$\mathbf{E}[O_{\mathrm{MT},i}] = \frac{\beta \cdot \mathbf{E}[d^{\alpha}] \cdot R_t}{\epsilon_{\mathrm{MT}} \epsilon_{\mathrm{char}}} \tag{3.12}$$

where β is a constant of proportionality, with the value 0.2 $\mathrm{fJm}^{-\alpha}$ [87], d is the distance between the transmitter and the receiver, α is the path loss exponent. For an urban scenario this value is in the range of $2.7 \sim 3.5$. In this work $\alpha = 3$. R_t represents the data transmission rate, ϵ_{MT} is the efficiency of the MT, and ϵ_{char} is the MT's charger efficiency. It should be noted that, since the usage of various applications and different customer preferences, the power consumed besides voice and data transmission, such as the power consumed by offline gaming, using the camera, and playing music, is not counted into this analysis.

In order to achieve the expected value of $O_{\mathrm{MT},i}$, the expected value of d^{α} should be calculated. First of all, we model a hexagonal as a circle of radius R_m, where $R_m = (\frac{3\sqrt{3}}{2\pi})^{\frac{1}{2}} \cdot R_{\mathrm{BS}}$.

Since active users are uniformly distributed within this area, the probability function describing the distance between one user and the BS is:

$$\Pr(d) = \frac{2d}{R_m^2} \tag{3.13}$$

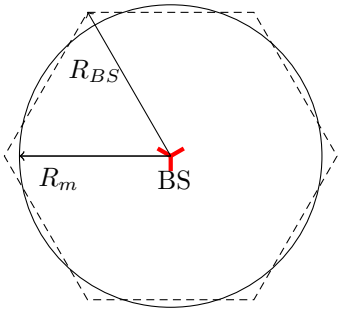

Figure 3.16: Scenario sketch of macrocell

when $\alpha = 3$, the probability of d^3 can be expressed as:

$$\Pr(d^3) = \frac{2}{3} \cdot \frac{1}{R_m^2 \cdot d} \tag{3.14}$$

Using the $t = d^3$ substitution, the expected value of d^3 is given as:

$$\mathbf{E}[d^3] = \mathbf{E}[t] = \int_0^{R_m^3} t \cdot \frac{2}{3} \cdot \frac{1}{R_m^2 \cdot t^{\frac{1}{3}}} dt = \frac{2}{5} R_m^3 \tag{3.15}$$

3.3.2 When a few femtocells are deployed

In a scenario where a few femtocells are introduced into the cellular system, the system embodied energy and operational energy are all affected, and expressed as follows.

Considering the embodied energy, only the extra N_{AP} femtocells' embodied energy is added compared with (3.7). It can be expressed as:

$$\overline{P}_{\mathrm{cap},f} = \frac{C_{\mathrm{BS}} + N_u \cdot C_{\mathrm{MT}} + N_{\mathrm{AP}} \cdot C_{\mathrm{AP}}}{\mathcal{A}} \tag{3.16}$$

On the other hand, the system operational energy consumption comprises three parts, BS, femtocell AP and user MT. Due to the deployment of femtocells, more active users are able to be switched to a local femtocell. BS's operational power will all decrease because fewer mobile users need to be supported compared with the baseline system. At the same time, MTs' transmission power will decrease as well, due to the shorter transmission distance to a local femtocell. The calculation of system operational energy

consumption is given as:

$$\overline{P}_{\mathrm{op},f} = \frac{O_{\mathrm{BS}} + \sum_{i=1}^{N_u} O_{\mathrm{MT},i} + O_{\mathrm{AP},1} + O_{\mathrm{AP},2}}{\mathcal{A}} \tag{3.17}$$

It is assumed that each femtocell is able to switch between two modes, ACTIVE and IDLE. The term IDLE describes the mode of operation of the femtocell when its radio transmissions are switched off due to the proposed scheme, and ACTIVE is when they are switched on. In (3.17), $O_{\mathrm{AP},1}$ denotes the power consumption of active femtocells, and $O_{\mathrm{AP},2}$ denotes the idle ones.

In this work, one femtocell switch-off scheme is proposed. Figure 3.17 shows the flowchart of this scheme. First of all, when a femtocell is initially installed, the default mode is IDLE. At this stage, the signal transmission and processing functions are switched off. The "sniffer" function is operating, in order to detect the macrocell uplink signal strength, to decide whether there is an eligible active user that can be handed over to this femtocell. If there are no active users located within its coverage area, this femtocell stays in the initial IDLE mode. Then, the "sniffer" detects the signal strength from the downlink of the nearest neighbouring femtocell. If the signal strength is stronger than the detection threshold, it means the neighbouring femtocell is likely to be located very close to the current femtocell, and able to provide the service for the active users covered by this femtocell. Therefore, this femtocell stays in the IDLE mode. Otherwise, this femtocell is switched to an ACTIVE mode.

Considering the mathematical model, when N_u active users and N_{AP} femtocells are all uniformly distributed within a macrocell coverage, and each femtocell with a target coverage radius of R_f, the probability of exactly k users located within a femtocell coverage can be modelled by Poisson Point Process (PPP), with parameter $\rho_u \cdot v_f$. Here ρ_u is the active user density in a macrocell, and v_f is one femtocell's coverage. Hence, the probability is given as:

$$\mathbf{P_r}(K = k) = \frac{(\rho_u \cdot v_f)^k}{k!} \cdot e^{-\rho_u \cdot v_f} \tag{3.18}$$

Therefore, the probability of one femtocell deployment with active users is $[1 - \mathbf{P_r}(K = 0)]$. Figure 3.18 shows a realisation of a Possion Point Process with k nodes and 4 femtocells.

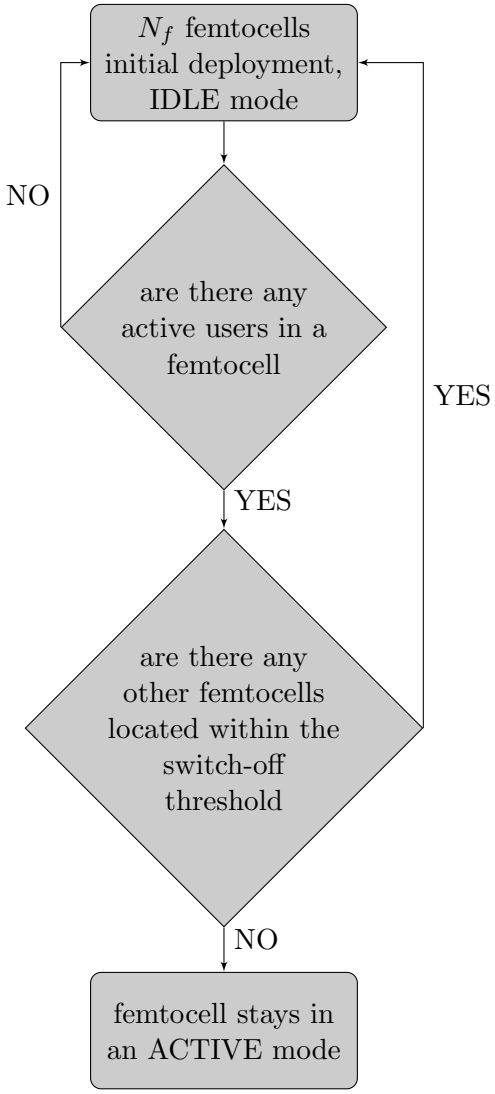

Figure 3.17: Flowchart of the proposed IDLE mode procedure for a femtocell BS

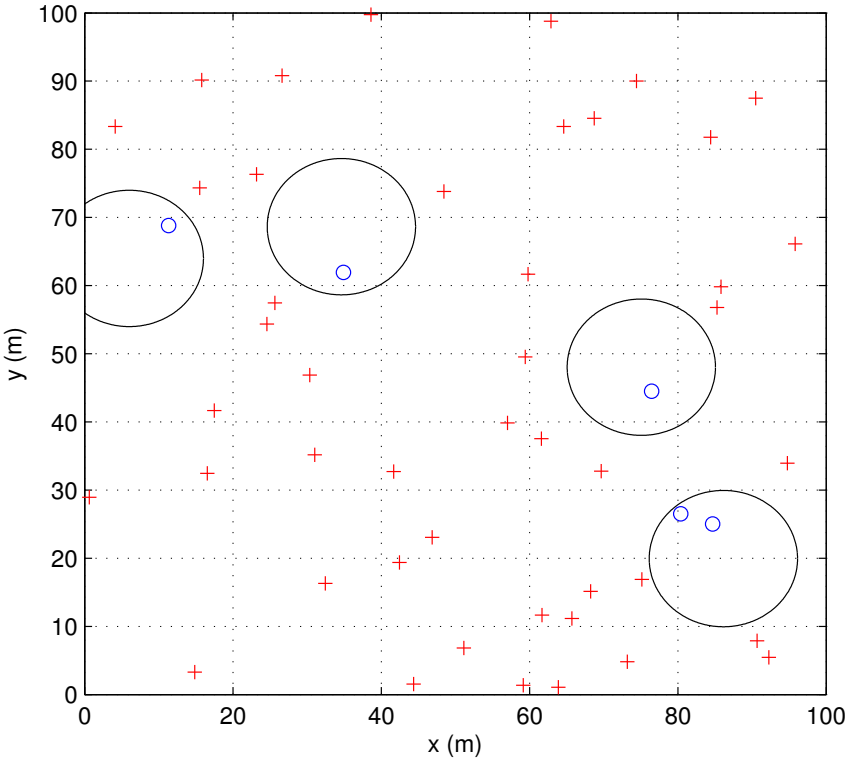

Figure 3.18: A realisation of Possion Point Process with k nodes and 4 femtocells.

The detection threshold between two nearest active femtocells should be decided. Assume that each femtocell downlink signal has the same signal propagation environment, then the switch off threshold can be expressed as the distance between two femtocells. Therefore, the distance between two neighbouring femtocells r is estimated in the following proposition.

Lemma 3.3.1 *Provided that, there are femtocells deployed within a certain area, with a density of ρ_f. The distance between two nearest femtocells, r, has the probability density function (PDF) and cumulative distribution function (CDF) as follows respectively:*

$$P_{\mathcal{R}}(r) = 2\pi r\rho_f \cdot e^{-\pi r^2 \rho_f}; \qquad F_{\mathcal{R}}(r) = 1 - e^{-\pi r^2 \rho_f} \tag{3.19}$$

The probability density function of the distance r between two nearest fem-

tocells follows a Rayleigh distribution, $r \sim Rayleigh(\sigma)$, where $\sigma^2 = \frac{1}{2\pi\rho_f}$. $P_{\mathcal{R}}(r < \tau)$ indicates the probability of femtocells to be switched to an idle mode, due to the neighbouring femtocell located within the threshold distance τ.

Proof The probability of the distance between two nearest femtocells can be described as, the probability that no femtocells exist interior to r times the probability that a femtocell does exist in the distance of $r + dr$. Therefore, it can be expressed as:

$$P_{\mathcal{R}}(r) = [1 - \int_0^r P_{\mathcal{R}}(r)dr] \cdot 2\pi r\rho_f \tag{3.20}$$

Therefore, it can be turned into a homogenous linear differential equation:

$$\frac{\mathrm{d}}{\mathrm{dr}}[\frac{P_{\mathcal{R}}(r)}{2\pi r\rho_f}] = -2\pi r\rho_f \cdot \frac{P_{\mathcal{R}}(r)}{2\pi r\rho_f} \tag{3.21}$$

By solving this equation, the $P_{\mathcal{R}}(r)$ can be easily obtained.

Based on the previous two criteria, the operational power consumption of active femtocells and idle femtocells are calculated as follows respectively:

$$O_{\mathrm{AP},1} = N_{\mathrm{AP}} \cdot P_{\mathrm{AP}} \cdot [1 - \mathbf{P_r}(K = 0)] \cdot [1 - P_{\mathcal{R}}(r < \tau)] \tag{3.22}$$

$$O_{\mathrm{AP},2} = N_{\mathrm{AP}} \cdot \delta_{\mathrm{AP}} \cdot \{1 - [1 - \mathbf{P_r}(K = 0)] \cdot [1 - P_{\mathcal{R}}(r < \tau)]\} \tag{3.23}$$

In the above equation, P_{AP} and δ_{AP} represent the operational power consumption for an active femtocell and an idle femtocell respectively. The power model is given by [98], and each hardware components energy consumption is listed in Table 3.5.

Integrating all hardware component power consumption, P_{AP} is equal to 12 W, including 85% power efficiency of the power supply. By switching to an idle mode, the femtocell BS switches off the PA, RF transmitter, RF receiver, and miscellaneous hardware components related to non-essential functionalities in the IDLE mode, such as data encryption, hardware authentication, etc. However, a low-power radio sniffer ($P_{\mathrm{sniff}} = 0.3$ W) is switched on to provide received power measurements on the macrocell uplink band. Therefore the operational energy consumption for a idle mode

Table 3.5: Energy Consumption Profile of Femtocell Hardware

Hardware Component	Energy Consumption (W)
Microprocessor	1.7
Associated Memory	0.5
FPGA	2.0
Associated Memory	0.5
Other Circuitry	2.0
RF Transmitter	1.0
RF Receiver	0.5
RF Power Amplifier	2.0

is:

$$\begin{aligned}\delta_{\mathrm{AP}} &= P_{\mathrm{AP}} - [(P_{\mathrm{PA}} + P_{\mathrm{TX}} + P_{\mathrm{RX}} + P_{\mathrm{misc}}) - P_{\mathrm{sniff}}]/0.85 \\ &= 12 - [(2.0 + 1.0 + 0.5 + 1.0) - 0.3]/0.85 = 7.0\,\mathrm{W}\end{aligned} \tag{3.24}$$

In Equation (3.17), $\sum_{i=1}^{N_u} O_{\mathrm{MT,i}}$ is the aggregation of operational energy consumption of all active users, including users covered by a macrocell and by a femtocell. Due to the different signal transmission distance and different data rate in macrocell and femtocell coverage, Equation (3.15) can be modified correspondingly. The number of users served by femtocells based on the mathematical model is:

$$N_{u,f} = N_{\mathrm{AP}} \sum_{k=1}^{k\to\infty} k \cdot \mathbf{P_r}(K = k) \tag{3.25}$$

Hence, the number of macrocell users is $N_{u,m} = N_u - N_{u,f}$. When $k > 5$, the value of $\mathbf{P_r}(K = k)$ is extremely small, and can be neglected. Therefore, we assume that the maximum capacity of a femtocell is 4 users, and in the simulation the maximum value of k is taken as 4. The $\sum_{i=1}^{N_u} O_{\mathrm{MT},i}$ can be replaced as:

$$\sum_{i=1}^{N_u} O_{\mathrm{MT},i} = N_{u,f} \cdot \frac{\beta \cdot \mathbf{E}[d_f^{\alpha}] \cdot R_{t,f}}{\epsilon_{\mathrm{MT}}\epsilon_{\mathrm{char}}} + N_{u,m} \cdot \frac{\beta \cdot \mathbf{E}[d_m^{\alpha}] \cdot R_{t,m}}{\epsilon_{\mathrm{MT}}\epsilon_{\mathrm{char}}} \tag{3.26}$$

where d_f is the distance between a femtocell user and its local femtocell, and $\mathbf{E}[d_f^3] = \frac{2}{5}R_f^2$ can be obtained based on the same methodology as Equation (3.15).

As described above, the BS's operational energy consumption deceases

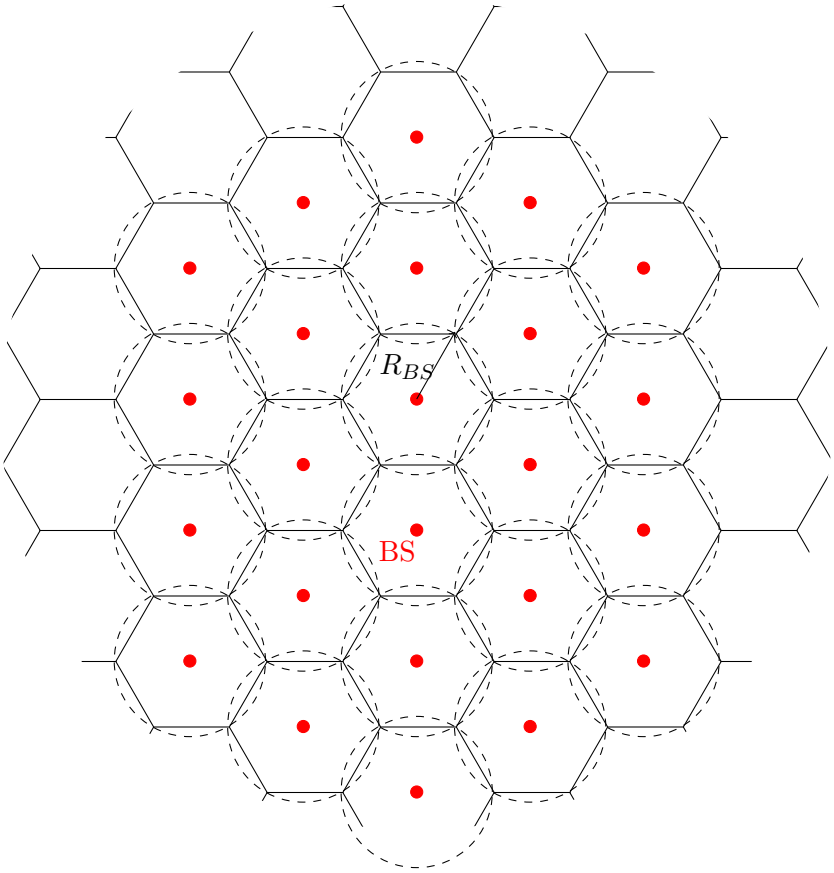

Figure 3.19: Baseline system macrocell BSs coverage layout

due to fewer users demanding service. It is assumed that, in the base line system the macrocell transmits at the maximum power, in order to achieve the maximum capacity of a macrocell. When a few femtocells are deployed, some users are offloaded to the femtocells, then the macrocell transmission power decreases proportionally. The P_{BS} in Equation (3.10) can be replaced as :

$$P_{\text{BS},f} = \max\left\{\frac{N_{u,m}}{N_u} \cdot P_{\text{BS}}, P_{\text{BS,min}}\right\} \tag{3.27}$$

where $P_{\text{BS,min}}$ is the minimum transmission power of a macrocell BS.

3.3.3 When femtocells are ubiquitously deployed

Figure 3.19 shows the baseline system scenario without femtocells in a coverage of $\mathcal{A}_{\text{sys}}$. Each macrocell has a radius of R_{BS}, and they are all active.

In the scenario where femtocells are deployed into the system, more

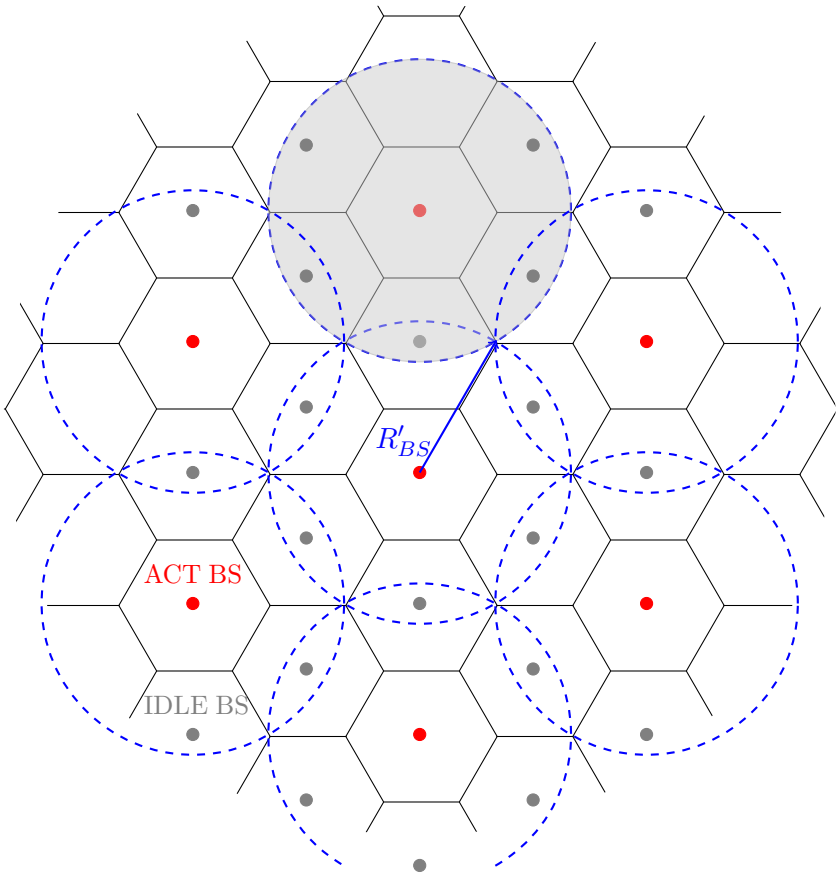

Figure 3.20: Macrocell BSs layout with ubiquitous femtocells deployment

active users are able to be serviced by local femtocells. Hence the number of users in the macrocell decreases significantly with the utilisation of femtocells. By using a certain central control node, some of the macrocells can transmit at a higher power lever, in order to cover the users in the neighbouring macrocells' territory. Correspondingly, the neighbouring macrocells' transmission power can be adjusted to a lower level, to have a smaller coverage and support fewer users.

When the macrocell's radius increases to $R'_{\mathrm{BS}} = 2 \cdot R_{\mathrm{BS}}$ with the increase of femtocell deployment, some macrocells can be switched to an IDLE mode, since the active macrocells are able to provide the service to all remaining users. Figure 3.20 illustrates this scenario. The red nodes represent the active macrocells, and grey nodes represent the idle macrocells. The radius of the active macrocell increases to 2 times that of R_{BS}, and accordingly, the coverage area increased to 4 times that of the macrocell compared to the baseline system. Therefore, the macrocell base station switched-off threshold can be defined as the point when over 75% of the macrocell coverage is covered by femtocells.

Since the femtocells are considered as uniformly distributed in this work, the coverage ratio of femtocells can be derived based on the different values of femtocell switch off threshold distance τ and ρ_f by enumeration. Each realisation of femtocells deployment based on one set value of τ and ρ_f is simulated 1,000 times. The Cumulative Distribution Functions (CDFs) of coverage ratio are presented in Figure 3.21 and 3.22. Figure 3.21 shows the effects of τ to the area coverage ratio of femtocells with the same value of ρ_f. Correspondingly, Figure 3.22 indicates the femtocell deployment coverage based on the different value of ρ_f and the same value of τ. In this enumeration simulation, $R_{\mathrm{cell}} = 500$ m and $R_f = 10$ m.

In Figure 3.21, the femtocell switch-off threshold $\tau = 10$ m, and $\rho_f = 0.0085$. It is equal to 5520 femtocells deployed within a macrocell area with radius of 500 m, which also means 85 femtocells are deployed in a area of 100 m$\times$ 100 m area. It gives a high femtocell usage scenario. It can be seen that, with the increase of τ, the femtocells coverage decreases dramatically. It indicates that more femtocells are switched to an IDLE mode. For a smaller τ setting, e.g. $\tau = 6$ m, with this femtocell usage, the local macrocell can definitely be switched off, since the coverage is always greater than 75%. Therefore, considering the power efficiency and femtocells utilisation rate,

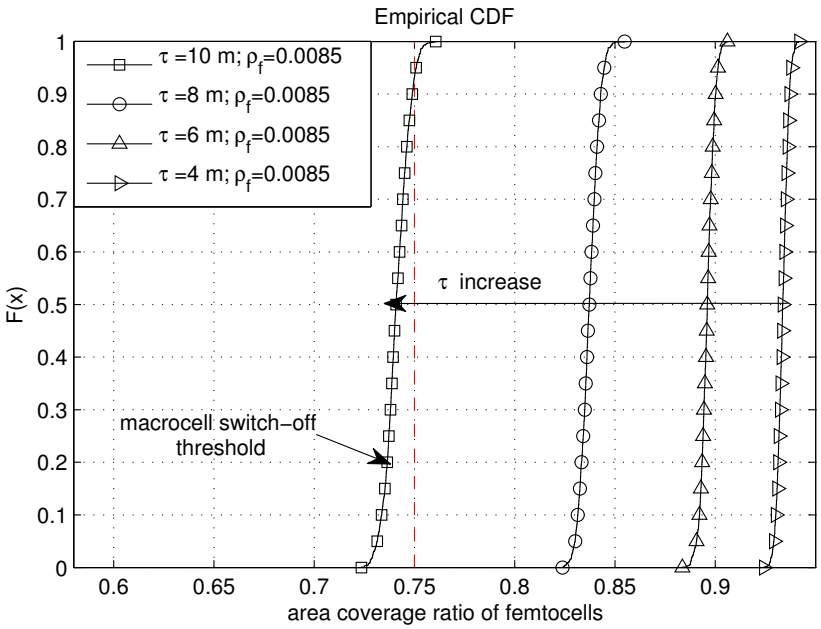

Figure 3.21: Femtocells coverage ratio based on the different τ

the value of τ should not be set under 10 m.

In Figure 3.22, the effects of ρ_f on the coverage ratio based on $\tau = 10$ m are examined. It shows that, with the increase of femtocell deployment, the coverage increases. When the femtocell density is 0.0105, there are 90% of cases when the femtocells' coverage ratio is larger than 75%. Therefore, the local macrocell can be considered to be switched off.

Table 3.6: Lookup table for mapping relationship of τ and $\rho_{f,\text{swi}}$

τ (m)	$\rho_{f,\text{swi}}$(number of femtocells per m^2)
0	0.0042
4	0.0043
6	0.0045
8	0.006
10	0.0105

Based on this methodology, the density of femtocell usage can be taken as an indicator of macrocell switch-off threshold, and which show in over 95% of cases that the coverage of femtocells is greater than 75%. Hence, for each τ, the femtocell deployment density that makes the local macrocell switch off ($\rho_{f,\text{swi}}$) can be derived and are presented in Table 3.6. It has

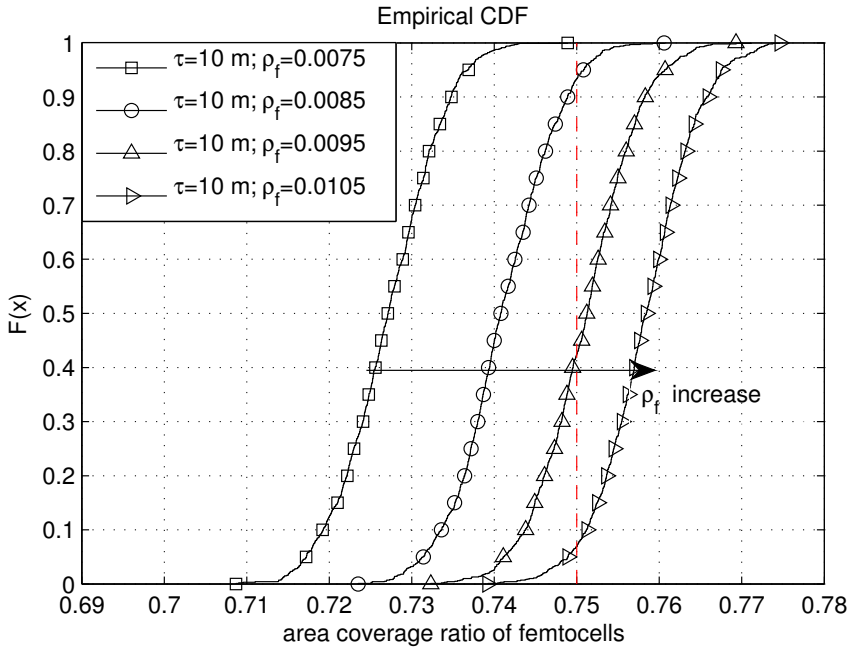

Figure 3.22: Femtocells coverage ratio based on the different ρ_f

two conclusions: First of all, for smaller values of τ, they have similar $\rho_{f,\text{swi}}$ for switching off the macrocell. To avoid significant interference between femtocells, τ should be set at a bigger value. Second, when τ is larger than 8 m, the value of $\rho_{f,\text{swi}}$ increases significantly, which means it requires a large number of femtocells to be deployed. For a practical and economical consideration, τ should not be set larger than 8 m.

Considering the system power consumption in a scenario where some macrocells are switched to an IDLE mode, the embodied energy is the same as Equation (3.16). However, if a developing system is considered, the increasing number of mobile users and equipment, together with user demand, requires further macrocell BS to be installed. The ubiquitously deployed femtocells may be able to fulfil the increasing demand, and avoid the installation for new BSs. Therefore, the macrocell BSs which are switched to an IDLE mode in the previous discussion, are considered as the extra BSs that were intended to be built in this scenario. Hence, the embodied and operational power are all saved. The calculations are given as follows:

$$\overline{P}_{\text{cap},f'} = \begin{cases} \overline{P}_{\text{cap},f}, & \text{developed system} \\ (C_{\text{BS}}/4 + N_u \cdot C_{\text{MT}} + N_{\text{AP}} \cdot C_{\text{AP}}) \cdot \dfrac{1}{\mathcal{A}}, & \text{developing system} \end{cases} \tag{3.28}$$

$$\overline{P}_{\text{op},f'} = \begin{cases} [(O_{\text{BS}} + 3 \cdot \delta_{\text{BS}})/4 \\ \quad + \displaystyle\sum_{i=1}^{N_u} O_{\text{MT},i} + O_{\text{AP},1} + O_{\text{AP},2}] \cdot \dfrac{1}{\mathcal{A}}, & \text{developed system} \\ (O_{\text{BS}}/4 + \displaystyle\sum_{i=1}^{N_u} O_{\text{MT},i} + O_{\text{AP},1} + O_{\text{AP},2}) \cdot \dfrac{1}{\mathcal{A}}, & \text{developing system} \end{cases} \tag{3.29}$$

3.3.4 Numerical results

In this section, the numerical results are given based on the theoretical analysis and Monte Carlo simulation. The simulation parameters are given in Table 3.7

Table 3.7: Simulation Parameters

Symbol	Parameter	Value
R_{cell}	modeled macrocell radius	500m
R_f	femtocell radius	10m
ρ_f	density of femtocells	0 to 0.0085
C_{BS}	macrocell BS embodied energy/s	1000 W
C_{AP}	femtocell AP embodied energy /s	1 W
C_{MT}	MT embodied energy/s	2.6 W
P_{BS}	macrocell BS transmission power	20 W
$P_{\text{BS,min}}$	minimum BS transmission power	31.6 mW
δ_{BS}	BS power consumption (not transmitting)	354.44 W
P_{AP}	AP power consumption (transmitting)	12 W
δ_{AP}	AP power consumption(not transmitting)	7 W

In the simulation, active mobile users and femtocells are all uniformly distributed, and the scenario is simulated 1,000 times. The average system power consumption per unit area in an urban environment is achieved based on 1,000 realisations. The results are illustrated in Figure 3.23.

Since the difference in system power consumption between a developed

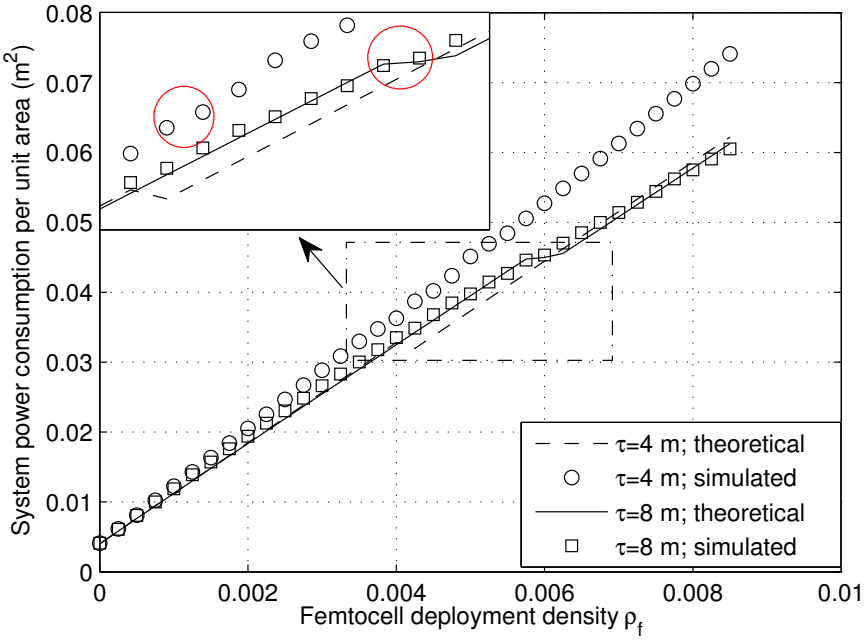

Figure 3.23: System power consumption per unit area with different femtocells deployments

system and a developing system is that, spreading one macrocell embodied energy and operational power over one macrocell coverage, or 4 times that coverage, we can calculate the developing system power consumption, then add the extra portion of macrocell BS power consumption into the developed system based on Equations (3.28) and (3.29). Figure 3.23 shows the theoretical and simulated results based on the different values of femtocell deployment densities ρ_f and femtocell switch-off threshold τ.

First of all, in the baseline system, when no femtocell is deployed, the average power consumption per unit area is 0.004 W/m^2, including embodied energy (Cap) and operational power (Op) of all equipment. The contributions from Cap and Op are approximately equal, which means they all contribute 0.002 Wm^2 (2,000 W/km^2) into the system respectively.

Second, all curves show a trend that, along with the increase usage of femtocells, the system power consumption increases dramatically. This is due to the intensive usage of femtocells. For example, when the femtocell deployment density achieves 0.004, then there are about 2,600 femtocells contributing approximately 0.030 W/m^2 into the system, while the whole

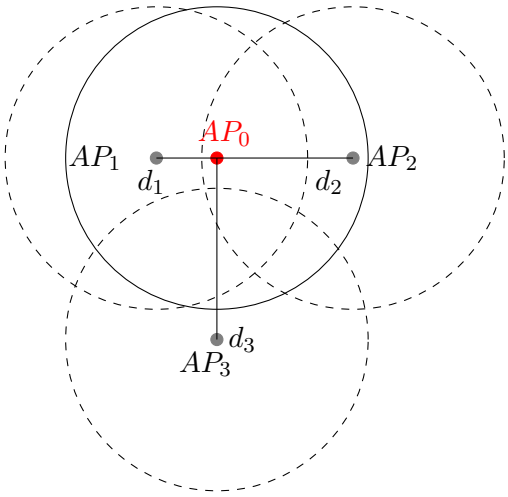

Figure 3.24: One example of femtocells deployment when ρ_f is relatively high

power consumption is 0.033 W/m^2. There is an urge to decrease the femtocell manufacturing power consumption and reduce the power consumption when a femtocell is in an IDLE mode. If these two factors can be reduced, the system power consumption will decrease significantly. On the other hand, the operational power of MT and macrocell BS are decreased because of the use of femtocells, so that a long distance transmission is replaced by a short distance transmission.

It can also be seen that, for the two theoretical results curves, at the macrocell switch-off point, i.e. when $\tau = 4$ m, the point at $\rho_f = 0.0043$; and when $\tau = 8$ m, the point at $\rho_f = 0.006$. The simulated curves also indicate a good match that at these points, the increments in system power consumption are relatively smaller, which are highlighted with two red circles. From the zoomed in sub-picture, when larger τ is set, a lower system power consumption can be achieved, since it is able to provide a larger coverage for mobile users.

The most notable result is that, when it's set at a higher value of τ, the simulated curve has a better match with the theoretical curve. Additionally, along with the increase of femtocells deployment, the bigger gap appears between the theoretical and simulated curves for a smaller τ. One possible explanation is that, when more femtocells utilised, the scenario shown in Figure 3.24 is more likely to happen, that several femtocells are overlapping

with each other. It is assumed that the distances from AP_0 to AP_1, AP_2 and AP_3 have this relationship: $d_1 < d_2 < \tau_1 < d_3 < \tau_2$. If the femtocell switch-off threshold is set at τ_1, both AP_1 and AP_2 should be switched off. However, in the theoretical formula, it is only able to find the nearest femtocell to AP_0, which means that only AP_1 can be switched off. Therefore, the femtocell coverage is bigger in theoretical analysis than the practical scenario. It results in more mobile users being offloaded to a femtocell, and less system power consumption. On the other hand, if a bigger value τ_2 is chosen, based on the theoretical analysis, AP_1 and AP_3 will be switched off. due to the short distances to AP_0, and so AP_0 and AP_2 will contribute to the coverage. However, in a practical scenario, AP_2 and AP_3 will remain working. Although they still do not present the same coverage, however, it is much closer than the previous setting.

3.4 Comparisons between a urban and a combination scenario

This section gives some discussion of the comparisons between an urban and a combined urban and rural scenarios, based on the previous two sections' analysis. First of all, the mobile user and femtocells densities are significantly larger in an urban scenario when compared with a combined scenario. It results in approximately a 4 times higher power consumption per user in urban area.

Second, in the urban scenario, the mobile users and femtocells are uniformly distributed, therefore there is no relationship between the location of users and femtocells. However, in the combined scenario, the femtocells are located in the high density user's area. Hence, it results in a better match compared with the urban scenario. In this case, it provides a better femtocell coverage, and leads to a lower power consumption. Therefore, in reality, the power consumption should be between these two scenarios.

Finally, in the combination scenario, the femtocell coverage is assumed to be a 100 m $\times$ 100 m area. If femtocells have smaller coverage, the system power consumption may be greater compared to the current results. As fewer users are able to be covered by a femtocell. The trade-off points may appear beyond 40%, or there may be no power rising trade-off point along with the increase of femtocell deployment. Figure 3.25 shows the system power consumption comparison for two femtocells, with a large and small coverage area. The dotted line represents the result for a femtocell with a

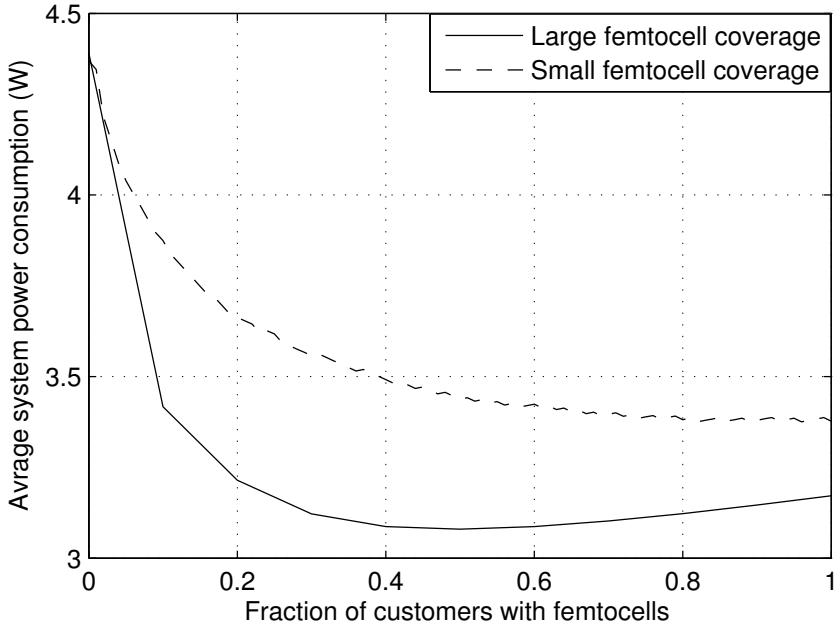

Fig. 3.25: System power consumption comparison of different femtocell sizes

circular coverage region of 10 m radius. It shows that along with the increase of femtocell deployment, the system power consumption always falls. This is because with the same density of femtocell deployment, but having smaller coverage, the femtocell network may not fulfill all the users' demand, and the probability of one user being covered by a femtocell declines. In this case, the fully installed femtocells scenario may still not be the scenario "when femtocells are over deployed".

3.5 Summary

From the large scale simulation results for system power consumption, there are three main conclusions. First, for all levels of macrocell support, a certain degree of femtocell implementation can reduce the system power consumption. However, excessive use of femtocells may lead to an even higher power consumption compared to the original cellular communication system, when the femtocells have a bigger coverage. On the other hand, if the femtocells have a smaller coverage, the system power consumption may always decrease as more femtocells are added. Second, after analysing

the composition of the system power consumption, it can be seen that the greatest power saving is from the BS's operational energy. Also if the rate of increase in new customers is high, the amount of BS's embodied energy is also saved. Third, if the femtocells with different capacities are available, only taking power consumption into consideration, the more users that a femtocell can support, the greater the power that can be saved.

On the other hand, based on the normalised small scale analysis, it has the following conclusions. One, due to the high density of mobile users and femtocells in an urban environment, the power consumption is approximately 4 times larger than the large scale analysis. The reduction of femtocell standby power is so crucial to the system power efficiency. Also, based on the simulation parameters, the switch-off threshold distance between two femtocells should be set at a relatively high value, i.e. 6 m or 8 m. It achieves a similar coverage as a low threshold setting, and also saves power by switching off a proper amount of femtocells. The proposed mathematical model shows a satisfactory match for the simulation results, specially when τ is set at a high value. This model can be used for the further analysis and research.

4

Combined Femtocell and Cellular Network Architecture: Capacity and Throughput analysis

Femtocells are considered as a promising low power complementary network to macrocells. They have been developed to work with various cellular standards, including GSM, CDMA and UMTS. The deployment of femtocells is attractive as they are able to offload traffic from the macrocell, and increase the network coverage and capacity. At the same time, the system power consumption can be reduced from both operational and capital perspectives. Our previous work [99] showed that, with appropriate uptake of femtocells, a communication system is able to achieve a high power efficiency and high QoS performance at the same time.

Wideband code division multiple access (WCDMA) is a UMTS technology that is widely deployed. Installing femtocells in a WCDMA system is problematic due to the co-channel interference that then exists in the network [100, 101, 102]. Power control algorithms have been proposed for the uplink [103] and downlink [25] scenarios respectively. Independently of this work, other researchers have investigated the QoS aspects for the uplink [63, 100] and downlink [104] separately. The commonly used QoS metrics for this evaluation are system capacity [15, 22] and coverage [23]. Analysis of the power efficiency should be linked to the QoS performance, to guarantee the quality of user experience. However, since the femtocell is able to provide the same bandwidth as the macrocell, and supports significantly fewer users, the femtocell can improve the user QoS significantly through increased throughput. Hence, in this chapter, the throughput of each user is investigated.

Here, the downlink for femtocells coexisting with a WCDMA macro-

cell is studied. The interference analysis is conducted using a geometric model, introduced in [105]. Two transmission power setting schemes, Power-Controlled and Fixed-Power schemes, are described and analysed. Results are presented from numerical evaluation of the theory. The main contributions of this work include a detailed theoretical analysis of femtocell transmission power, in conjunction with throughput, including both system level performance and single user performance.

The reminder of this chapter is organised as follows. Section 4.1 defines the propagation model in different communication scenarios and describes the simulation assumptions. The simulation parameters are given in this section. Section 4.2 proposes two femtocell transmission power setting schemes, and presents and compares them theoretically. In the following two sections, two power setting schemes are compared through simulation of system capacity and single user throughput. In the first of these the interference scenarios are studied from the perspectives of a macrocell and a femtocell user in a single-macrocell scenario and in the second, a multiple-macrocell. Finally, the last section summarises this chapter.

4.1 Simulation Model

4.1.1 Propagation Model

In wireless communication scenarios, the transmitted signal experiences attenuation due to different reasons, such as scattering, reflection or refraction caused by a multi-path channel. These attenuation effects can be divided into two types of propagation: large-scale propagation and small-scale propagation [106].

Large-scale propagation includes pathloss and shadowing, which are caused by large terrain features and environments, such as hills and buildings, or other obstacles, between the transmitter and receiver. Small-scale fading is normally defined as rapidly changing signal strength caused during a short period, or distance. This phenomenon may result in deep fading or contribute to multiuser diversity gain. In this chapter, both large-scale and small-scale propagation losses will be taken into consideration for evaluation of system capacity and throughput performance. The related propagation models are defined in the following section.

Pathloss and Large-scale propagation

Outdoor propagation model

The outdoor propagation model adopted in this chapter is developed for a typical cellular system. This model is given by: [107]

$$PL_o[\text{dB}] = \begin{cases} PL_{fs}(f_c, d), & d \leqslant d_0 \\ PL_{fs}(f_c, d_0) + 10 \cdot \alpha \log_{10}(\frac{d}{d_0}) + \gamma, & d > d_0 \end{cases} \tag{4.1}$$

where $\alpha = a - b \cdot h_b + c/h_b$, h_b is the base station height, and d_0 is breakpoint and selected as 100 m. γ is the log-normal distribution of the random variable due to shadowing with a standard deviation of 10 dB, and a, b, and c are constants that depend on the type of environment. In this work, $a = 4, b = 0.0065$, and $c = 17.1$, which models a low tree density, or medium tree density environment[107]. f_c is the frequency of the carrier, 2 GHz. PL_{fs} represents the free space attenuation, given by:

$$PL_{fs}[\text{dB}] = 32.44 + 20 \log_{10} f_c + 20 \log_{10} d \tag{4.2}$$

Indoor propagation model

The indoor propagation model is given by[108], which is developed from[109].

$$PL_i[\text{dB}] = \begin{cases} PL_{fs}(f_c, d), & d \leqslant d_0 \\ PL_{fs}(f_c, d_0) + 35 \log_{10}(\frac{d}{d_0}) + \gamma, & d > d_0 \end{cases} \tag{4.3}$$

The breakpoint for the indoor environment is selected as 5 m. Within the breakpoint distance, the signal experiences a free space attenuation, which is proportional to d^2 , whilst for higher distances the additional attenuation increase is $d^{3.5}$. The shadowing can also be accounted for through a random variable, γ.

Complex scenario propagation model

As femtocells may share the same frequency with macrocells, interference will exist between femtocells and macrocells, or between femtocells themselves. Hence, a new propagation scenario needs to be investigated, in which, the transmitted signal may experience a more complex scenario, such as from a macrocell to a femtocell (outdoor-to-indoor), from a femto-

cell to another femtocell (indoor-to-outdoor-to-indoor), or from a femtocell to a macrocell (indoor-to-outdoor). In order to evaluate these scenarios, the following equation is employed, which is developed from a indoor-to-outdoor scenario of ITU-R(M.1225) [110]. The equation is written as:

$$PL_c[\text{dB}] = 40\log_{10} d + 30\log_{10} f_c + 19 + \omega \cdot PL_{\text{wall}} + \gamma \tag{4.4}$$

where PL_{wall} indicates the wall attenuation, with a average value of 15 dB. ω sets the number of walls crossed during a transmission process. For instance, in a indoor-to-outdoor propagation, ω equals 1, and in a indoor-to-outdoor-to-indoor scenario, ω equals 2.

Small-scale propagation

Rayleigh Channel

Considering the small-scale propagation, the outdoor propagation model can be described as a Rayleigh channel. A Rayleigh fading channel can be modeled by generating the real and imaginary parts of a complex number according to independent normal Gaussian variables. The following equation is employed:

$$H = \frac{|X + jY|}{\sqrt{2}} \tag{4.5}$$

where $X \sim N(0, \sigma^2)$ and $Y \sim N(0, \sigma^2)$ are independent normal random variables.

Nakagami Channel

The indoor environment can be modeled by a Nakagami distribution. The parameters are m and Ω, which are given as follows [111]:

$$m = \frac{\mathbf{E}^2[R^2]}{\mathbf{Var}[R^2]} \tag{4.6}$$

$$\Omega = \mathbf{E}[R^2] \tag{4.7}$$

where R is the signal strength measured from a realistic communication scenario. $\mathbf{E}[\cdot]$ and $\mathbf{Var}[\cdot]$ denote the expected value and the variance of $[\cdot]$ respectively.

Based on the moment measurements from [112], it is found that the Nakagami model fits better than other fading models for the indoor scenario.

In this work, the parameters are adopted from the same paper; m is around 1.5, and Ω is 1.

It is possible to generate a Nakagami channel by using a Gamma distribution generator, it can be written as:

$$N = \sqrt{\Gamma(k, \theta)} \tag{4.8}$$

where $\Gamma(\cdot)$ is the gamma function, $k = m$ and $\theta = \Omega/m$.

4.1.2 Simulation Descriptions and Assumptions

The investigated system model is the downlink scenario of a WCDMA cellular system with a hexagonal cell of radius R_{cell}. In this work, a single macrocell or a multiple macrocell scenario are considered respectively, each macrocell supporting a constant number of macrocell users N_{mu}. It is assumed that a macrocell is divided into 3 sectors. A hexagonal coverage is modelled as a circle of radius R_m.

Within a macrocell coverage, N_{mu} macrocell users and N_f femtocells are independently uniformly distributed. In order to avoid significant interference between femtocells, it is assumed that the femtocell switch-off threshold distance τ is set as 8 m. Figure 4.1 shows the modelled macrocell coverage and co-channel femtocell deployment. The other summarised assumptions are listed as follows:

1. Although the number of macrocell users is constant, if femtocells are deployed, users can be offloaded to femtocells, the number of remaining macrocell users will decrease.

2. Each user is allocated the same transmission power at the macrocell base station. All macrocell users belong to the same service class.

3. An open access scheme is assumed for femtocells in this work. Each user located within a femtocell's coverage can be served by this femtocell. In practice, an open access scheme can be encouraged by means of compensation from network operators, etc. It is able to avoid the strong interference for unauthorized users who are passing by a femtocell or guesting in a house with femtocell.

4. In the following two scenarios a femtocell will be switched to a sleep mode: first, when there is no active user located in this femtocell's

coverage; second, when all the active users within its coverage can get service from other neighbouring femtocells.

Other system simulation parameters are listed in Table 4.1.

Table 4.1: Simulation Parameters

Symbol	Parameter	Value
R_{cell}	modelled macrocell radius	500m
R_m	modelled macrocell radius	455m
R_f	femtocell radius	10m
W	macrocell and femtocell Bandwidth	5 Mbps
P_{fmax}	maximum femtocell transmission power	125 mW
P_m	macrocell transmission power	20 W
N_{fmax}	maximum number of users per femtocell	4
R_s	information rate per symbol	2
$SINR_{tar,m}$	target SINR for macrocell users	5 dB
$SINR_{tar,f}$	target SINR for femtocell users	5 dB
SF_m	spreading factor for macrocell users	256
SF_f	spreading factor for femcell users	1-256
G_{max}	antenna boresight gain	16 dBi
G_β	3 dB antenna beamwidth	70 degrees

4.2 Femtocell Transmission Power Analysis

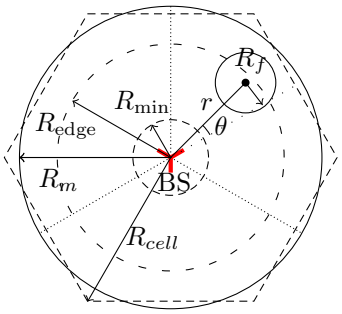

Figure 4.1: Scenario sketch of macrocell and co-channel femtocell

Two scenarios are investigated, where the femtocell 's transmission power depends on the received base station power at the edge of the femtocell (Power-Controlled Scheme), and where it is fixed at a maximum value (Fixed-Power scheme).

For the Power-Controlled scheme, the transmission power of a femtocell is calculated by (4.9). Due to the strength of the macrocell, a femtocell should not be installed within R_{min}, to avoid the significant macrocell interference to femtocell users. Secondly, femtocell transmission power is calculated by the received power level from the local macrocell at the target coverage edge of a femtocell, with a maximum value constraint of P_{fmax}.

$$P_f = \begin{cases} 0, & (0 \leqslant r \leqslant R_{\min}) \\ P_{\text{fmax}}, & (R_{\min} < r \leqslant R_{\text{edge}}) \\ \dfrac{P_m G(\theta) PL_i(R_f)}{PL_o(r - R_f)}, & (R_{\text{edge}} < r \leqslant R_m) \end{cases} \tag{4.9}$$

In (4.9), P_m is the macrocell's antenna transmission power, $PL_o(r - R_f)$ and $PL_i(R_f)$ are the linear values calculated with Equations (4.1) and (4.3) respectively, where $PL_i(R_f)$ is constant with a given R_f. $G(\theta)$ is the antenna gain at an angle θ from the azimuth plane. Its dB value is calculated by [32]:

$$G(\theta)[\text{dB}] = G_{\max} - \min\left\{12 \times \left(\frac{\theta}{G_\beta}\right)^2, G_s\right\} \tag{4.10}$$

where $G_{\max} = 16$dBi is the boresight gain and $G_\beta = 70\pi/180$ is the 3 dB reduction point in the antenna patten, and $G_s = 20$dBi.

Considering Equation (4.9), for the first two pieces' values, the probabilities are constant, given by the following equations:

$$\begin{aligned} &\Pr(P_f = 0) = \Pr(0 \leqslant r \leqslant R_{\min}) = \frac{R_{\min}^2}{R_m^2} \\ &\Pr(P_f = P_{\text{fmax}}) = \Pr(R_{\min} \leqslant r \leqslant R_{\text{edge}}) = \frac{R_{\text{edge}}^2 - R_{\min}^2}{R_m^2} \end{aligned} \tag{4.11}$$

For the third piece, the probability is a condition function with two functions of random variables, i.e. $G(\theta)$ and $1/PL_o(r - R_f)$. Using $Q(r)$ to replace $1/PL_o(r - R_f)$, i.e.:

$$Q(r) = \frac{1}{PL_o(r - R_f)} \tag{4.12}$$

Therefore, when $R_{\text{edge}} < r \leqslant R_m$, P_f is a function of $G(\theta)$ and $Q(r)$. Since $G(\theta)$ and $Q(r)$ are independent, the probability of the third piece is:

$$\begin{aligned}\Pr(P_f = P_i) =& \Pr(R_{\text{edge}} \leqslant r \leqslant R_m) = \frac{R_m^2 - R_{\text{edge}}^2}{R_m^2} \cdot \Pr(G(\theta))\Pr(Q(r)), \\ & where \quad P_i \in (0, P_{\text{fmax}})\end{aligned} \tag{4.13}$$

Functions $G(\theta)$ and $Q(r)$ are given by Equations (4.10) and (4.12) respectively, where θ and r are random variables as well. Their probability density functions (PDF) are:

$$\begin{aligned}\Pr(\theta) &= \frac{3}{2\pi}, & \theta &\in [-\frac{\pi}{3}, \frac{\pi}{3}] \\ \Pr(r) &= \frac{2r}{R_m^2 - R_{\text{edge}}^2}, & r &\in (R_{\text{edge}}, R_m]\end{aligned} \tag{4.14}$$

Hence, the cumulative distribution functions (CDF) for $G(\theta)$ and $Q(r)$ can be expressed as:

$$\mathcal{F}(G(\theta)) = 1 - \frac{3}{\pi}\sqrt{\frac{G_{\max}/10 - \log_{10}G(\theta)}{1.2/G_\beta^2}} \tag{4.15}$$

$$\mathcal{F}(Q(r)) = 1 - \frac{[(\frac{1}{p \cdot Q(r)})^{\frac{1}{\alpha}} + R_f]^2 - R_{\text{edge}}^2}{R_m^2 - R_{\text{edge}}^2} \tag{4.16}$$

where α is given by Equation (4.1), and $p = PL_{fs}/d_0^\alpha$. Equation (4.13) can be re-written as:

$$\Pr(P_f = P_i) = \frac{R_m^2 - R_{\text{edge}}^2}{R_m^2} \cdot \frac{\mathcal{F}(G(\theta))}{\mathrm{d}G(\theta)} \frac{\mathcal{F}(Q(r))}{dQ(r)} \tag{4.17}$$

Equation (4.11) and (4.17) indicate the probability of the value of single femtocell transmission power based on the location of the femtocell. It is assumed that $\overline{P_f}$ is the mean of P_f, and $\sigma_{P_f}^2$ is the variance of P_f. When more femtocells are deployed in the system, the average femtocell transmission power tends to be a normal distribution, i.e. $\overline{P_{f,n}} \sim \mathcal{N}(\overline{P_f}, \frac{\sigma_{P_f}^2}{n})$. Figure 4.2 shows the theoretical and simulated CDF of average femtocell transmit power distribution for multiple femtocells. In the simulation, 120 users and multiple femtocells are uniformly distributed within a coverage of $R_m = 152$ m radius, where the macrocell BS is located in the centre of this area. The deployment scenarios of users and femtocells are simulated 10,000

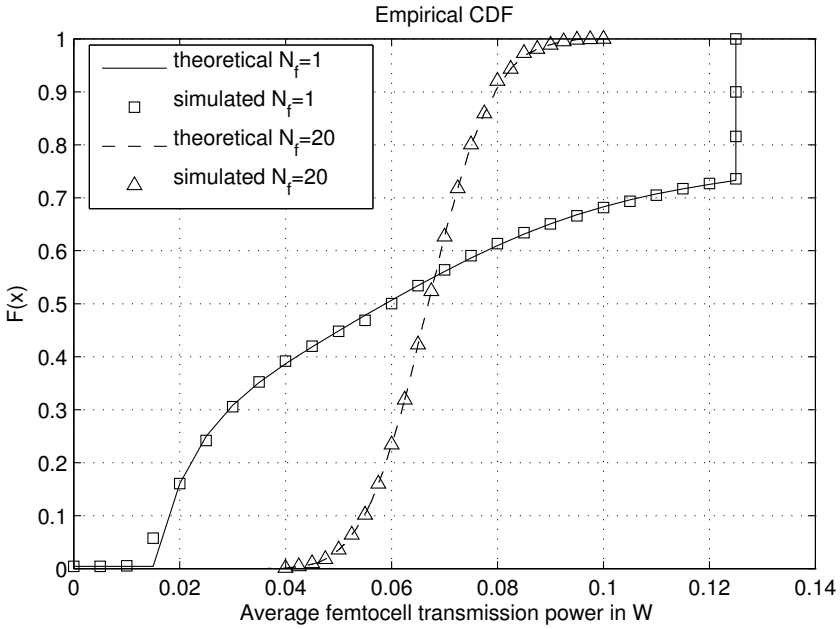

Figure 4.2: CDF of transmission power of femtocell in W when femtocell's transmission power is controlled

times by using Monte Carlo method. By assuming $P_{\text{fmax}} = 125$ mW, in the case of one femtocell deployment, the expected value of P_f is 67 mW, with a variance of 0.0018. Compared with the Fixed-Power scheme, with femtocell transmission power set at P_{fmax}, the Power-Controlled scheme is able to save power of around 50%. However, there may be a trade-off between the power consumption and throughput. In the following sections, this power consumption will be analysed along with the system performance, to achieve an optimal solution for both power efficiency and throughput.

4.3 System Capacity and Single User Throughput: Single Macrocell

In this section, system capacity and single user throughput performance are analysed in the single macrocell scenario, for a macrocell and femtocell user respectively.

4.3.1 Macrocell users' performance

In a WCDMA system where macrocells and femtocells co-exist, when only one macrocell is considered, a user's received signal is affected by two interferers: first is self-interference from the macrocell base station (BS); another is from femtocell access points (AP). Figure 4.3 shows the interference scenarios for a macrocell user.

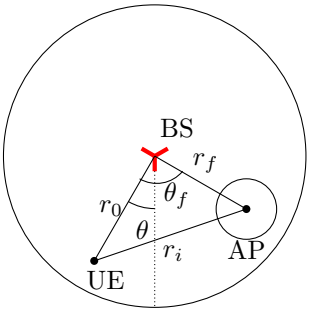

Figure 4.3: Interference scenarios for a macrocell user

In the downlink scenario, data for each user is transmitted with the same power by the BS, i.e. $P_{\text{tx}} = P_m/(N_{mu,\max}/3)$, where P_m is the transmission power of each macrocell antenna, and $N_{mu,\max}$ is the maximum number of users that a macrocell can support as specified by the system design. Assume that each user has a target SINR level, SINR_{tar}, hence, the maximum number of users for all 3 sectors can be expressed as [113]:

$$N_{mu,\max} = 3 \cdot \frac{SF_m/R_s}{\text{SINR}_{\text{tar}}} \tag{4.18}$$

However, due to the significant interference from the environment, normally the maximum number can not be supported. Self-interference from the local macrocell BS is:

$$I_{m1} = \frac{N_{mu}/3 \cdot P_{\text{tx}}[G(\theta) + G(\theta') + G(\theta'')]}{PL_o(r_0)} - P_{m0} \tag{4.19}$$

where $G(\theta')$ and $G(\theta'')$ denote the antenna gains from the other sectors. P_{m0} is the received power for a macrocell user from the BS, the calculation is given by:

$$P_{m0} = \frac{P_{\text{tx}}G(\theta)}{PL_o(r_0)} \tag{4.20}$$

The total interference from femtocell APs to a macrocell user can be expressed by:

$$I_{m2} = \int_0^{2\pi} \int_{R_m}^{R_{\min}} \rho_f \frac{P_f(r_f)}{PL_c(r_i(r_f, \theta_f))} r_f dr_f d\theta_f \tag{4.21}$$

where ρ_f is the density of femtocell deployment. It is given by:

$$\rho_f = \frac{N_f \cdot \pi R_f^2}{\pi R_m^2} \tag{4.22}$$

$P_f(r_f)$ is defined in Equation 4.9, and r_i is a given by $(r_0^2 + r_f^2 + 2r_0 r_f \cos\theta_f)^{\frac{1}{2}}$.

The received SINR at the macrocell users should satisfy the following inequality:

$$\text{SINR}_{\text{tar},m} \leqslant \frac{|h_0|^2 P_{m0}}{|h_1|^2 I_{m1} + |h_2|^2 I_{m2} + \sigma^2} \cdot \frac{SF_m}{R_s} \tag{4.23}$$

where h_0, h_1 and $h_2 \sim \mathcal{C}N(0,1)$, are Rayleigh channel coefficients. σ^2 denotes the background noise.

Combined with (4.19), the actual number of users that one macrocell can support, based on single user evaluation, can be obtained by:

$$N_{mu,i} \leqslant \begin{cases} \dfrac{3P_{\text{tx}} G(\theta)[|h_0|^2 SF_m/(\text{SINR}_{\text{tar},m} \cdot R_s) + |h_1|^2]}{|h_1|^2[G(\theta) + G(\frac{2}{3}\pi + \theta) + G(\frac{2}{3}\pi - \theta)]} \\ - \dfrac{3PL_o(r_0)(|h_2|^2 I_{m2} + \sigma^2)}{|h_1|^2 P_{\text{tx}}[G(\theta) + G(\frac{2}{3}\pi + \theta) + G(\frac{2}{3}\pi - \theta)]} \end{cases} \tag{4.24}$$

It can be seen from this inequality that, the macrocell capacity will be affected by the deployment of femtocells, i.e. I_{m2}, since more femtocells results in more interference being introduced into the system.

Based on the accumulation of all users' evaluation, the macrocell capacity can be expressed as:

$$N_{mu} \leqslant \int_{-\frac{\pi}{3}}^{\frac{\pi}{3}} \int_0^{R_m} N_{u,i} dr_0 d\theta / N_{mu,\max} \tag{4.25}$$

where $N_{mu,i}$ is a function of θ and r_0 according to (4.24).

The macrocell system capacity is obtained by the sum of data rates for the actual maximum number of macrocell users after considering the

interference, which is given by:

$$\mathcal{C}_m = \frac{N_{mu} \cdot W \cdot R_s}{SF_m} \tag{4.26}$$

where W is the chip rate, R_s is the information rate per symbol, and SF_m is the macrocell spreading factor.

Each user's throughput performance can be obtained as follows:

$$\mathcal{T}_m = \log_2(1 + \frac{SF_m}{R_s} \cdot \frac{|h_0|^2 P_{m0}}{|h_1|^2 I_{m1} + |h_2|^2 I_{m2} + \sigma^2}) \tag{4.27}$$

4.3.2 Femtocell users' performance

Considering a femtocell user, the interference is from three sources: first is self-interference, second is from the nearest macrocell BS, and the final source is the other femtocells which are located around it.

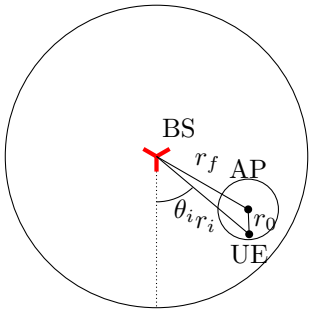

Figure 4.4: Interference scenarios for a femtocell user: Interferers are macrocell BS and intra femtocell AP

Figure 4.4 indicates the interference scenario for a femtocell user. It can be seen that the interferers are local femtocell and the macrocell BS. I_{f1} and I_{f2} denote the interference from those interferers respectively. They can given by:

$$I_{f1} = \frac{(N_{fu} - 1)P_{f0}}{N_{fu} PL_i(r_0)} \tag{4.28}$$

P_{f0} is the transmission power of the local femtocell, given by (4.9).

$$I_{f2} = \frac{[G(\theta_i) + G(\theta_i') + G(\theta_i'')]P_{\text{tx}} N_{mu}/3}{PL_c(r_i)} \tag{4.29}$$

where θ_i is the angle between this femtocell user and the macrocell BS.

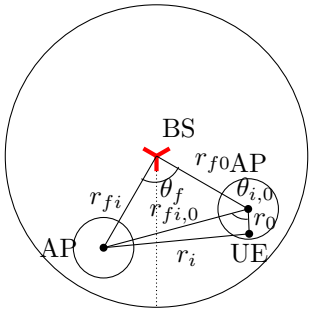

Figure 4.5: Interference scenarios for a femtocell user: Interferers are inter femtocell APs

Figure 4.5 depicts the scenario of the interference from neighbouring femtocells. It can be computed as:

$$I_{f3} = \int_0^{2\pi} \int_{R_{\min}}^{R_m} \rho_f \frac{P_{fi}(r_{fi})}{PL_c(r_i)} r_{fi} dr_{fi} d\theta_f \tag{4.30}$$

where the distance between i^{th} interferer femtocell and the femtocell user, r_i, is a function of r_{fi}, θ_f and $\theta_{i,0}$.

A femtocell user's received SINR should be guaranteed to be larger than $\text{SINR}_{tar,f}$, including all interference and background noise, thus:

$$\text{SINR}_{\text{tar},f} \leqslant \frac{|h_0|^2 P_{f0}/[PL_i(r_0) \cdot N_{fu}]}{|h_1|^2 I_{f1} + |h_2|^2 I_{f2} + |h_3|^2 I_{f3} + \sigma^2} \cdot \frac{SF_f}{R_s} \tag{4.31}$$

where h_0 and $h_1 \sim$ Nakagami(m, Ω), and h_2 and $h_3 \sim \mathcal{CN}(0, 1)$.

It is assumed that each femtocell can support a maximum of 4 users, i.e. $N_{fu} \leqslant 4$. For each femtocell, based on the different number of users, the spreading factor can be obtained as:

$$SF_f \geqslant \begin{cases} \text{SINR}_{\text{tar},f} \cdot R_s \cdot PL_i(r_0) \cdot N_{fu} \\ \cdot \dfrac{|h_1|^2 I_{f1} + |h_2|^2 I_{f2} + |h_3|^2 I_{f3} + \sigma^2}{|h_0|^2 P_{f0}} \end{cases} \tag{4.32}$$

Therefore, each femtocell capacity and single femtocell user's performance can be given by the following equations.

$$\mathcal{C}_f = \frac{N_{fu} \cdot W \cdot R_s}{SF_{\text{fmin}}} \tag{4.33}$$

$$\mathcal{T}_f = \log_2(1 + \frac{SF_f}{R_s} \cdot \frac{|h_0|^2 P_{f0}/[PL_i(r_0)N_{fu}]}{|h_1|^2 I_{f1} + |h_2|^2 I_{f2} + |h_3|^2 I_{f3} + \sigma^2}) \tag{4.34}$$

4.3.3 Simulation Results

Macrocell capacity with effects of femtocell deployment

The macrocell capacity is investigated in this section, with different femtocell deployments. Figure 4.6 shows the ensemble average result of the total number of users per macrocell when femtocells are using the two transmission power setting schemes. First of all, it can be observed that, when femto-

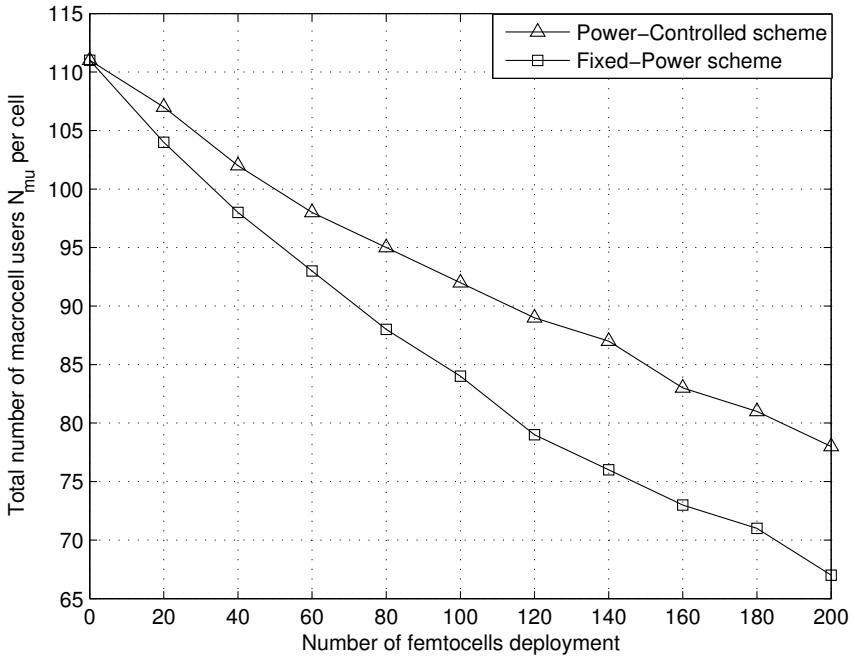

Figure 4.6: Macrocell capacity based on the different femtocell transmission power setting schemes in a single macrocell scenario

cells have not been introduced into the system, a macrocell can support approximately 110 users, although the designed number is 120 users. This is due to the self-interference from the macrocell. Then, when femtocells are adopted, the interference for a macrocell user is higher, since femtocells are allocated in the same channel as the macrocell. Comparing the two femtocell transmission power setting schemes, Figure 4.6 shows that a Power-Controlled scheme presents significantly less interference to a macro-

cell user than the Fixed-Power scheme. It can be noted from Figure 4.6 that, when around 200 femtocells are deployed within a macrocell coverage, by using the Fixed-Power scheme, the macrocell capacity is around 67 users, whereas the Power-Controlled scheme enables approximately 80 users to be supported by the macrocell.

Single user throughput analysis

Figure 4.7 indicates the single user throughput in macrocell and femtocell respectively, by applying (4.27) and (4.34). It illustrates the comparisons between two femtocell transmission power setting schemes, and the effects of using multiple femtocells.

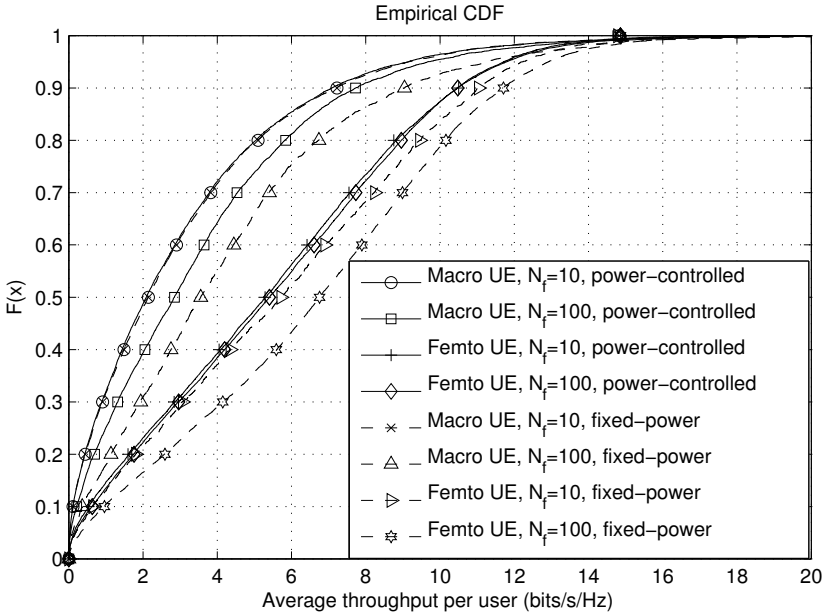

Figure 4.7: Available throughput per user with multiple femtocells

The four solid lines give the results of the Power-Controlled scheme. As the deployment of femtocells increases, more macrocell users can be offloaded to a femtocell, and the self-interference from the macrocell decreases. Hence, the single macrocell user's throughput is improved. Considering a femtocell user's performance, when more femtocells are deployed, although the number of interferers increases, only nearby femtocells are major interferers. Additionally, as femtocells are installed in buildings, the intercell femtocell interference experiences two walls of attenuation. Therefore, high

femtocell deployment results in a limited effect on the femtocell users' performance. On the other hand, more femtocell deployment is able to provide high throughput to more users.

The four dashed lines indicate the results of a Fixed-Power scheme. Comparing these two power setting schemes, based on the different usage of femtocells, the following conclusions can be drawn: for low femtocell deployment, the two schemes have a similar performance for a macrocell user. However, a Fixed-Power scheme is able to provide a significantly better performance for a femtocell user, since in this scheme, each femtocell transmits at a relatively high power. On the other hand, for high femtocell deployments, a Fixed-Power scheme results in a better throughput performance for a macrocell user. Figure 4.6 shows that, in this case the macrocell capacity decreases significantly. Therefore, the higher single macrocell user throughput is at the cost of the whole macrocell capacity.

4.4 System Capacity and Single User Throughput: multiple macrocell

In this section, QoS performance, including system capacity and single user throughput are investigated in the multiple macrocell scenario. The performance for macrocell users and femtocells users are both considered.

4.4.1 Macrocell Users' performance

For a macrocell user, the interference is from four sources in a multiple macrocell scenario. One interferer is the local macrocell. The transmission power to other macrocell users cause a significant interference to the studied user. The second interferer is the neighbouring macrocells. It is assumed that due to the long distance transmission, only adjacent macrocells are considered as interferers. The following two interferers are the femtocells located in the same macrocell and the femtocells located in the neighbouring femtocells respectively.

Figure 4.8 shows the interference from macrocells to a macrocell user. The interference from the local macrocell is given by Equation 4.19, i.e. $\tilde{I}_{m1} = I_{m1}$. The interference from the neighbouring macrocells can be cal-

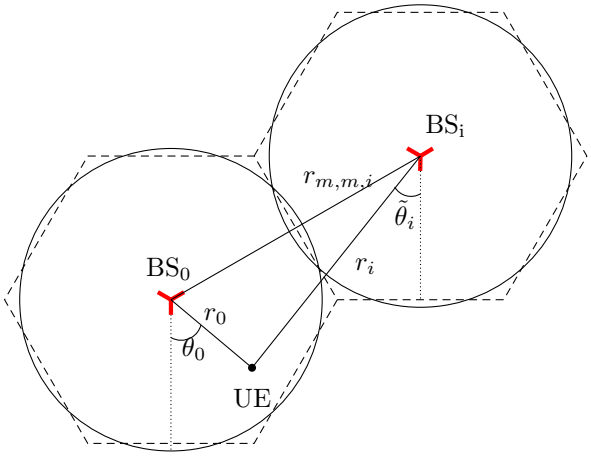

Figure 4.8: Interference scenarios for a macrocell user: Interferers are macrocells

culated as follows:

$$\tilde{I}_{m2} = \sum_{i=1}^{6} \frac{N_{mu}/3 \cdot P_{\text{tx}} \cdot [G(\tilde{\theta}_i) + G(\tilde{\theta}_i') + G(\tilde{\theta}_i'')]}{PL_o(r_i)} \tag{4.35}$$

where $\tilde{\theta}_i$ is the angle to a neighbouring macrocell base station, and r_i is the corresponding distance from the macrocell user to this macrocell base station. The value of i is from 1 to 6. This equation gives the aggregation of interference from all neighbouring macrocells.

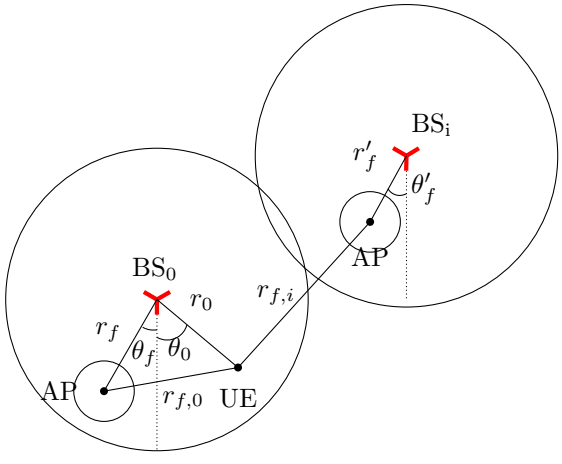

Figure 4.9: Interference scenarios for a macrocell user: Interferers are femtocell APs

Figure 4.9 shows the interference scenario for a macrocell user, where the interference from femtocells. $\tilde{I}_{m3}$ and $\tilde{I}_{m4}$ represent the femtocell interference that is located in the local macrocell area and the neighbouring macrocells. $\tilde{I}_{m3}$ is considered in the single macrocell scenario, i.e. $\tilde{I}_{m3} = I_{m2}$. $\tilde{I}_{m4}$ can be expressed by:

$$\tilde{I}_{m4} = \sum_{i=1}^{6} \int_{0}^{2\pi} \int_{R_{min}}^{R_m} \rho_f \cdot \frac{P'_f(r'_f)}{PL_c(r_{f,i}(r'_f, \theta'_f))} r'_f dr'_f d\theta'_f \tag{4.36}$$

where P'_f is a function of r'_f, which is the distance between the interferer femtocell in the neighbouring macrocell to its local macrocell base station. $r_{f,i}$ is the distance between the interferer femtocells to the investigated macrocell user. Finally, this equation aggregates the femtocells, interference in all six adjacent macrocells.

As it has been mentioned, each macrocell user received signal SINR should be higher than a target value. Therefore, it can be expressed as the following inequality:

$$SINR_{tar,m} \leqslant \frac{|h_0|^2 P_{m0}}{\sum_{k=1}^{4} |h_k|^2 \tilde{I}_{mk} + \sigma^2} \cdot \frac{SF_m}{R_s} \tag{4.37}$$

where h_0 and $h_k \sim \mathcal{C}N(0,1)$, are Rayleigh channel coefficients. Combined with $\tilde{I}_{m3}$ and $\tilde{I}_{m4}$ expressions, the actual system capacity of this macrocell, based on single user evaluation, can be expressed as:

$$N_{mu} \leqslant 3 \cdot \frac{\frac{SF_m \cdot |h_0|^2 P_{m0}}{SINR_{tar,m} \cdot R_s} + |h_1|^2 P_{m0} - (|h_3|^2 \tilde{I}_{m3} + |h_4|^2 \tilde{I}_{m4} + \sigma^2)}{P_{\text{tx}} \cdot \{\frac{|h_1|^2 [G(\theta) + G(\theta') + G(\theta'')]}{PL_o(r_0)} + |h_2|^2 \sum \frac{G(\tilde{\theta}_i) + G(\tilde{\theta}'_i) + G(\tilde{\theta}''_i)}{PL_o(r_i)}\}} \tag{4.38}$$

It can be seen that, the system capacity is affected by two factors. First is the deployment of femtocells. When more femtocells are deployed, $\tilde{I}_{m3}$ and $\tilde{I}_{m3}$ increase, which results in a smaller value of N_{mu}. The other factor is the interference from the adjacent macrocells. If the investigated macrocell shares the same frequency channel with its adjacent macrocells, it leads to a lower system capacity.

In a multiple macrocell scenario, each macrocell user's throughput can

be obtained as follows:

$$\tilde{\mathcal{T}}_m = \log_2(1 + \frac{SF_m}{R_s} \cdot \frac{|h_0|^2 P_{m0}}{\sum_{k=1}^{4} |h_k|^2 \tilde{I}_{mk} + \sigma^2}) \tag{4.39}$$

4.4.2 Femtocell Users' performance

For a femtocell user's performance consideration, it may be affected by the following interferers: if more than one user is located in the same femtocell, the transmission power from the local femtocell to the other user(s) causes interference to the investigated femtocell user; the local macrocell and adjacent macrocells are all introducing interference to a femtocell user; the adjacent femtocells, whether located in the local macrocell, or neighbouring macrocell, all cause interference to a femtocell user. Based on this analysis, each interference is calculated as follows.

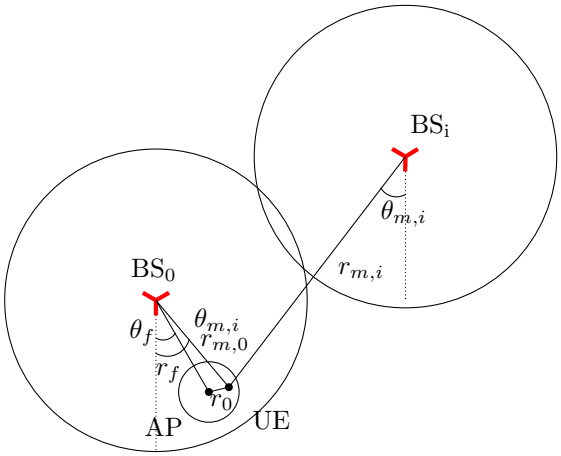

Figure 4.10: Interference scenarios for a femtocell user: Interferers are macrocells

Figure 4.10 shows an interference scenario that the interferers are the local femtocell, local macrocell and adjacent macrocells. $\tilde{I}_{f1}$ is the interference from the local femtocell, when this femtocell is supporting more than one active mobile users. It has $\tilde{I}_{f1} = I_{f1}$. $\tilde{I}_{f2}$ represents the interference from macrocells. The calculation is given as:

$$\tilde{I}_{f2} = \sum_{i=0}^{6} \frac{N_{mu}/3 \cdot P_{\text{tx}} \cdot [G(\theta_{m,i}) + G(\theta_{m,i})' + G(\theta_{m,i})'']}{PL_c(r_{m,i})} \tag{4.40}$$

where i indicates the index of the adjacent macrocells. r_0 is the distance to the local femtocell, and $r_{m,i}$ is the distance to the macrocells. $G(\theta_{m,i})$ is the angle to each macrocell, and $G(\theta'_{m,i})$ and $G(\theta''_{m,i})$ denote the antenna gains from the other two sectors. $\tilde{I}_{f2}$ aggregates the interference from all macrocells, including the local macrocell and adjacent macrocells.

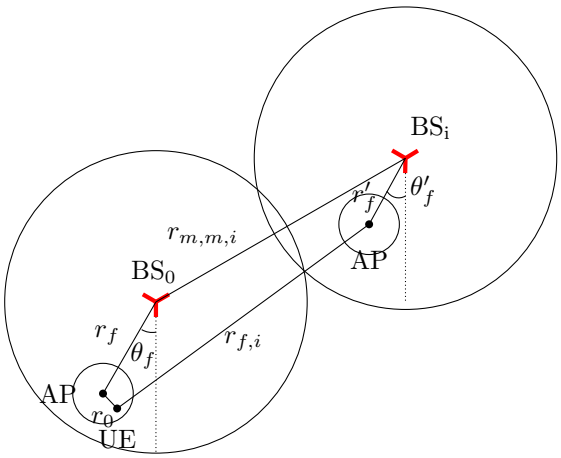

Figure 4.11: Interference scenarios for a femtocell user: Interferers are femtocell APs

A femtocell user also suffers as a result of the interference from neighbouring femtocells. They could be intra femtocells, which are deployed in the local macrocell, or could be inter femtocells, which are deployed in other adjacent macrocells. Figure 4.11 shows a scenario with the interference to a femtocell user from other femtocells. The analysis of interference from the intra femtocells is given in a single macrocell scenario, therefore, $\tilde{I}_{f3} = I_{f3}$. The interference from inter femtocells can be calculated by:

$$\tilde{I}_{f4} = \sum_{i=1}^{6} \int_{0}^{2\pi} \int_{R_{\min}}^{R_m} \rho_f \cdot \frac{P'_f(r'_f)}{PL_c(r_{f,i}(r'_f, \theta'_f))} r'_f dr'_f d\theta'_f \tag{4.41}$$

where the transmission power $P'_f$of the interferer femtocell is a function of the distance between it's nearest macrocell and itself, r'_f. The distance between the interferer femtocell and the victim femtocell user is $r_{f,i}$, and i represents the index of the adjacent macrocells.

Based on the above interference analysis for a femtocell user, its received SINR should be larger than $\text{SINR}_{\text{tar},f}$. Therefore, the following inequality should be satisfied:

$$\mathrm{SINR}_{\mathrm{tar},f} \leqslant \frac{|h_0|^2 P_{f0}/[PL_i(r_0)\cdot N_{fu}]}{\sum_{k=1}^{4}|h_k|^2\tilde{I}_{fk}+\sigma^2}\cdot\frac{SF_f}{R_s} \tag{4.42}$$

where h_0 ~Nakagami(m,Ω), and $h_k \sim \mathcal{CN}(0,1)$. In this equation, SF_f is adjustable, to achieve an optimal femtocell capacity. Therefore, the constraint for the possible value of SF_f is:

$$SF_f \geqslant \frac{\mathrm{SINR}_{\mathrm{tar},f}\cdot R_s\cdot(\sum_{k=1}^{4}|h_k|^2\tilde{I}_{fk}+\sigma^2)}{|h_0|^2 P_{f0}/[PL_i(r_0)\cdot N_{fu}]} \tag{4.43}$$

Therefore, each femtocell user's throughput in a multiple macrocell scenario can be expressed as:

$$\tilde{\mathcal{T}}_f = \log_2\left(1+\frac{SF_f}{R_s}\cdot\frac{|h_0|^2 P_{f0}/[PL_i(r_0)\cdot N_{fu}]}{\sum_{k=1}^{4}|h_k|^2\tilde{I}_{fk}+\sigma^2}\right) \tag{4.44}$$

4.4.3 Simulation Results

Simulation scenario realisation

Figure 4.12 shows an example of simulation realisation of a seven-macrocell communication system with femtocells deployed. In each macrocell's coverage, there are 120 active mobile users and 10 femtocells are deployed uniformly. Based on the femtocell switch-off mechanism, which is described in the previous chapter, some femtocells are switched to IDLE mode. In the figure, these IDLE femtocells are distinguished by green circles. The simulation parameters are given by Table 4.1. The following simulation results are based on these parameters and simulation scenario set-ups.

Macrocell capacity with effects of femtocell deployment

It can be noted from Equation (4.38) that the capacity of a WCDMA system is limited by the interference from the adjacent macrocells and femtocells in the same and in different cells. Figure 4.13 shows the comparisons of a WCDMA macrocell capacity for a single macrocell scenario and multiple macrocell scenario. Three major conclusions can be drawn from this figure. First of all, when no femtocells are deployed, a multiple macrocell scenario has a much lower capacity compared with a single macrocell scenario. It is because the adjacent macrocells contribute significant interference if they are allocated in the same channel with the local macrocell. Second, along with the increasing use of femtocells, the capacity decline rate for a multiple

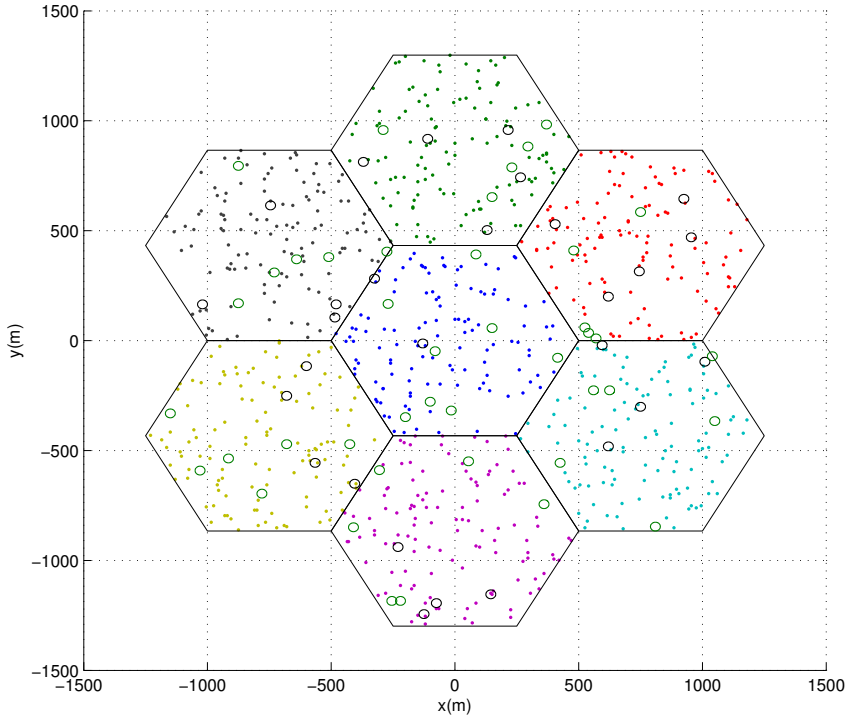

Figure 4.12: A simulation realisation of a seven-macrocell system with femtocells deployment

macrocell case is slower compared with a single macrocell analysis. This is due to the major interference from the macrocells, both the local and adjacent, and the affects from femtocells are weakened. Finally, the Power-Controlled scheme results in a better capacity performance for the system compared with the Fixed-Power scheme, which has the same conclusion as Figure 4.6.

These comparisons provide the basic idea of the range of the systems' capacity performance when the adjacent macrocells are allocated in the same channel, or in different channels. If the adjacent macrocells are allocated in different frequency channels, it results in the performance indicated by the single macrocell analysis, which can be considered as the upper bound. On the other hand, if all macrocells are allocated in the same channel, the system capacity is provided by the multiple macrocell analysis which can be considered as the lower bound. When certain resource allocation algorithms

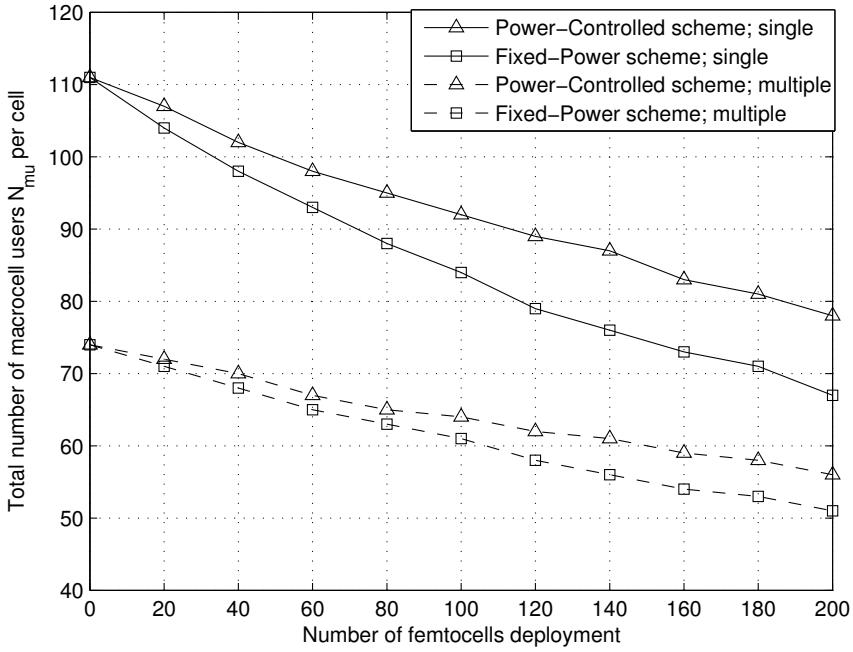

Figure 4.13: Macrocell capacity comparison based on the different femtocell transmission power setting schemes

are applied, the results may fall in the range of previous two analysis.

In the following section, each interference level from the different interferers for a macrocell user and a femtocell user is investigated in order to obtain a comprehensive understanding of the composition of the interference and understand the major interferer to a certain mobile user.

Detailed interference analysis for a single user

Figure 4.14 shows the detailed analysis of interference for a macrocell user, and each interference level is expressed in unit dBm. PC and FP represent Power-Controlled scheme and Fixed-Power scheme in the figure. I_{m1} is the interference from its local macrocell, which is the transmission signal to other mobile users. I_{m2} is the interference from all the adjacent macrocells. It can be seen that, I_{m1} contributes the major interference, and both I_{m1} and I_{m2} are slightly affected by the utilisation of femtocells. I_{m3} and I_{m4} represent the interference from the intra femtocells and inter femtocells respectively. The femtocells located in the local macrocell introduce a higher interference compared with the femtocells in the adjacent macro-

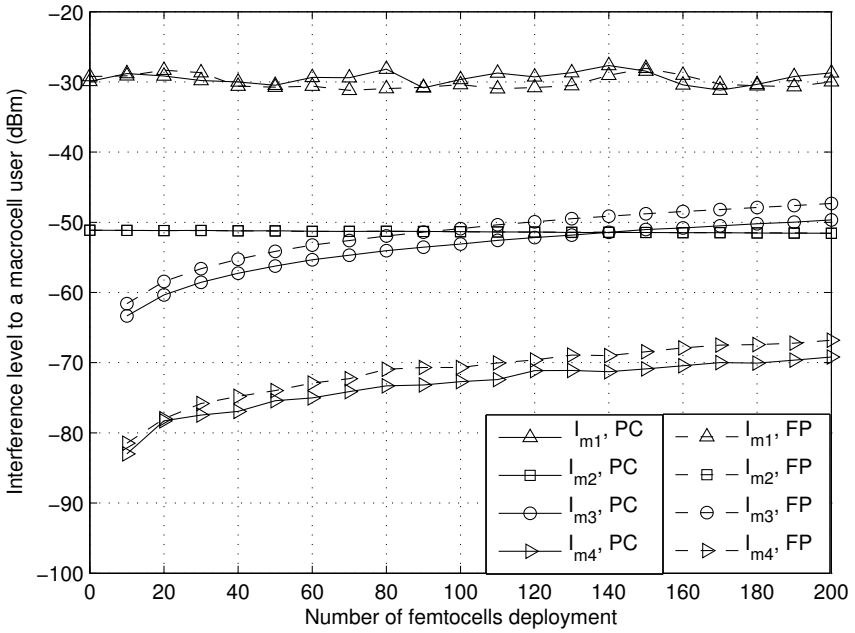

Figure 4.14: Detailed interference analysis for a macrocell user

cells, due to the long transmission distance. With the increase of femtocell deployment, both interference factors increase. It should be noted that, when femtocell deployment is greater than 100 per macrocell with Fixed-Power scheme (or 140 per macrocell with Power-Controlled scheme), the intra femtocells' interference is more significant than the adjacent macrocell interference. Therefore, when femtocells are ubiquitously deployed, the intra femtocells will become one of the major interferers to a macrocell user. At the same time, it also shows that a Fixed-Power scheme results in more interference when compared with the Power-Controlled scheme.

Figure 4.15 gives the interference analysis for a femtocell user. In the majority of simulation realisations, each femtocell is able to cover one active mobile user. In real life, users tend to operate in bursts, and they may not be transmitting at the same time. Therefore, the interference caused by its serving femtocell, which is transmitting signals to other mobile users at the same time, can be neglected. Therefore, the investigated interference for a femtocell user are: I_{f2}, the interference from the local and adjacent macrocells; I_{f3}, the interference from the intra femtocells; and I_{f4}, the interference

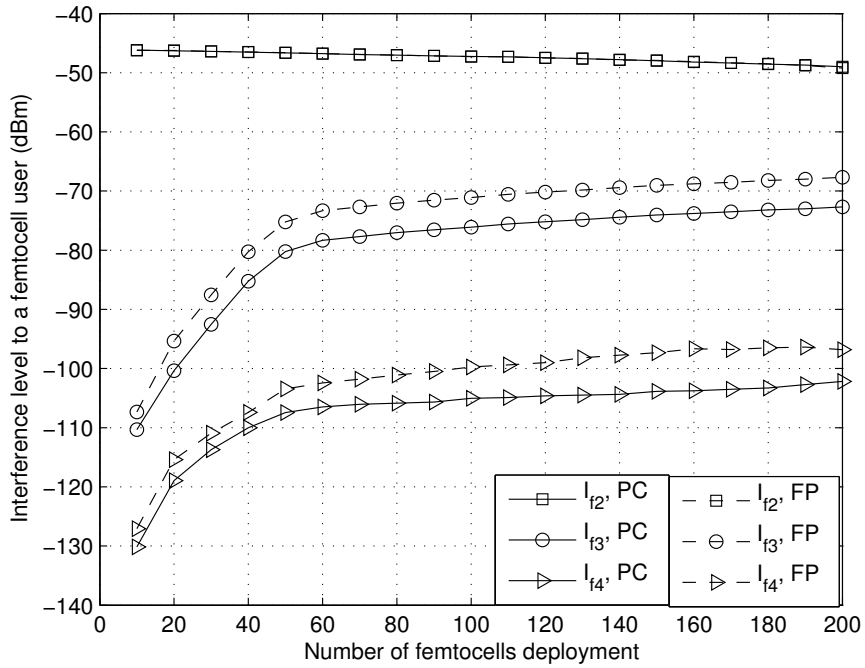

Figure 4.15: Detailed interference analysis for a femtocell user

caused by the inter femtocells. It can be noted that, I_{f2} contributes the major interference to a femtocell user, and it is slightly affected by the utilisation of femtocells. Increased femtocell deployment results in a lower user capacity for the macrocell. Therefore, lower transmission power is required for a macrocell to serve fewer users and lower interference for a femtocell user. I_{f3} and I_{f4} all increase due to more femtocells in the system. It is easy to understand that the intra femtocells cause more interference compared with the inter femtocells, due to the short transmission distance. Additionally, one of the reasons that macrocells cause more interference to a femtocell user than the adjacent femtocells, is that all femtocells are assumed to be installed in homes, and the interference from a femtocell to another experiences two walls of attenuation. The interference from a macrocell to a femtocell user only experiences one wall of attenuation. Finally, the comparison between two femtocell transmission power setting schemes shows that a Power-Controlled scheme results in a slightly lower interference when compared with the Fixed-Power scheme to a femtocell user.

Single user throughput analysis

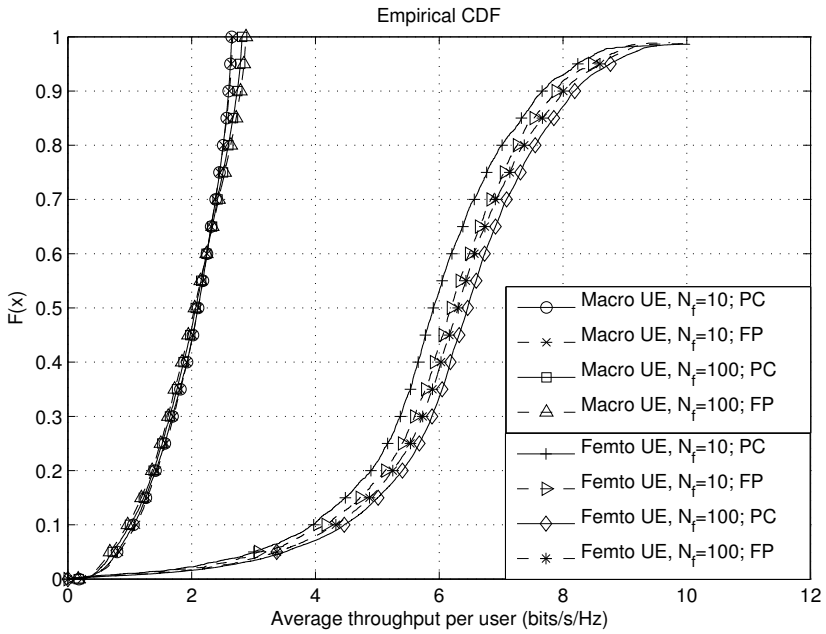

Figure 4.16: Available throughput per user in multiple macrocell scenario

Based on the previous detailed interference analysis to a single user, this section gives the single user throughput performance, by using Equations (4.39) and (4.44). The results are given in Figure 4.16.

It can be noted that, macrocell users have significantly lower throughput compared with femtocell users, since the interference from macrocells is dominant for all users, and it has more influence to a macrocell user. Considering a macrocell user, different femtocell transmission power setting schemes do not result in a significant difference to its throughput performance. When more femtocells are deployed, a macrocell can only support fewer mobile users at the same time. Therefore, there is less resource competition for a macrocell user, and it is more likely to have a higher throughput, as can be seen from the results.

As has been previously mentioned, femtocell users experience a significantly higher throughput compared with macrocell users in a multiple macrocell scenario. It presents approximately a 3 times improvement in throughput. If more femtocells are used, the available throughput for a femtocell user tends to be better. It can be explained by aid of Figure 4.15.

More femtocell utilisation results in a lower I_{f2} contribution, which is the major interference to a femtocell user. Additionally, when the density of femtocell deployment is low, the Fixed-Power scheme is able to provide a relatively better performance. However, if the femtocell usage increases, the femtocells with the Fixed-Power scheme introduce significant interference to the neighbouring femtocells, and a femtocell user will have a reduced throughput performance when compared with the Power-Controlled scheme.

4.5 Summary

This chapter focuses on the mathematical analysis of the trade-off between the system power consumption and QoS, with different femtocell deployments. In this work, the downlink of a WCDMA system is considered, where femtocells are allocated in the same spectrum as a macrocell. Both single macrocell scenario and multiple macrocell scenario are investigated. A comprehensive investigation of two femtocell transmission power setting schemes is applied, which are a Power-Controlled and a Fixed-Power scheme.

The results show that, by using the Power-Controlled scheme for defining femtocell transmission power, it is possible to save around 50% power compared with a Fixed-Power scheme. It is shown that femtocell usage decreases the macrocell capacity significantly in the co-channel configuration, to the extent that, in a high femtocell deployment scenario, the macrocell capacity drops significantly. On the other hand, when femtocells are sparsely deployed, the Fixed-Power scheme can improve the throughput for femtocell users, without introducing a significant interference to the macrocell. Thus, below a certain density of femtocell deployments, femtocells should transmit with full power. However, above this threshold, the Power-Controlled scheme should be adopted.

5

Combined WLAN and Cellular Network Architecture

Femtocells save power by offloading long distance communication traffic from the macrocell, avoiding the construction of new base stations due to the expanding demand, as shown by previous chapters. However, they still give rise to extra power consumption from hardware investment, which is also known as the embodied energy [99].

At the same time, due to the increase of smartphone penetration, more mobile users are able to access the Internet via a WLAN, by employing an 802.11 air interface. The utilisation of WLANs has grown dramatically, with statistics showing that there are nearly 13,000 and 37,000 hotspots in the UK and US respectively [29, 30]. Because WLANs are ubiquitously deployed in residences and public area, there is no extra embodied energy input to be considered, which is an advantage compared to femtocell deployment. In addition, WLANs occupy the unlicensed spectrum, which leads to a much broader bandwidth than the cellular network. For these reasons, the WLAN is another potential network for reducing power consumption and also provides a better bandwidth. Therefore, it should be considered as a means of offloading traffic from the macrocell.

In this chapter, a cooperative heterogeneous network combining femtocells and WLANs is studied. It includes investigation of the power efficiency and user QoS experience, in different configuration scenarios. In particular, the embodied energy of equipment is considered, which leads to a comprehensive power analysis. The effects of data traffic volume and smartphone usage are also studied. To assess the QoS of users, the available bandwidth per user is analysed.

5.1 Femtocell and WLAN Cooperative Network

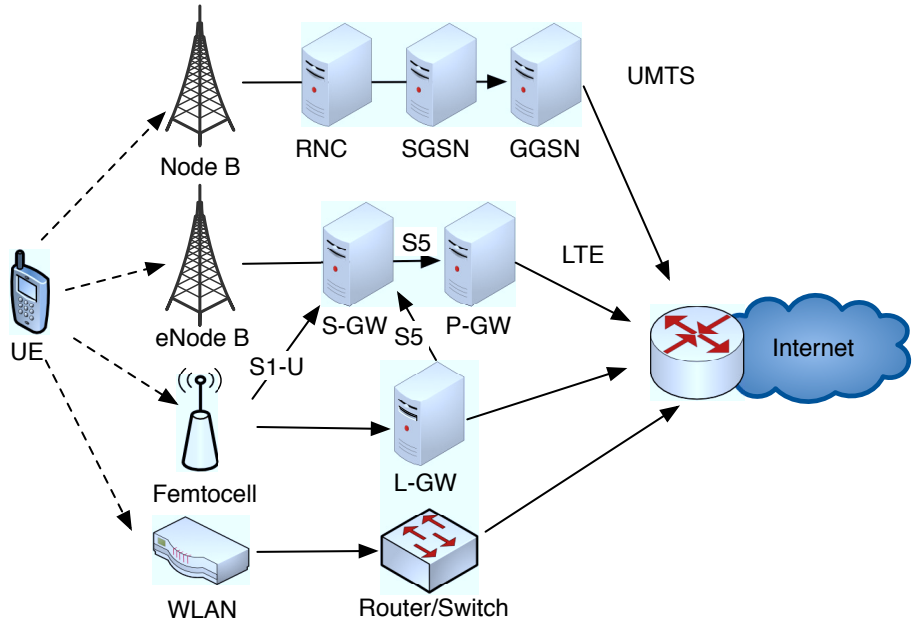

Fig. 5.1: Overview of data traffic flow in heterogeneous network architectures

Due to the significant increase of data traffic over an IP network, the different network architectures are able to cooperate with each other, and are likely to achieve both an energy efficiency and a high QoS communication solution [114]. The possible network architectures, that are able to cooperate with each other, are shown in Figure 5.1. It can be seen that, the four network architectures are UMTS macrocell, LTE macrocell, Femtocell and WLAN. They deliver IP packets through different servers and units. For instance, the uplink IP packet, delivered from a mobile user in a UMTS network, will firstly send to the nearest UMTS base station (Node B), then it will be delivered via Radio Network Controller (RNC), Serving GPRS support node (SGSN) and Gateway GPRS support node (GGSN). Within these units, the data traffic is processed, re-directed and forwarded to the Internet, or other networks. In an LTE network, a base station controller is not required, and instead the LTE base station (eNode B) connects to a Serving Gateway (S-GW) directly. It can route and forward the data packets and is able to reduce the latency and improve the mobility. Then

the data traffic is handled by a PDN Gateway (P-GW). It provides the connectivity for a mobile user to the external network, including the Internet. A mobile user may have simultaneous connectivity with more than one P-GW for accessing multiple PDNs (Packet Data Network). For a femtocell, or a WLAN access, the data packets are delivered in a simpler fashion. If the service from a femtocell, or a WLAN is available, a smartphone user can transmit the data to a femtocell or WLAN access point, then they connect with a Local Gateway (L-GW) or a router, or a third layer switch respectively. These network units are able to forward the data to other networks or to the Internet. Based on these possible data packet routings, the data offloading specifications are discussed in 3GPP standards, which are described in the following section.

5.1.1 Data offloading specifications in 3GPP

The 3rd Generation Partnership Project (3GPP) has been working on the data offloading specifications since Release 8, and it has been well developed after Release 10 [115, 116]. There are three concepts proposed for defining the different data offloading scenarios. They are Local IP Access (LIPA), Selected IP Traffic Offload (SIPTO) and IP Flow Mobility (IFOM). LIPA and SIPTO methods are specified by the data offloading scenarios occurring within 3GPP accesses, such as GPRS, UMTS, EDGE, HSPA, LTE and LTE Advanced. IFOM is focusing on the data offloading between 3GPP accesses and non-3GPP accesses, including trusted accesses, e.g. CDMA 2000, and untrusted accesses, e.g. WLAN. These three IP based data offloading methods are described as follows:

LIPA

The detailed specifications of LIPA is defined in [64, 65], which give the technical requirements and typical communication scenarios and configurations. LIPA describes the connectivities within a local cellular network, i.e. femtocell. A mobile user in a femtocell is able to access all the other resources within this local network, such as laptops, tablets, printers and video conferencing units, without the data packets detouring via the macrocell cellular network. It also allows the mobile user to access the external network through an L-GW. Its function is similar to a Local Area Network (LAN), but with a cellular air interface. For example, the interface between

femtocell (HeNB) and S-GW in LTE is S1-U, and the interface between femtocell L-GW and the S-GW is S5.

SIPTO

SIPTO overcomes the limitation that LIPA can only be used within one femtocell, or femtocells (in an enterprise scenario). It provides the ability to offload the data packets between femtocells and macrocells based on topological or geographical location of users [65, 117]. It's able to reduce the load on the system, and save the transmission power at the macrocell base station. The data offload between macrocells and femtocells is transparent to mobile users, with minimal impacts on the user's experience. On the other hand, it doesn't ease the congestion in the cellular core network, and it is constrained by the limited spectral resource of each operator.

IFOM

IFOM provides a method that enables the data offloading between typical cellular networks and WLAN [61]. It is possible for a mobile user to have multiple PDN connections simultaneously with a 3GPP network and WLAN by using IFOM. The user has the ability to add, or delete, any PDN connection over either of the accesses [62]. Due to the complexity of the data offloading between cellular network and WLAN, such as the data packet formatting, handover decision making and network selection, Dual Stack Mobile IPv6 (DSMIPv6) protocol and Access Network Discovery and Selection Function (ANDSF) are proposed for the aids of technical specifications and configurations for this scenario.

5.1.2 Data Offload Priority Analysis

In reality, the operators have control over selecting the data offload network and offload method. In this work, one data offload priority setting is proposed, in order to balance the system energy efficiency and user QoS.

Considering that most IP based data applications do not require real time communication, a WLAN becomes a viable option for offloading this mobile traffic. However, because of the need to maintain QoS, it may not be possible to also offload voice traffic onto WLAN systems. Hence, with the consideration of the technical specifications described previously, the possible four scenarios of the cooperation of macrocell, femtocell and WLAN can be observed in Figure 5.2 and are discussed in the following sections.

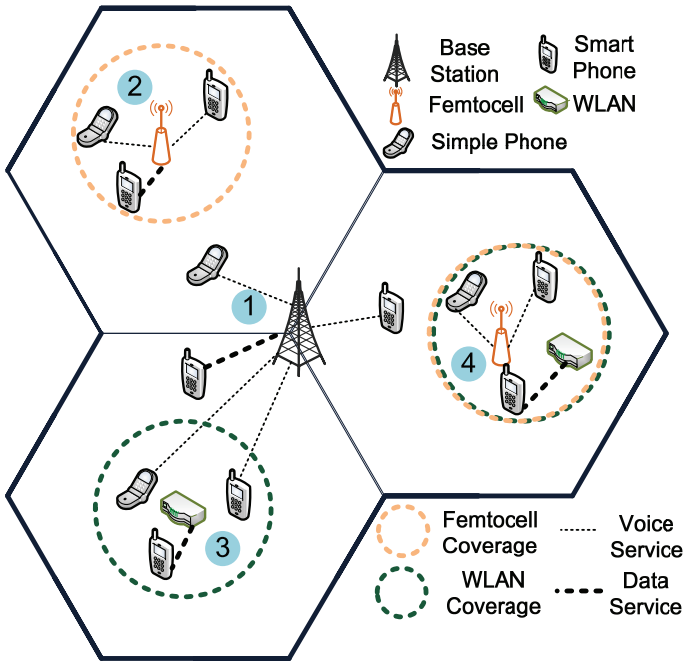

Fig. 5.2: A snapshot of the cooperative architecture of femtocells and WLANs

No local network coverage

In the first scenario, if one user is not covered by any local network, this user will receive service form the nearest macrocell. This user may experience a low QoS, or high power consumption, due to the long distance transmission. When a smartphone requires a data service from the macrocell, the QoS cannot be guaranteed, since a lot of users are competing for the same resource.

Only femtocell coverage

When one user is covered by a femtocell, the traffic can be offloaded from the macrocell for both the voice and the data service by using LIPA/SIPTO method. This results in a significant reduction in power and also provides a relatively higher QoS when compared with the macrocell [99]. However, note that the capacity of the femtocell may be affected by the limited spectrum and interference from the macrocell and the neighbouring femtocells. Additionally, when the number of users in a femtocell exceeds the capacity that one femtocell can support, the traffic from the extra users cannot be

offloaded from the macrocell to the femtocell.

Only WLAN coverage

In this scenario, the ability to offload traffic depends on two factors: first, the user is using a smartphone to get service from a WLAN, because it requires an 802.11 air interface to connect with a WLAN; second, due to the need to maintain QoS, only data services can be offloaded to a WLAN. In these cases, the IFOM mechanism is implemented, enabling the traffic to be offloaded from a cellular network to a WLAN. It can be seen from Figure 5.2, that the traffic from a simple phone, and the voice services from a smartphone, are all retained with the macrocell. Because of the constraints for offloading, only a limited number of users can experience the benefit from it. However, with the move to higher rate WLAN support by network operators, the WLAN is more able to provide a better QoS compared with the femtocell, and increases the system capacity.

Both femtocell and WLAN coverage

When a femtocell and a WLAN all cover the same area, which is highly likely, if the femtocell and the WLAN are both home-installed, the scenario is complex. The service from a simple phone user, or the voice service of a smartphone, will be switched to the local femtocell by using LIPA/SIPTO configuration. The data service will be switched to the WLAN in the first instance, with the aid of IFOM.

5.2 Status of Communication System and Problem Overview

5.2.1 Status

In order to evaluate the heterogeneous network performance, a baseline system should be set. A report from Ofcom [118] indicates some key figures of the current communication system, which help to set a reasonable baseline system.

It shows that, a quarter of mobile customers claim that they own a smartphone in Q1 2010, whilst this figure was lower than 15% one year previously. The increase is significant; the smartphone usage of adults in the UK around 40% in Q1 2012. This report suggests that 66% of UK homes used wireless routers in Q1 2010. Considering the home broadband speed, although the advertised value can achieve 24 Mbps, 50 Mbps or even greater,

the average actual speed is 5.2 Mbps (May 2010). This value was 4.1 Mbps the year before. In this report, it is indicated that 56% of smartphone users claimed to use data services frequently, and only 22% said that they did not use them at all. Table 5.1 lists all related data.

Table 5.1: Ofcom Data [118]

Description	Value	Reported Time
Smartphone Usage	15%	Q1, 2009
Smartphone Usage	25%	Q1, 2010
WLAN Deployment Rate	66%	Q1, 2010
Average Home Broadband Speed	4.1 Mbps	April, 2009
Average Home Broadband Speed	5.2Mbps	May, 2010
Smartphone user frequently use data service	56%	Q1, 2010
Smartphone user never use data service	22%	Q1, 2010

Based on the current communication system status, the baseline parameters are selected for the simulations: smartphone usage is 25%, average home broadband speed is 5 Mbps, and WLAN deployment rate is 70%.

5.2.2 Problems

It has been previously shown that femtocell adoption is able to decrease the system power consumption significantly by offloading the mobile traffic from the macrocell. However, along with the increase of the femtocell usage, the embodied energy of the femtocells becomes significant, and may offset the benefits. On the other hand, since WLANs are already commonly installed in homes and in public areas, no further embodied energy investment is required. Thus WLANs may be considered as an alternative low power consumption traffic-offloading network.

From the QoS point of view, a femtocell is able to provide a similar bandwidth for relatively fewer customers compared to a macrocell, resulting in a better QoS provision. However, due to the limited spectrum of cellular networks, the available bandwidth for the femtocell is restricted. There is less of a constraint for WLANs. They use unlicensed spectrum, there is much more room for the WLAN to offer a broader bandwidth. Additionally, since only the data service is offloaded to the WLAN, fewer users are competing for the resource, which means each user is able to achieve a better data

rate. Finally, the WLAN uses cable or ADSL as a backhaul, which is low cost. On the contrary, there are a number of options for backhaul for a femtocell, which may result in a high power consumption from a wireless backhaul or an comparable requirement where the backhaul is achieved over cable or ADSL. These reasons mean that WLANs have the potential to be a significant component in next generation communications.

The study conducted in this chapter is tackling three scenarios that need to be considered in order to understand the femtocell and the WLAN cooperation benefits, for both power efficiency and QoS:

1. The baseline system is discussed first, which shows where we stand in the current communication system, and sets a comparison target for the following scenarios.

2. Over the long term prediction, an increase in the volume of data service is expected. In this scenario, the cooperative network will be examined based on different volumes of data usage.

3. It has been already noted that the increase of smartphone usage is explosive. Given this trend, smartphones will eventually replace the simple phone in the future. Therefore in the final scenario, smartphone usage is discussed. Finally, some conclusions are drawn, combining the data volume and smartphone usage analysis.

5.3 Simulation Setup

In this section, the considered simulation model and parameters are discussed respectively.

5.3.1 Simulation Model

The same large scale scenario as Chapter 3 is considered. The scenario area is 10 km×10 km, with a population of 200,000 of which 95% are mobile users. There are 65,000 homes located in this area. It is assumed that each customer is considered as an active user for about one hour per 12 hours of day time, including internet usage and SMS messaging. It should be noted that, in the previous assumption the cell phone usage is limited to half an hour of the day, which only accounts for voice service. In this chapter the average usage time is increased to one hour to account for both voice

and data traffic. During the day time, these active users' positions follow a normal distribution, and the peak point can be considered as the city centre. The distribution of homes has multiple peaks, with each concentration being normally distributed. The femtocell access point distribution corresponds to residence distribution, since the femtocells are currently being targeted at residential users. As WLANs are ubiquitously installed in both homes and public areas, it is assumed that the distribution of WLAN is a combination of active users and homes.

The resolution of this area is 100 m×100 m, it means that this area is divided into 10,000 units. It is assumed that the radius of the femtocell and WLAN are R_f and R_w respectively. In this chapter it is assumed that a femtocell and a WLAN coverage is a round area with 10 m radius. The number of femtocells and WLANs in a unit is N_f and N_w respectively. Therefore, the probabilities of one user being covered by a femtocell or a WLAN are given by the following equations, assuming there is no overlap between internal networks:

$$\eta_f = N_f \cdot \left(\frac{\pi R_f^2}{100^2} \right) \tag{5.1}$$

$$\eta_w = N_w \cdot \left(\frac{\pi R_w^2}{100^2} \right) \tag{5.2}$$

If in one unit there are N_u active users, the number of users who are likely served by a femtocell or a WLAN are given as $N_u \cdot \eta_f$ and $N_u \cdot \eta_w$.

In order to calculate the sum of users serviced by a local network, the following constrains are applied. For femtocells, the number of users should be within the capacity of femtocell; any additional users are not considered as femtocell users. For WLANs, users that are located in a WLAN coverage and using a smartphone for a data service, are considered as a WLAN user. By applying the above rules for each user, the overall numbers of femtocell users and WLAN users are given as:

$$n_f = \sum_i N_{u_i} \cdot \eta_{f_i} \tag{5.3}$$

$$n_w = \sum_i N_{u_i} \cdot \eta_{w_i} \tag{5.4}$$

The corresponding required numbers of femtocells and WLANs can be cacculated as well (n_{femto} and n_{wlan}). The number of outdoor active users can be calculated from Equations. 5.3 and 5.4.

$$n_{\text{active\_user}} = n_{\text{user}} - (n_f + n_w) \tag{5.5}$$

Hence, the required number of base stations can be derived as:

$$n_{\text{BS}} = n_{\text{active\_user}}/\rho_{\text{BS}} \tag{5.6}$$

where ρ_{BS} is the capacity of a macrocell.

Based on all the analysis of the above, the system power consumption can be computed as:

$$P_{\text{user}} = \sum_i \frac{n_i \cdot P_{\text{Cap}_i} + n_i \cdot P_{\text{Op}_i}}{n_{\text{user}}} \tag{5.7}$$

where i selects between the BS, MT, Femtocell and WLAN. It consists of Embodied Power (P_{Cap}) and Operational Power (P_{Op}). The parameters values are listed in Table. 5.3. The mobile terminal's operational energy is given by the equation 3.5.

It is assumed that each user asks for the same QoS requirement, thus, the available bandwidth is based on the total bandwidth and the number of users of sharing the same resource.

5.3.2 Other Parameters

Based on the discussion of above, the related parameters are concluded and listed in Table. 5.2 and Table. 5.3. It should be noted that the embodied energy of a WLAN is neglected in this work. Since WLANs are already ubiquitously installed in the UK, it requires no further hardware investment.

5.4 Baseline System

In the following sections, the cooperative network of femtocells and WLANs is investigated. To begin with, the baseline system will be studied, with the different deployment patterns of femtocells and WLANs. In order to investigate the effects of the data service on the power efficiency and QoS, different volumes of data traffic compared to total traffic are employed in

Table 5.2: Reference Simulation Parameters

Parameter	Value
Scenario	10 km × 10 km
Population	200,000
Number of Homes	65,000
Proportion of Mobile Phone Users	95%
Average Usage of Cell Phone	1 hour/day (incl. data service)
User Demand Distribution	normal distribution
Home Density Distribution	combination of normal distributions
BS Bandwidth	5 MHz [119]
Femtocell Bandwidth	5 MHz
WLAN Bandwidth	5.2 MHz
Femtocell radius	10 m
WLAN radius	10 m

Table 5.3: Cross Reference Table of Embodied Energy and Operational Power of each entity.

Facilities and Equipment	Embodied Energy per sec(W)	Operational Power(W)
RBS	∼1000W (P_{Cap_BS})	∼1500 W (P_{Op_BS})
Femtocell AP	1W (P_{Cap_Femto})	6 W(P_{Op_Femto})
WLAN AP	—	5.6 W(P_{Op_WLAN})
Simple Phone	2.6 W (P_{Cap_MT})	—
SmartPhone	5.2 W (P_{Cap_MT})	—

section 5.5 for analysis. Smartphone usage also is discussed, since it is likely to be widely used in the future, and also has a significant impact on the power consumption and QoS. Finally, some conclusions are drawn, combining the analysis of the effects of data volume and smartphone usage. In the baseline system it is assumed there is no data service requirement. This is because information of the actual proportion of data traffic as a fraction of the total traffic is not available, and it is also depends on the different operators and market strategies. The effect of different levels of data service volume will explored in the next section.

Figure 5.3 shows the result of the system power consumption, with different femtocell and WLAN deployment rates respectively. It can be seen that femtocell adoption can result in a significant power saving for the system. At the same time, the adoption of WLAN does not affect the power

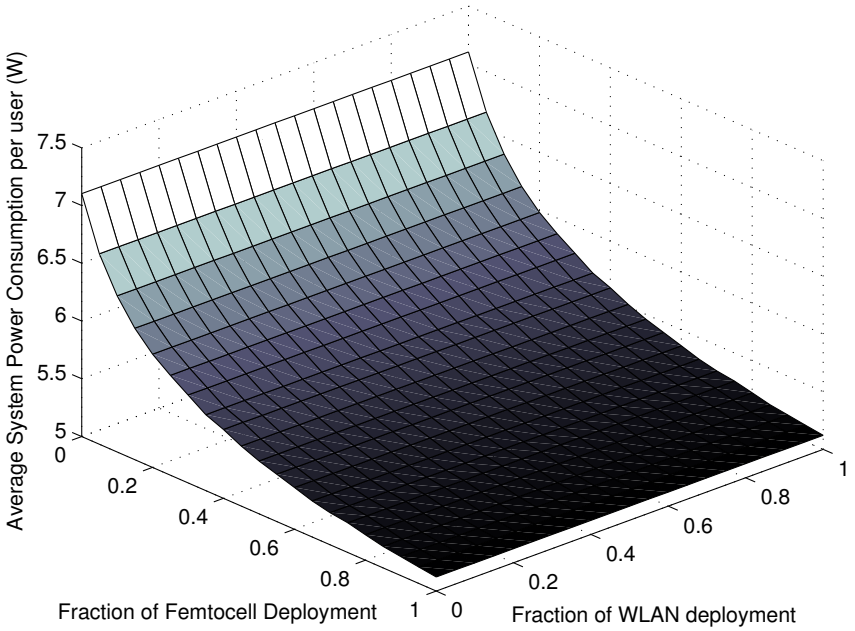

Fig. 5.3: Average power consumption per user with different deployments of femtocells and WLANs: smartphone usage 25%, data traffic 0%

consumption. This is because there is no data service, thus the WLAN does not provide service for mobiles. Moreover, since the WLAN is ubiquitously deployed, there is no hardware investment needed. For the above reasons, the curve is invariant to the increase of WLAN deployment.

Figure 5.4 shows the contribution of each piece of equipment to the overall total power consumption. The main power saving is from the macrocell base stations, since part of the traffic is offloaded to the local network. The rise of data demand is eased by the local network, it can avoid new macrocell construction, and embodied energy is saved significantly. The mobile phone's embodied energy is the major contribution, which consists of 25% smartphones and 75% simple phones. Although along with the increase of femtocell usage, more power consumption from femtocells is added into the system, the mainstream trend of the whole system power consumption declines.

It is noted that the result of Figure 5.4 is significantly different from

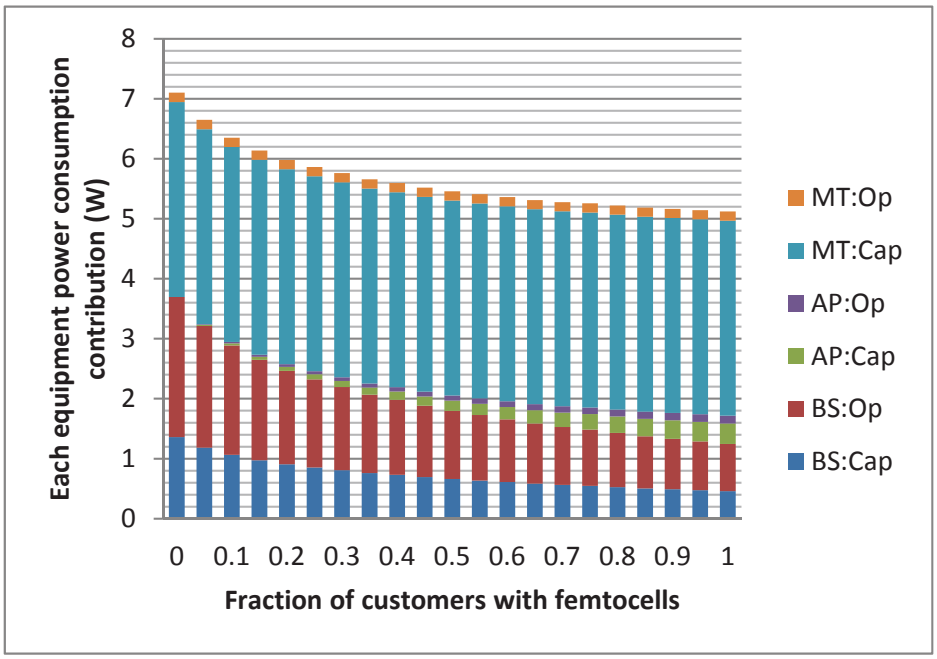

Fig. 5.4: Power consumption of each network component per user when different fractions of users operate femtocells

Figure 3.10, because of three different assumptions between chapter 3 and chapter 5. They are described as follows, the effects of each factor to the system power consumption is illustrated in Figure 5.5. First, the mobile usage increases from half hour per 12 hours of day time in chapter 3 to one hour in chapter 5. In chapter 3, only voice service is considered. However, in chapter 5, both data and voice are included. Two circles indicate the effects of different phone usage patterns. It shows that longer usage contributes higher power consumption when femtocells are not deployed. It also show that, the increasing the deployment of femtocells monotonically decreases the system power consumption. Second, single femtocell coverage is adjusted from 100 m $\times$ 100 m in chapter 3 to a round area of 10 m radius in chapter 5. It shows the smaller size results in more power consumption, since less users are able to be covered by a femtocell. Finally, in chapter 5, smartphone analysis is introduced. For the baseline system, the smartphone usage is 25%. Due to high power consumption of a smartphone, the system power consumption increases. The red curve shows the result from chapter 5, which

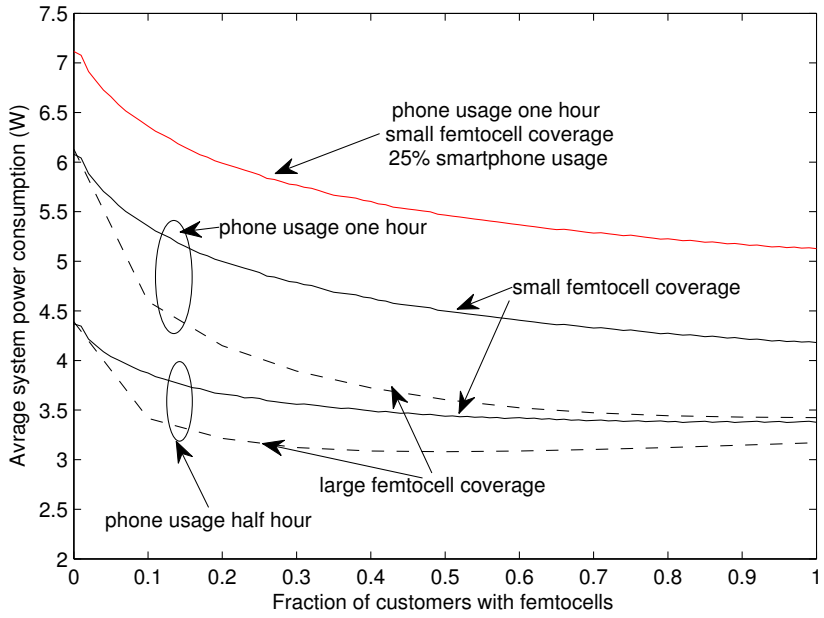

Fig. 5.5: Comparison of simulation results based on different assumptions

considers the smartphone usage, uses the improved model, and has a longer phone usage time. The comparison results between Figure 3.10 (chapter 3) and Figure 5.4 (chapter 5) also shows that, if the coverage of femtocells increases, it is possible to achieve a power efficiency saving by deploying fewer femtocells.

The Energy Reduction Gain is calculated in Figure 5.6, as a function of different femtocell usage. The equation is give by Equation (3.6) in Chapter 3. The overall operational ERG can be as high as 60%. The traffic offloading scheme results in more short-distance local communications, therefore, the operational power saving is from a reduction in operational energy at the macrocell base station and in mobile phones. However, the embodied ERG can only achieve a reduction of 12%. The resulting system ERG can achieve gains of almost 40%.

To determine the QoS benefits, the available bandwidth is evaluated. The results can be seen in Figure 5.7. More femtocell deployments result in a significant bandwidth growth. When the femtocell is 100% utilised, the maximum bandwidth is 1.6 MHz per user on average. On the contrary,

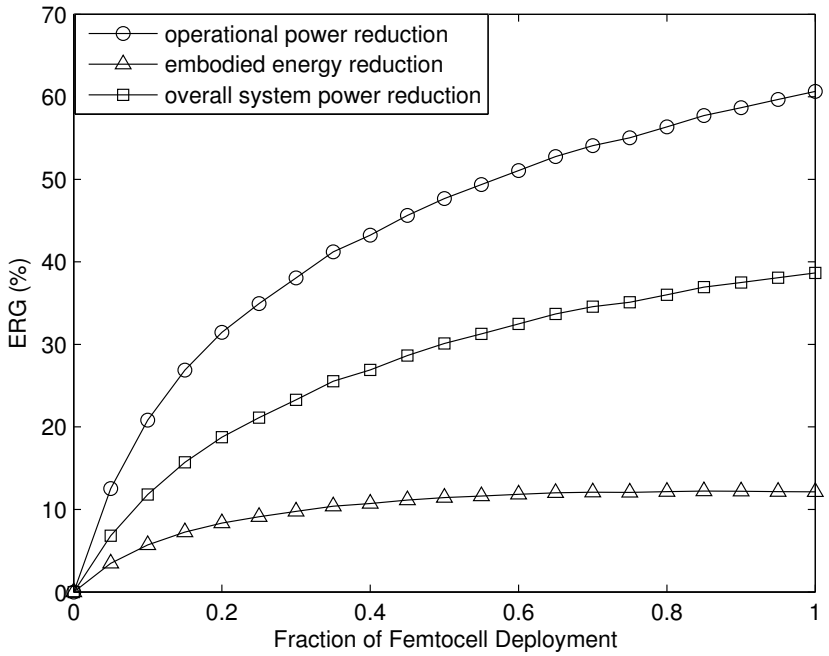

Fig. 5.6: Energy Reduction Gain(ERG) of system power consumption, when different fractions of customers are operating femtocells

before the femtocell is adopted, the average bandwidth is only 80 kHz per user.

This figure also distinguish the performance of the macrocell users and the femtocell users. In this research, it is assumed that each macrocell serves a finite number of users, therefore, the macrocell users are provided a constant available bandwidth. It shows that, the femtocell users' performance increases significantly along with the increase of femtocell usage. Hence, the average QoS for each user is improved as well. When the femtocell is 100% utilised, the maximum bandwidth of femtocell users can achieve to 2.4 MHz per user on average, which is 30 times of the macrocell user's bandwidth.

5.5 Data Service Volume Analysis

In this section, the data service usage is increased compared with the baseline system, and different proportions are evaluated for comparison.

Figure 5.8 shows the results of system power consumption, with the co-

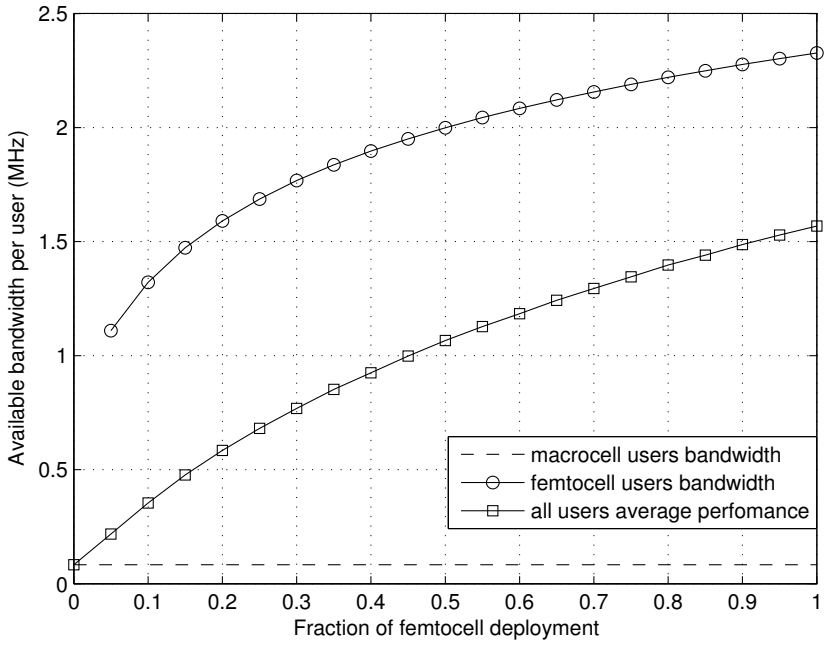

Figure 5.7: Average system available bandwidth when different fractions of customers are operating femtocells

operation of femtocells and WLANs. It can be seen that, the growth of the data service requirement gives prominence to the benefit of WLAN utilisation. A bigger proportion of data service results in a more obvious power saving from WLAN deployment. It can be seen from the simulation results that, when the data traffic increases to 50%, WLAN adoption can achieve an extra 7% power saving compared to the pure femtocell deployment scenario. Similarly, when the data traffic is 100%, the extra power saving from WLAN use is 11%.

Figure 5.9 gives a detailed analysis of power consumption based on different data service requirements. Generally, the growth of data traffic can reduce the power consumption in each scenario. When more femtocells are deployed, less power is consumed from a system's point of view. In addition, when more WLANs are used, the system power decreases, although it is not a significant drop.

Figure 5.10 describes the ERG for different femtocell deployment rates, along with the increase of data traffic. In this result, the WLAN uptake is

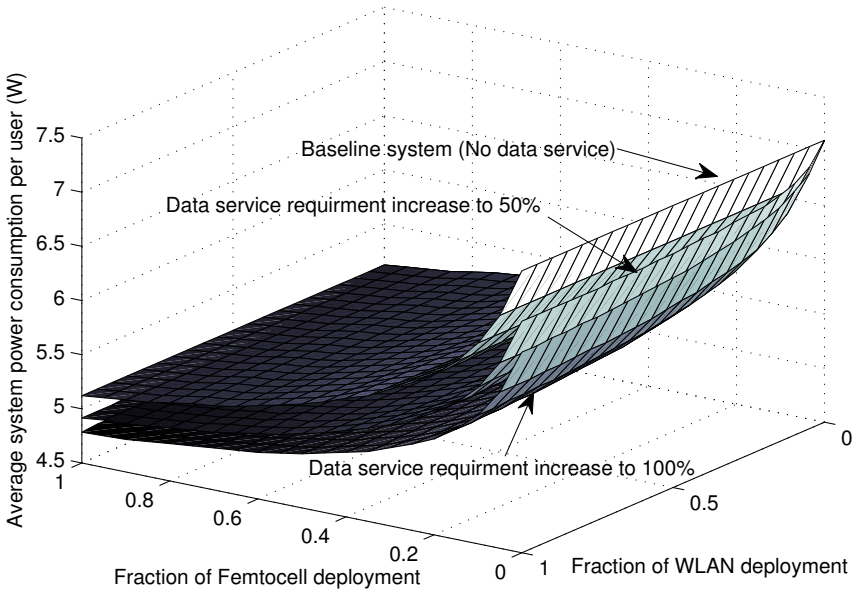

Fig. 5.8: Average power consumption per user for 0%, 50% and 100% data traffic scenarios, with different deployments of femtocells and WLANs: smartphone usage 25%

at a level of 70% of households. It indicates that the deployment of fewer femtocells is able to achieve a higher ERG. This is because a lot of mobile users still receive service from the macrocell. When the data traffic increases, more smartphone users can switch their service from the macrocell to the WLAN, which results in a significant power saving. On the contrary, when the femtocell is ubiquitously used, and the data traffic increases, the users just switch the service from the femtocell to the WLAN. Therefore, the power saving is limited.

Figure 5.11 shows results of system power consumption and available bandwidth, with the cooperation of femtocells and WLANs. From Table 5.1, we know that by Q1 2010 the utilisation rate of WLAN was around 70% in the UK. And the usage of WLAN is still increasing. This is consistent with usage in other countries. Therefore, the cases of 70% and 100% of WLAN adoption are investigated respectively, based on different data traffic volume.

Compared to the baseline system, the offloaded data traffic increases

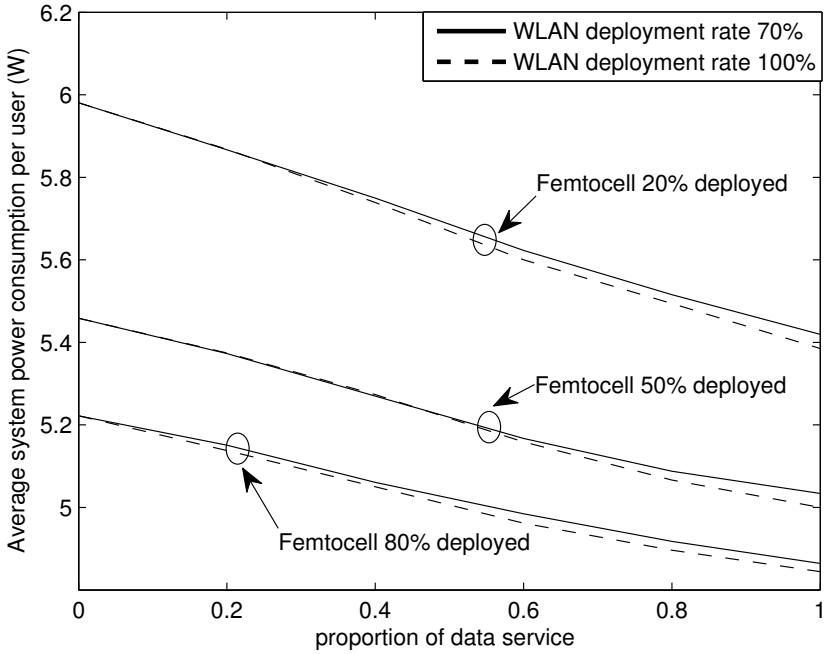

Fig. 5.9: Average power consumption per user, with different proportions of data traffic.

to 50% with 25% smartphone usage, and the average power consumption decreases from 7.1 W to 6.6 W, without femtocell deployment. It results in a 7% energy reduction gain (ERG). If the femtocell is fully installed in this area, the ERG is 4%. This is because in this scenario some of active users are switched from femtocells to WLANs. Since femtocells and WLANs are all low power consuming substitute networks, the benefit from WLANs offloading in a femtocell deployed system is not significant compared to the traditional communication system. Hence, the ERG is reduced. When the data service reaches 100%, the ERG resulting from WLAN offloading is between 6% and 11%. Also, lower femtocell deployment rates contribute a higher ERG, with the aid of WLAN traffic offloading.

Meanwhile, the available bandwidth increases dramatically when the data traffic increases compared to the baseline system. It can be observed that if the femtocell is not adopted yet, but the data traffic increases to 50%, the ubiquitously adopted WLAN can increase the available bandwidth

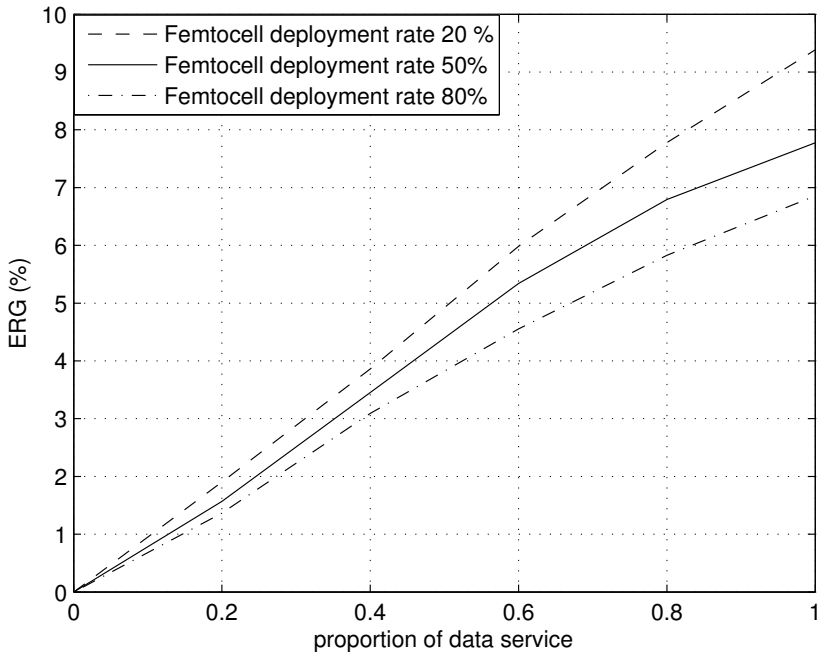

Fig. 5.10: Energy Reduction Gain (ERG) of different deployment rates of femtocells, with different proportions of data traffic.

from 80 kHz to around 600 kHz per user. Again, when the data traffic is 100% of all traffic, more mobile users are able to be switched to the local WLAN, and the bandwidth increases to 800 kHz. Even in the scenario that the femtocells are ubiquitously installed, the WLAN is still able to increase the bandwidth by 12% and 20%, for 50% and 100% data traffic scenarios respectively. The cooperation of two local networks is able to increase the bandwidth to over 1 MHz.

Furthermore, if the proportion of WLAN usage increases beyond 70%, the system power continues reducing, while the user bandwidth improves at the same time, albeit the improvements are not significant.

5.6 Smartphone Usage Analysis

Figure 5.12 indicates the power consumption results with different smartphone usage, when the data service occupies a large proportion of all traffic. When smartphone ownership increases from 25% to 50%, or even 100% over

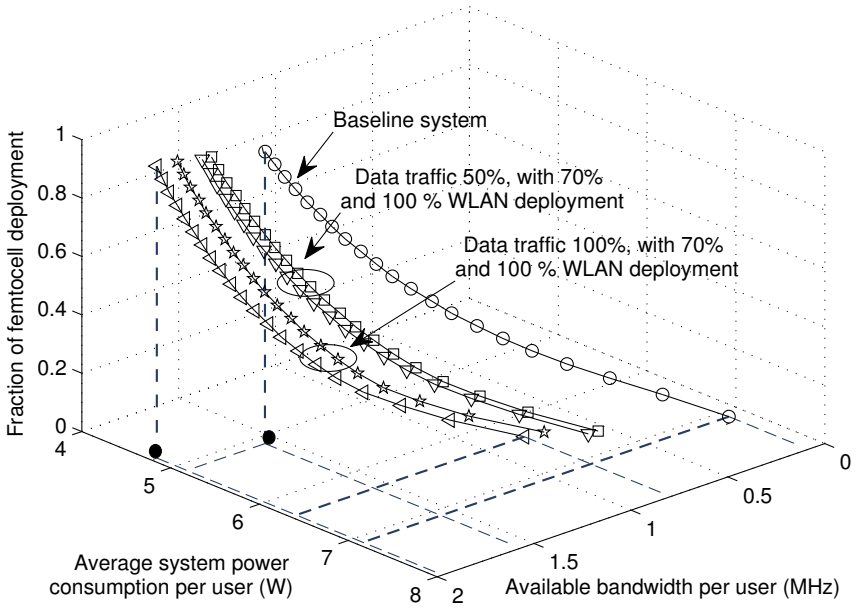

Figure 5.11: System power consumption and available bandwidth per user, with the cooperation of femtocells and WLANs deployment. The data traffic proportion, which can be offloaded, are 0%, 50% and 100% respectively.

a long term period, the power consumption per user grows, which is expected, since a smartphone requires at least double the embodied energy consumption compared to a simple phone.

On the other hand, if the proportion of the data traffic increases to a relatively high value, around 100%, a higher proportion of smartphone users enables more mobile users to get service from the WLAN, and contributes to a significant power saving. As can be seen from Figure 5.12, it is pointed out when the femtocell and WLAN are both ubiquitously adopted, in a high data traffic scenario, high smartphone usage has a lower power consumption compared to a low smartphone usage scenario.

The following results describe the influence of the femtocell deployment, the WLAN deployment and the variable data traffic on the power consumption, in the different smartphone usage scenarios.

In the first scenario, it is assumed that the WLAN uptake is 70%, and that data traffic forms 50% of all traffic. The result is presented in Figure 5.13. All curves show the same trend that, along with the increase of

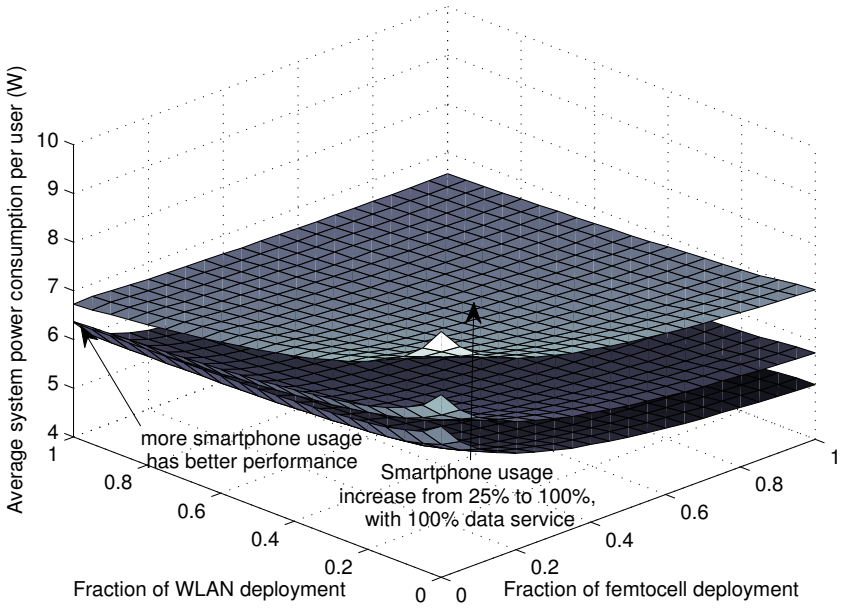

Fig. 5.12: Average power consumption per user for 25%, 50% and 100% smartphone usage scenarios, with different deployments of femtocells and WLANs: data traffic 100%

smartphone usage, the power consumption grows dramatically, due to the significant hardware investment of smartphones. It is clear that increasing the proportion of femtocells results in a higher power saving. However the reduction is moderated by the femtocell's embodied energy contribution.

Figure 5.14 describes the effects of WLAN deployment on the power consumption based on different smartphone usage. The femtocell deployment rate and the data service proportion are set at 50%. Since the WLAN is installed in 70% of homes in the UK in Q1 2010, the starting curve shows the result based on the current status, with the increasing adoption of smartphones. Similarly to Figure 5.13, more smartphones result in higher power consumption. Although the WLAN is already commonly used, if this usage continues to increase, it only results in a limited power saving.

Figure 5.15 examines the influence of the variable data service on the power consumption, with different smartphone usage. In this part, the WLAN and femtocell have a fixed deployment rate of 70% and 50% re-

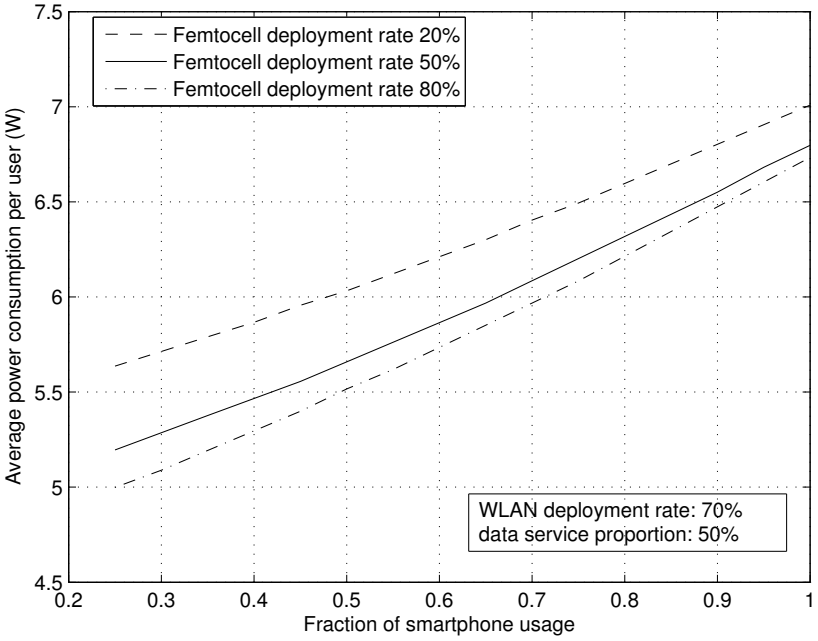

Fig. 5.13: Average power consumption for the different deployment rates of femtocells, in the various smartphone usage scenarios

spectively. It shows that more data traffic leads to more power saving. This is because as more users are using data service, then more users are able to switch their service to a WLAN.

Figure 5.16 indicates the power consumption and bandwidth results with different smartphone usage, when the WLAN installation rate is 70%. Generally, when smartphone ownership increases from 25% to 50%, or even 100%, and the data forms 50% of all traffic, the power consumption per user grows, which is expected, since a smartphone requires at least double the embodied energy consumption compared to a simple phone. On the other hand, the bandwidth benefits from the increase of smartphone usage can be observed. It can be seen that, as more smartphones are used, the higher the bandwidth that can be achieved per user for all different deployment scenarios of femtocells. This is due to the ability to offload more mobile users on to the WLAN, where there is less competition for the resource, and a relatively high bandwidth compared to the macrocell and the femtocell. It should also be noted that, when smartphone usage is 100%, with a lower

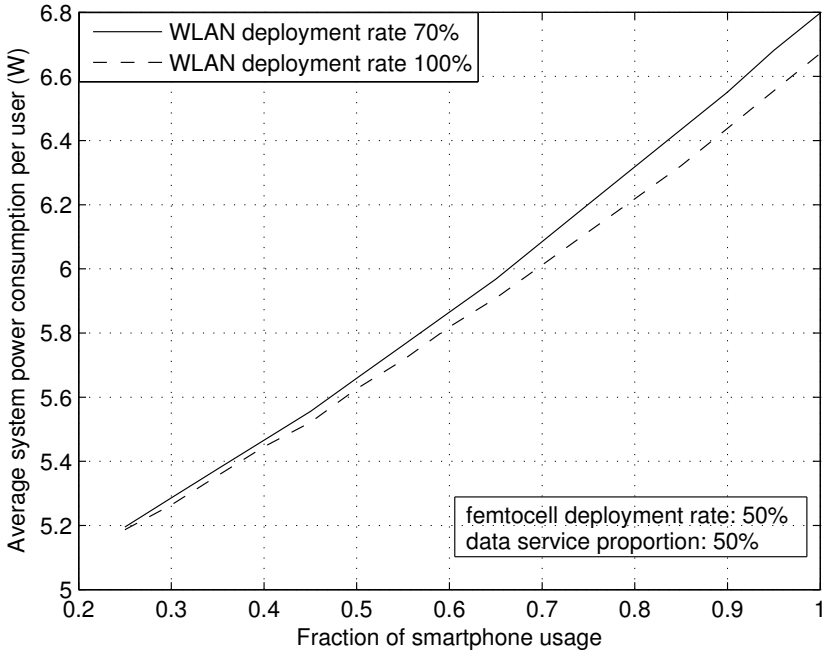

Figure 5.14: Average power consumption for the different deployment rates of WLANs, in the various smartphone usage scenarios

femtocell deployment rate, the cooperative network is still able to provide a high bandwidth for users, compared to the 80 kHz bandwidth for macrocell users.

On the other hand, if the proportion of data traffic increases to a relatively high value, a higher proportion of smartphone users enables more mobile users to get service from the WLAN, and contributes to a significant power saving. In Figure 5.16, the curve representing 25% smartphone usage and 50% data traffic and the curve with 50% smartphone usage and 100% data traffic, show that although higher smartphone usage contributes significant embodied energy, the power saving from WLAN traffic offloading is even greater. In this case, it is less desirable to encourage femtocell deployment, since the extra embodied energy of femtocell access point is significant.

Based on the above analysis, the following conclusions can be drawn:

From the baseline analysis, the femtocell can offload traffic from the macrocell, and contribute a significant power saving, and also increases the

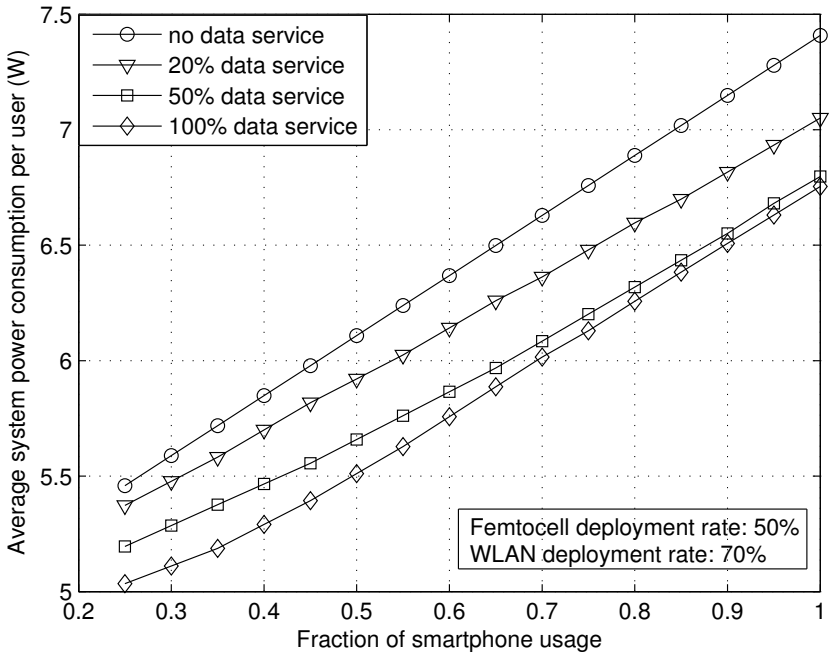

Figure 5.15: Average power consumption for the different proportion of data traffic, in the various smartphone usage scenarios

available bandwidth for users. In this scenario, the WLANs do not provide any service to mobile users.

If the proportion of data traffic is increased, based on the current 25% smartphone customers, the benefit of the WLAN starts to show. The more data traffic within the overall traffic, the more users can be offloaded to the WLAN. This results in a win-win situation for both the power consumption and QoS.

It is a trend that the smartphone is becoming an essential commodity in the longer term. It brings a drawback that it increases the system power consumption significantly, due to the higher embodied energy of the phone itself. However, based on the premise that this increase will happen due to market forces, increased adoption of femtocells and WLAN deployments can reduce the power consumption. In addition, the encouragement of using data services also can decrease the power, due to the increased usage of the WLAN.

Finally, Figure 5.17 gives the detailed power analysis of all system com-

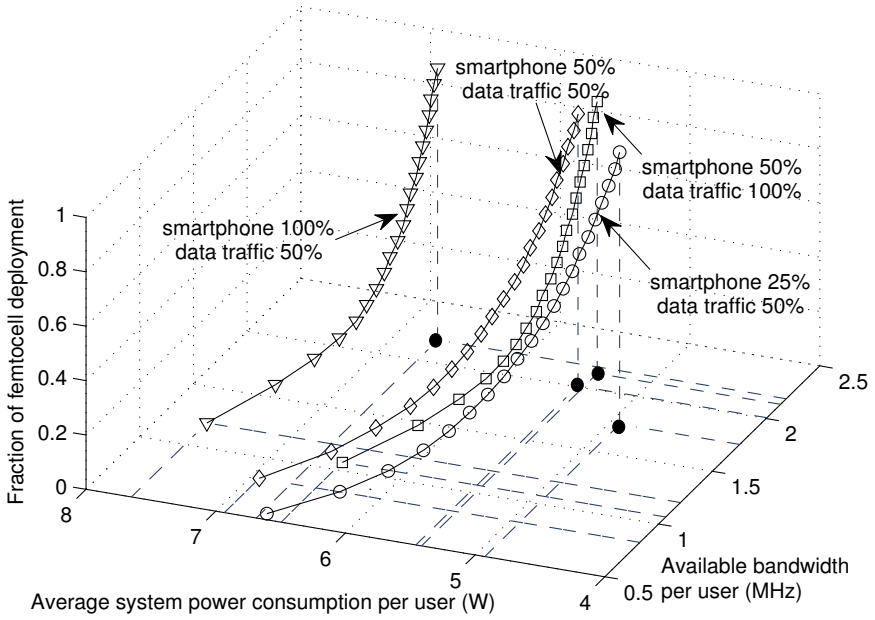

Figure 5.16: System power consumption and available bandwidth per user, with the cooperation of femtocells and WLANs deployment. The smartphone usage increases from 25% to 50% and 100% .

ponents, assuming a mix of 50% of data traffic and 50% smartphone usage. Comparing this with Figure 5.4, it can be seen that the mobile terminal's embodied energy increases significantly, but the base station's power consumption is reduced, since more users get service from the WLANs. The WLAN's operational power increases, but not significantly. Note that the WLAN's embodied energy contribution is neglected, since they are already widely used.

5.7 Summary

In this chapter, a cooperative network architecture was investigated, where femtocells and WLANs are utilised for offloading traffic from a macrocell. Based on this network configuration, the system power consumption and customer QoS were studied, as a function of the data traffic proportion and the smartphone usage. The embodied energy is considered in the power consumption analysis, since femtocell deployment and the growth of smart-

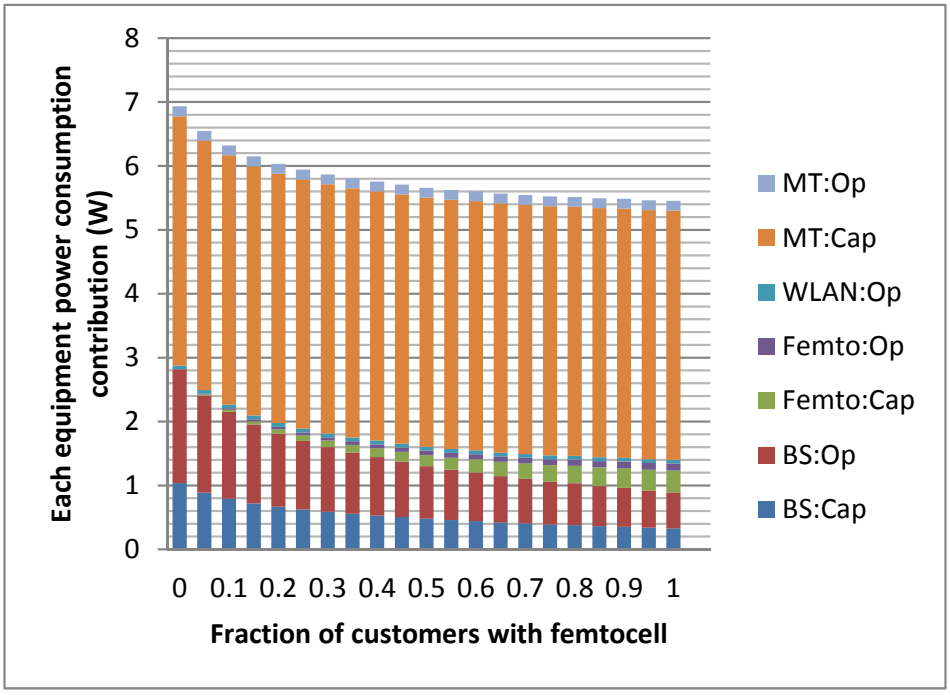

Figure 5.17: Power consumption of each network component, with the different fraction of users operate femtocells, when the proportion of data traffic and smartphone usage are all 50%.

phone usage may result in a significant hardware investment, which cannot be ignored. Some statistics from Ofcom that indicate the status of the communication system in Q1 2010, suggests that WLANs are commonly used in the UK, and the growth of the smartphone usage is rapidly increasing.

The simulation results are presented, for various levels of data volume and smartphone usage. The following conclusions can be drawn:

It can be derived that the adoption of femtocells can reduce power significantly, although they contribute extra embodied energy. For low data service requirement and low smartphone usage, WLANs are not able to bring in more benefits either for power consumption or for QoS, since few users can be offloaded to a WLAN access point. However, along with the increasing use of data traffic and the trend of smartphone popularity, WLANs become more important in this cooperative network. In addition, as WLANs are already ubiquitously installed, e.g. they are installed in 70% of the residences in the UK, there is no further embodied energy input required, resulting in

a significant power saving compared to femtocell deployment. The cooperative network is able to provide a broader available bandwidth to users, since more users can be offloaded to a less busy resource of the local network.

The results show that when femtocells are introduced into the current system, the power consumption can be decreased by up to 40%, mainly arising from the operational power saving of up to 60%. At the same time, the average available bandwidth per user that can be achieved is 20 times better compared to a conventional macrocell system. When the data service volumes increase, the WLAN offloading scheme can lead to an extra 7% to 9% ERG gain with different femtocell deployment rates, and the user experience is also able to be improved. Also, due to the premise that the smartphone usage will increase in the future, and the significant energy consumption of producing a smartphone compared to a simple phone, the system power consumption will increase over the long-term. However, as WLANs are able to be utilised more frequently, they become more important for traffic offloading.

Overall, the cooperative network shows a significant improvement in both power efficiency and QoS. With the current market development trend and the pattern of the traffic composition, WLANs will play a more important role in the future, to minimise power and improve QoS.

6

Conclusion

6.1 Summary of findings

In this thesis a novel comprehensive energy consumption analysis is presented, based on different types of heterogeneous networks. The energy reduction is considered in terms of operational energy and embodied energy from the operator and mobile users. To evaluate the system QoS, the available bandwidth, system capacity and throughput per user are used to evaluate system performance. The trade-off between energy efficiency and QoS is investigated in this thesis.

A combined cellular and femtocell heterogeneous network is studied. The effects of some practical factors are evaluated in a large scale analysis, such as user capacity of a femtocell and a macrocell and femtocell deployment rate. The results show that combining cellular communications with femtocells can significantly reduce the overall energy consumption, depending on the uptake of femtocells. When a macrocell is able to support more users, the system energy consumption is relatively low, since fewer macrocell base stations are required for a certain number of mobile users and traffic demand. In this scenario the femtocell deployment does not result in significant energy saving, since the macrocell system itself consumes relatively little power. However, the femtocell deployment significantly increases the bandwidth for users. On the other hand, when a macrocell supports fewer users, femtocell adoption can reduce the system energy more substantially, while the bandwidth can be improved, but not as much as in the previous scenario. If a femtocell can support more users, the system energy is reduced compared to a femtocell supporting fewer users. However, to achieve a better QoS, the fewer users a femtocell can support the better.

Increasing the number of femtocells deployed may result in an increase

in the energy consumption due to more embodied energy. This can be observed from a normalised small scale analysis. It happens when the mobile users and femtocells distribution are independent, and most of the deployed femtocells are switched to a sleep mode, due to no active users located in its coverage. They cause a significant increase in embodied energy. It shows that if a proper femtocell switch-off threshold or mechanism is adopted, the system power consumption can be reduced significantly. However, in this case more users are likely to achieve a better local network service from a femtocell. The conflict between energy efficiency and QoS must be balanced for different system configurations, requirements and preferences.

Following the exploration of femtocell deployment, the thesis explores a cooperative architecture combining femtocells and WLANs. In this architecture, the data traffic and smartphone usage are considered to evaluate the trade-off of energy efficiency and QoS. Since the QoS of real time communications, such as voice calls and video conferences, can not be guaranteed in 802.11 and TCP/IP protocols, in this thesis WLANs are only able to offload the data traffic from a cellular network. Therefore, in this scheme a femtocell is used for offloading voice traffic, and a WLAN only offloads data traffic, when they are both available for a mobile user. The results show that when there is a high demand for data service, the WLAN utilization can achieve significantly higher energy saving compared to a femtocell heterogeneous network, and also more users are able to experience a higher QoS. This is because the WLANs are commonly used, thus there is no embodied energy introduced into the system. Due to the premise that the usage of smartphones will increase significantly in the future, the energy efficiency benefits of WLAN deployment will become more significant, since more mobile users can offload their data traffic to a WLAN access point. A localised heterogenous network is a promising technique for achieving power efficiency and a high QoS system.

In a macrocell base station's lifetime, approximately 20% of total energy consumption is embodied energy. For a mobile phone, the figure is 80%. Hence, the embodied energy contributes a significant part in the whole system energy consumption. Data for embodied energy of each system element are derived from the major operators and device producers. For the embodied energy of a smartphone, as it is not available in the public domain, three approaches are proposed to estimate a reasonable value for the evalua-

tion. They are a price approach, a proportion approach and a CO_2 emission approach.

Finally, two femtocell transmission power setting schemes are proposed, a power-controlled and a fixed-power scheme. The results show that considering both energy efficiency and QoS, a femtocell should use a power-controlled mode, when the femtocells are densely deployed. This can avoid the significant interference between the femtocells and the macrocell or within the femtocells. On the other hand, when the femtocells are sparsely deployed, they should switch to a higher fixed transmission power, to provide a better QoS to the local users.

6.2 Limitations

The limitations of this thesis is listed as follows:

1. In this thesis, all the simulation assumptions are derived from current telecommunication systems. Along with the development of technology, some of these simulation parameters may not be valid in the future. For example in Chapter 5, due to the current 70% of WLAN access point usage, the embodied energy from WLAN is neglected. It has not taken into account further upgrade and replacement of the access point. The analysis from this thesis can be considered as a starting point for other researchers in the future.

2. It has been mentioned that the femtocell has two access methods, one is closed access, the other is open access. In order to investigate the potential of energy saving with femtocell deployment, in this thesis it is assumed that all femtocells are available for all users, which is open access. In this case, many issues need to be addressed in the future, such as billing, authentication and authorisation. These issues are not studied in this thesis, whereas, they are very important in a practical application.

3. In this thesis, cell boundary effects have not been considered, not only within macrocells, but also between femtocells and the macrocell. In this scenario, the related issues, such as handover between different cells, connection establishment and cooperative algorithms, should be investigated. These issues can be considered in future work.

4. In Chapter 4, a WCDMA standard based femtocell technique is studied. Since at the time of commencing this research femtocells were mainly deployed using this technology. However, during the time that the research carried out, LTE standards with OFDM techniques were drawing more attention. Although in this thesis the analysis was not applied to an LTE system, the proposed stochastic geometry model can be utilised for analysing LTE femtocell deployment.

5. In the majority of the simulations in this thesis, the sensitivity of assumptions is not evaluated. It should be considered in further work. However, there is an example of the effects of different values of assumptions on simulation results in Chapter 5, Figure 5.5. It shows that, with the different values for the assumptions, the shapes and trends of the results do not change significantly.

6.3 Future Work

Although the this thesis target has been achieved, more work can be done in the future. This can be described as follows.

6.3.1 Frequency planning for the macrocell and the femtocell

In the thesis, it shows that when the femtocells are allocated in the same frequency as the macrocell, both femtocell users and macrocell users performance are affected significantly, due to the interference between each other. This is a case where users who are authorised to access the femtocell whenever this user is located in a femtocell's coverage. One the other hand, if the femtocell owner is not willing to share the femtocell resource with the public, then there can be an isolated poor coverage area around the femtocell for the passing-by users. Therefore, in this case, the service for the macrocell users are even worse than the scenario which is evaluated in this thesis. Therefore, the frequency planning is crucial for the femtocell deployment in an underlay macrocell network.

There are three possible solutions to this problem. First, since currently more operators are deploying more than one carrier due to the significant increase of traffic volume, they are able to switch the femtocells to a different carrier from the local macrocell. Second, some operators may also have sectorised basestations, where the same frequency is reused three or six

times, one for each segment. The femtocells are able to be allocated in the frequency sectors that not the local macrocell is using. Finally, cognitive radio technology can be used for frequency planning by monitoring the radio environment, such as radio frequency spectrum, user behaviour and network state. In this case the femtocells can be dynamically allocated in the different spectrum to avoid the interference to the macrocell.

6.3.2 Interference cancellation between femtocells

By using the above described techniques, the femtocell and macrocell can be considered that they are allocated in separate channels. However, the interference still exist between femtocells. This issue is more notable in apartment residence areas, where the femtocells are likely densely deployed, and the signal attenuation between apartments are small. Hence, interference cancellation techniques should be considered to improve the femtocell performance.

One possible solution for this problem is using Orthogonal Frequency-Division Multiple Access (OFDMA) to allocate orthogonal subbands to neighbouring femtocells, also considering femtocell power setting in different bandwidth to mitigate the interference between femtocells. Another solution is Inter-cell Interference Coordination (ICIC). This technique is originally designed for macrocell networks, when they are using one frequency. The ICIC technique can be used for avoidance of interference between femtocells, which can be highly efficiency in terms of spectrum, but requires close coordination between femtocells.

6.3.3 Femtocell sleep mode mechanism

In the thesis, it is assumed that in the following two scenarios, a femtocell will be switched to a sleep mode: First, when there is no active user located in this femtocell's coverage; Second, in this femtocell's coverage, all active user are served by other neighbouring femtocells, and this femtocell becomes redundant. For these two scenarios, more technique details need to be considered in the future.

First, in order to determine whether there is any active user located in a femtocell's coverage, the femtocell may be required to broadcast signal from time to time to detect the user's existence. Considering the power efficiency during user detection, specific protocols are needed to be proposed to ad-

dress this issue. Second, the coordination between femtocells are essential to decide which femtocell should be treated as a redundant access point in the second scenario. One possible solution is to place a centralised control node for femtocells in a certain region, to make the sleep mode decision with consideration of the optimal performance of this region. Finally, the power model for the femtocell sleep mode need to be clarified in the future. For example, how much power consumed by a femtocell when it's in a sleep mode, and how much power consumed when it's switched from sleep mode to active.

6.3.4 Handover for combined WLAN and femtocell network

The handover mechanism is not considered in this thesis, which is can be considered as a possible topic for future work.

In a combined WLAN and femtocell network, four possible types of handover may take place in the following scenarios: between WLAN and macrocell, between femtocell and macrocell, between WLAN and femtocell, and between homogeneous access points (i.e. between WLAN nodes, or femtocell nodes). The handover decision can be reactive or proactive. One possible reactive strategy is based on Location Based Service (LBS). When a mobile user enter to a different network, the LBS reports the available network based on the location of user, then the handover takes place. The proactive strategy can be based on mobility prediction, which may be derived by user's movement speed, direction or other factors. For each handover process, it may have the following phases: preparation, signal measurement, authentication, processing and execution. In each phase, transmission protocols need to be designed, and considered carefully based on different types of networks.

Bibliography

[1] Secretary of State for Environment. Climate Resilient Infrastructure: Preparing for a Changing Climate. Technical report, Presented to Parliament, May 2011.

[2] Jack Rowley and Dawn Haig-Thomas. Unwiring the Planet-Wireless Communications and Climate Change. available at http://www.itu.int/dms_pub/itu-t/oth/06/0F/T060F0000090013PDFE.pdf, 2011. [Online; accessed 6-September-2011].

[3] Sunil Vadgama. Trends in Green Wireless Access. *Fujitsu*, 45(4):404–408, 2009.

[4] Y. G. Yohanis and B. Norton. Life-cycle operational and embodied energy for a generic single-storey office building in the UK. *Energy*, 27(1):77 – 92, 2002.

[5] D. Cavalcanti, D. Agrawal, C. Cordeiro, Bin Xie, and A. Kumar. Issues in Integrating Cellular Networks WLANs, AND MANETs: A Futuristic Heterogeneous Wireless Network. *Wireless Communications, IEEE*, 12(3):30–41, June 2005.

[6] A. Khandekar, N. Bhushan, Ji Tingfang, and V. Vanghi. Lte-advanced: Heterogeneous networks. In *Wireless Conference (EW), 2010 European*, pages 978 –982, april 2010.

[7] Weisi Guo and T. O'Farrell. Green cellular network: Deployment solutions, sensitivity and tradeoffs. In *Wireless Advanced (WiAd), 2011*, pages 42 –47, june 2011.

[8] David Lister. An Operators View on Green Radio. available at http://www.green-communications.net/icc09/docs/GreenComm-ICC09-Keynote3-Lister.pdf, 2011. [Online; accessed 10-October-2011].

[9] Cisco Virtual Networking Index: Forecast and Methodology, 2011-2016. Technical report, May 2012.

[10] Gordon Peters. Mobile data demand increases, mobile voice declines. available at http://www.itwire.com/it-industry-news/market/42125-mobile-data-demand-increases-mobile-voice-declines, 2010. [Online; accessed 10-October-2011].

[11] S. Videv and H. Haas. Energy-Efficient Scheduling and Bandwidth-Energy Efficiency Trade-Off with Low Load. In *Communications (ICC), 2011 IEEE International Conference on*, pages 1 –5, june 2011.

[12] Jianhua He, P. Loskot, T. O'Farrell, V. Friderikos, S. Armour, and J. Thompson. Energy efficient architectures and techniques for Green Radio access networks. In *Communications and Networking in China (CHINACOM), 2010 5th International ICST Conference on*, pages 1 –6, aug. 2010.

[13] Wei Wang and Gang Shen. Energy Efficiency of Heterogeneous Cellular Network. In *Vehicular Technology Conference Fall (VTC 2010-Fall), 2010 IEEE 72nd*, pages 1 –5, sept. 2010.

[14] U. Varshney and R. Jain. Issues in emerging 4G wireless networks. *Computer*, 34(6):94 –96, jun 2001.

[15] Youngju Kim, Sungeun Lee, and Daesik Hong. Performance analysis of two-tier femtocell networks with outage constraints. *Wireless Communications, IEEE Transactions on*, 9(9):2695 –2700, september 2010.

[16] R.Y. Kim, Jin Sam Kwak, and K. Etemad. WiMAX femtocell: requirements, challenges, and solutions. *Communications Magazine, IEEE*, 47(9):84 –91, september 2009.

[17] N. Nasser, A. Hasswa, and H. Hassanein. Handoffs in fourth generation heterogeneous networks. *Communications Magazine, IEEE*, 44(10):96 –103, oct. 2006.

[18] Gang Wu, M. Mizuno, and P.J.M. Havinga. MIRAI architecture for heterogeneous network. *Communications Magazine, IEEE*, 40(2):126 –134, feb 2002.

[19] Y Lu B Bhargava, X Wu and W Wang. Integrating Heterogeneous Wireless Technologies: A Cellular Aided Mobile Ad hoc Network (CAMA). *Mobile Networking and Applicaitons*, 9(4):393–408, 08 2004. ACM Special Issues of the Journal on Special Topics.

[20] Rui Zhang and M.A. Labrador. Energy-aware topology control in heterogeneous wireless multi-hop networks. In *Wireless Pervasive Computing, 2007. ISWPC '07. 2nd International Symposium on*, feb. 2007.

[21] H. Claussen and D. Calin. Macrocell offloading benefits in joint macro- and femtocell deployments. In *Personal, Indoor and Mobile Radio Communications, 2009 IEEE 20th International Symposium on*, pages 350 –354, sept. 2009.

[22] Alfonso Fernandez-Durán and Gloria García Carrasco. Umts femtocell performance in massive deployments: Capacity and gos implications. *Bell Labs Technical Journal*, 14(2):185–202, 2009.

[23] J. Weitzen and T. Grosch. Comparing coverage quality for femtocell and macrocell broadband data services. *Communications Magazine, IEEE*, 48(1):40 –44, january 2010.

[24] P. Pirinen. Co-channel co-existence study of outdoor macrocell and indoor femtocell users. In *Wireless Conference (EW), 2010 European*, pages 207 –213, april 2010.

[25] Xiangfang Li, Lijun Qian, and D. Kataria. Downlink power control in co-channel macrocell femtocell overlay. In *Information Sciences and Systems, 2009. CISS 2009. 43rd Annual Conference on*, pages 383 –388, march 2009.

[26] A. Rabbachin, T.Q.S. Quek, Hyundong Shin, and M.Z. Win. Cognitive network interference. *Selected Areas in Communications, IEEE Journal on*, 29(2):480 –493, february 2011.

[27] Fair and qos-oriented spectrum splitting in macrocell-femtocell networks. In *GLOBECOM 2010, 2010 IEEE Global Telecommunications Conference*, pages 1 –6, dec. 2010.

[28] Yong Bai, Juejia Zhou, and Lan Chen. Hybrid spectrum usage for overlaying lte macrocell and femtocell. In *Global Telecommunications Conference, 2009. GLOBECOM 2009. IEEE*, pages 1 –6, 30 2009-dec. 4 2009.

[29] E. Chlebus and G. Divgi. The pareto or truncated pareto distribution? measurement-based modeling of session traffic for wi-fi wireless internet access. In *Wireless Communications and Networking Conference, 2007.WCNC 2007. IEEE*, pages 3625 –3630, march 2007.

[30] G. Divgi and E. Chlebus. User and traffic characteristics of a commercial nationwide wi-fi hotspot network. In *Personal, Indoor and Mobile Radio Communications, 2007. PIMRC 2007. IEEE 18th International Symposium on*, pages 1 –5, sept. 2007.

[31] Jaehoon Roh, Yungha Ji, Yong Gyoo Lee, and Taehyo Ahn. Femtocell traffic offload scheme for core networks. In *New Technologies, Mobility and Security (NTMS), 2011 4th IFIP International Conference on*, pages 1 –5, feb. 2011.

[32] H. Claussen, L.T.W. Ho, and F. Pivit. Effects of Joint Macrocell and Residential Picocell Deployment on The Network Energy Efficiency. In *Personal, Indoor and Mobile Radio Communications, 2008. PIMRC 2008. IEEE 19th International Symposium on*, pages 1–6, Sept. 2008.

[33] Bo Han, Pan Hui, and Aravind Srinivasan. Mobile data offloading in metropolitan area networks. *SIGMOBILE Mob. Comput. Commun. Rev.*, 14:28–30, November 2010.

[34] Aruna Balasubramanian, Ratul Mahajan, and Arun Venkataramani. Argumenting Mobile 3G Uing WiFi. In *MobiSys '10: Proceedings of*

the 8th international conference on Mobile systems, applications, and services, pages 209–222, New York, NY, USA, June. ACM.

[35] P. Fuxjager, H.R. Fischer, I. Gojmerac, and P. Reichl. Radio resource allocation in urban femto-wifi convergence scenarios. In *Next Generation Internet (NGI), 2010 6th EURO-NF Conference on*, pages 1 –8, june 2010.

[36] B. Han, P. Hui, V. Kumar, M. Marathe, J. Shao, and A. Srinivasan. Mobile data offloading through opportunistic communications and social participation. *Mobile Computing, IEEE Transactions on*, PP(99):1, 2011.

[37] Qian Zhang, Chuanxiong Guo, Zihua Guo, and Wenwu Zhu. Efficient mobility management for vertical handoff between WWAN and WLAN. *Communications Magazine, IEEE*, 41(11):102 – 108, nov. 2003.

[38] Specification of the Bluetooth System, Volume 1: Core, v1.1. Bluetooth SIG, February 2001.

[39] S. Grech and P. Eronen. Implications of Unlicensed Mobile Access (UMA) for GSM security. In *Security and Privacy for Emerging Areas in Communications Networks, 2005. SecureComm 2005. First International Conference on*, pages 3 – 12, sept. 2005.

[40] Steven H. Blumenthal. UNLICENSED MOBILE ACCESS, June 2008.

[41] L.T.W. Ho and H. Claussen. Effects of User-Deployed, Co-Channel Femtocells on the Call Drop Probability in a Residential Scenario. In *Personal, Indoor and Mobile Radio Communications, 2007. PIMRC 2007. IEEE 18th International Symposium on*, pages 1–5, Sept. 2007.

[42] V. Chandrasekhar, J. Andrews, and A. Gatherer. Femtocell Networks: A Survey. *Communications Magazine, IEEE*, 46(9):59–67, September 2008.

[43] Yumin Wu, Kun Yang, and Jie Zhang. An Adaptive Routing Protocol for An Integrated Cellular and Ad-Hoc Network with Flexible Access. In *IWCMC '06: Proceedings of the 2006 international conference on*

Wireless communications and mobile computing, pages 263–268, New York, NY, USA, 2006. ACM.

[44] G. Srivastava, P. Boustead, and J.F. Chicharo. Topology control in heterogeneous ad-hoc networks. In *Networks, 2004. (ICON 2004). Proceedings. 12th IEEE International Conference on*, volume 2, pages 665 – 670 vol.2, nov. 2004.

[45] Hung yu Wei and R.D. Gitlin. Two-Hop-Relay Architecture for Next-Generation WWAN/WLAN Integration. *Wireless Communications, IEEE*, 11(2):24–30, Apr 2004.

[46] Taehwan Choi, Sunghoon Seo, and Jooseok Song. ABC^2: A New Approach to Seamless Mobility Using Cellular Networks and WLANs. In *Wireless Communications and Networking Conference, 2008. WCNC 2008. IEEE*, pages 2675–2680, 31 2008-April 3 2008.

[47] S.F. Hasan, N.H. Siddique, and S. Chakraborty. Femtocell versus WiFi - A survey and comparison of architecture and performance. In *Wireless Communication, Vehicular Technology, Information Theory and Aerospace Electronic Systems Technology, 2009. Wireless VITAE 2009. 1st International Conference on*, pages 916 –920, may 2009.

[48] Holger Claussen, Lester T. W. Ho, and Louis G. Samuel. An Overview of The Femtocell Concept. *Bell Labs Technical Journal*, 13(1):221–245, 2008.

[49] Charles E. Perkins and Pravin Bhagwat. Highly dynamic Destination-Sequenced Distance-Vector routing (DSDV) for mobile computers. In *Proceedings of the conference on Communications architectures, protocols and applications*, volume 24 of *SIGCOMM '94*, pages 234–244, New York, NY, USA, October 1994. ACM.

[50] Shree Murthy and J.J. Garcia-Luna-Aceves. An Efficient Routing Protocol for Wireless Networks, 1996.

[51] C.E. Perkins and E.M. Royer. Ad-hoc on-demand distance vector routing. In *Mobile Computing Systems and Applications, 1999. Proceedings. WMCSA '99. Second IEEE Workshop on*, pages 90 –100, feb 1999.

[52] David B. Johnson and David A. Maltz. Dynamic source routing in ad hoc wireless networks. In *Mobile Computing*, pages 153–181. Kluwer Academic Publishers, 1996.

[53] N. Li and J.C. Hou. Topology control in heterogeneous wireless networks: problems and solutions. In *INFOCOM 2004. Twenty-third AnnualJoint Conference of the IEEE Computer and Communications Societies*, volume 1, pages 4 vol. (xxxv+2866), march 2004.

[54] P. Johansson, N. Johansson, U. Korner, J. Elg, and G. Svennarp. Short range radio based ad-hoc networking: performance and properties. In *Communications, 1999. ICC '99. 1999 IEEE International Conference on*, volume 3, pages 1414 –1420 vol.3, 1999.

[55] D. Westhoff. The Role of Mobile Device Authentication with respect to Domain overlapping Business Models. In *The 6th World Multiconference on Systemics, Cybernatics and Informatics (SCI 2002), Orlando, Florida*, 2002.

[56] Ruay-Shiung Chang, Wei-Yeh Chen, and Yean-Fu Wen. Hybrid Wireless Network Protocols. *Vehicular Technology, IEEE Transactions on*, 52(4):1099–1109, July 2003.

[57] Hongyi Wu, Chunming Qiao, S. De, and O. Tonguz. Integrated Cellular and Ad Hoc Relaying Systems: iCAR. *Selected Areas in Communications, IEEE Journal on*, 19(10):2105–2115, Oct 2001.

[58] Dave Cavalcanti Bin Xie, Anup Kumar and Dharma P. Agrawal. Multi-Hop Cellular IP: A New Approach to Heterogeneous Wireless Networks. *International Journal of Pervasive Computing and Communications*, 2:370 – 383 370 – 383 370–383, 2006.

[59] I. Glover and P.M. Grant. *Digital Communications*. Prentice Hall, 2009.

[60] A.R. Mishra. *Cellular Technologies for Emerging Markets: 2G, 3G and Beyond*. John Wiley & Sons, 2010.

[61] 3GPP. TS 23.261, IP flow mobility and seamless Wireless Local Area Network (WLAN) offload, Release 10. Technical report, March 2012.

[62] 3GPP. TS 23.402, Architecture enhancements for non-3GPP accesses, Release 11. Technical report, June 2012.

[63] V. Chandrasekhar and J. Andrews. Uplink capacity and interference avoidance for two-tier femtocell networks. *Wireless Communications, IEEE Transactions on*, 8(7):3498 –3509, july 2009.

[64] 3GPP. TS 22.220, Service requirements for Home Node B (HNB) and Home eNode B (HeNB), Release 11. Technical report, June 2012.

[65] 3GPP. TS 23.829, Local IP Access and Selected IP Traffic Offload (LIPA-SIPTO), Release 10. Technical report, October 2011.

[66] G. Hammond and C Jones. Inventory of Carbon and Energy (ICE) version 1.6a. Technical report, University of Bath: Department of Mechanical Engineering, 2008.

[67] J.T. Louhi. Energy efficiency of modern cellular base stations. In *Telecommunications Energy Conference, 2007. INTELEC 2007. 29th International*, pages 475 –476, 30 2007-oct. 4 2007.

[68] T Edler and Susanne Lundberg. Energy efficiency enhancements in radio access networks. *Ericsson Review*, (1):42–51, 2004.

[69] D.F. Kimball, Jinho Jeong, Chin Hsia, P. Draxler, S. Lanfranco, W. Nagy, K. Linthicum, L.E. Larson, and P.M. Asbeck. High-Efficiency Envelope-Tracking W-CDMA Base-Station Amplifier Using GaN HFETs. *Microwave Theory and Techniques, IEEE Transactions on*, 54(11):3848 –3856, nov. 2006.

[70] J.S. Blogh and L. Hanzo. *Third-Generation Systems and Intellignet Wireless Networking - Smart Antennas and Adaptive Modulation.* John Wiley & Sons, April 2002.

[71] S.C. Swales, M.A. Beach, D.J. Edwards, and J.P. McGeehan. The performance enhancement of multibeam adaptive base-station antennas for cellular land mobile radio systems. *Vehicular Technology, IEEE Transactions on*, 39(1):56 –67, feb 1990.

[72] O. Arnold, F. Richter, G. Fettweis, and O. Blume. Power consumption modeling of different base station types in heterogeneous cellular

networks. In *Future Network and Mobile Summit, 2010*, pages 1 –8, june 2010.

[73] M.F. Hossain, K.S. Munasinghe, and A. Jamalipour. A protocooperation-based sleep-wake architecture for next generation green cellular access networks. In *Signal Processing and Communication Systems (ICSPCS), 2010 4th International Conference on*, pages 1 –8, dec. 2010.

[74] Rui Wang, J.S. Thompson, and H. Haas. A novel time-domain sleep mode design for energy-efficient LTE. In *Communications, Control and Signal Processing (ISCCSP), 2010 4th International Symposium on*, pages 1 –4, march 2010.

[75] F. Richter, A.J. Fehske, and G.P. Fettweis. Energy Efficiency Aspects of Base Station Deployment Strategies for Cellular Networks. In *Vehicular Technology Conference Fall (VTC 2009-Fall), 2009 IEEE 70th*, pages 1 –5, sept. 2009.

[76] Fred Richter, Albrecht J. Fehske, Patrick Marsch, and Gerhard P. Fettweis. Traffic Demand and Energy Efficiency in Heterogeneous Cellular Mobile Radio Networks. In *Vehicular Technology Conference (VTC 2010-Spring), 2010 IEEE 71st*, pages 1 –6, may 2010.

[77] F. Richter and G. Fettweis. Cellular Mobile Network Densification Utilizing Micro Base Stations. In *Communications (ICC), 2010 IEEE International Conference on*, pages 1 –6, may 2010.

[78] Francis Mullany. OPERA-Net: Optimising Power Efficiency in Mobile Radio Networks. available at http://www.celtic-initiative.org/Events/Old-events/Event2011/Presentations/Workshops/Get-connected/04-OperaNet2%20bis.pdf, 30 April 2009. Bell Labs Ireland, Alcatel-Lucent, Mobile VCE Green Radio, Education Day.

[79] T. Sowlati and D.M.W. Leenaerts. A 2.4-GHz 0.18- μm CMOS self-biased cascode power amplifier. *Solid-State Circuits, IEEE Journal of*, 38(8):1318 – 1324, aug. 2003.

[80] P Singhal. Stage I Final Report: Life Cycle Environmental Issues of Mobile Phones. Technical report, Integrated Product Policy Pilot Project, Nokia Corp., 2005.

[81] The Carphone Warehouse Group. Sim Free Phones. available at http://www.carphonewarehouse.com/mobiles/handset-only, 2011. [Online; accessed 9-March-2011].

[82] Hossein Falaki, Ratul Mahajan, Srikanth Kandula, Dimitrios Lymberopoulos, Ramesh Govindan, and Deborah Estrin. Diversity in smartphone usage. In *MobiSys '10: Proceedings of the 8th international conference on Mobile systems, applications, and services*, pages 179–194, New York, NY, USA, June 2010. ACM.

[83] Nokia Corporation. Nokia sustainability report. available at http://nds1.nokia.com/NOKIA_COM_1/Corporate_Responsibility/Sustainability_report_2009/pdf/sustainability_report_2009.pdf, 2009. [Online; accessed 9-March-2011].

[84] Sony Ericsson Mobile Communications AB. Mats Pellbäck Scharp. Using the power of our products to create a movement and build consumer trust. available at http://www.kemi.se/upload/Presentationer/Mats%20Pellback-Scharp.pdf, 2010. [Online; accessed 9-March-2011].

[85] Apple Inc. iPhone 3G Environmental Report. available at http://images.apple.com/environment/reports/docs/iPhone-3G-Environmental-Report.pdf, June 8, 2009. [Online; accessed 9-March-2011].

[86] Apple Inc. iPhone 4 Environmental Report. available at http://images.apple.com/environment/reports/docs/iPhone_4_Product_Environmental_Report.pdf, June 24, 2010. [Online; accessed 9-March-2011].

[87] J. Rabaey, J. Ammer, Jr. da Silva, J.L., and D. Patel. PicoRadio: Ad-hoc Wireless Networking of Ubiquitous Low-Energy Sensor/Monitor Nodes. In *VLSI, 2000. Proceedings. IEEE Computer Society Workshop on*, pages 9–12, 2000.

[88] Theodore S. Rappaport and Theodore Rappaport. *Wireless Communications: Principles and Practice (2nd Edition)*. Prentice Hall PTR, December 2001.

[89] Nokia Corporation. Nokia's Charger Energy Rating. available at http://www.nokia.com/environment/we-energise/how-you-can-save-energy/charger-energy-rating, 2011. [Online; accessed 9-March-2011].

[90] Cornelia Kappler. *UMTS Networks and Beyond*. John Wiley & Sons, Ltd, February 2009.

[91] Simon Davies. O2 Loses UK Appeal Over GSM Spectrum Reuse for 3G Services. available at http://www.cellular-news.com/story/45857.php, 2011. [Online; accessed 6-September-2011].

[92] H. Holma and A. Toskala. *HSDPA/HSUPA for UMTS: high speed radio access for mobile communications*. John Wiley, 2006.

[93] S.I. Maniatis, E.G. Nikolouzou, and I.S. Venieris. QoS Issues in The Converged 3G Wireless and Wired Networks. *Communications Magazine, IEEE*, 40(8):44–53, Aug 2002.

[94] T. Robles, A. Kadelka, H. Velayos, A. Lappetelainen, A. Kassler, Hui Li, D. Mandato, J. Ojala, and B. Wegmann. QoS support for an all IP system beyond 3G. *Communications Magazine, IEEE*, 39(8):64 –72, aug 2001.

[95] 3rd Generation Partnership Project. 3GPP TS 23.107, Technical Specification Group Services and System Aspects; Quality of Service (QoS) concept and architecture (Release 7). Technical Report V7.1.0, 3GPP.

[96] The Communications Market 2009, Annual Communications Market Report. Technical report, United Kingdom, Office of Communications (Ofcom) <http://www.ofcom.org.uk/research/cm/cmr09/>, Aug.2009,.

[97] S. Sarkar, B.K. Butler, and Jr. Tiedemann, E.G. Phone Standby Time in CDMA2000: The Quick Paging Channel in Soft Handoff. *Vehicular Technology, IEEE Transactions on*, 50(5):1240–1249, Sep 2001.

[98] Imran Ashraf, Lester T. W. Ho, and Holger Claussen. Improving Energy Efficiency of Femtocell Base Stations Via User Activity Detection. In *2010 IEEE Wireless Communications and Networking Conference (WCNC 2010)*, pages 1–5, April 2010.

[99] Ying Hou and David I. Laurenson. Energy Efficiency of High QoS Heterogeneous Wireless Communication Network. *Vehicular Technology Conference Fall (VTC 2010-Fall), 2010 IEEE 72nd*, pages 1 –5, sep. 2010.

[100] Zhenning Shi, He Wang, Ming Zhao, and Mark C. Reed. An uplink analytical model for two-tiered 3g femtocell networks. In *Modeling and Optimization in Mobile, Ad Hoc and Wireless Networks (WiOpt), 2010 Proceedings of the 8th International Symposium on*, pages 367 –372, 31 2010-june 4 2010.

[101] He Wang, Ming Zhao, and M.C. Reed. Optimal adaptive uplink attenuation algorithms for wcdma femtocell. In *Global Telecommunications Conference (GLOBECOM 2011), 2011 IEEE*, pages 1 –5, dec. 2011.

[102] D. Knisely, T. Yoshizawa, and F. Favichia. Standardization of femtocells in 3gpp. *Communications Magazine, IEEE*, 47(9):68 –75, september 2009.

[103] V. Chandrasekhar, J.G. Andrews, T. Muharemovic, Zukang Shen, and A. Gatherer. Power control in two-tier femtocell networks. *Wireless Communications, IEEE Transactions on*, 8(8):4316 –4328, august 2009.

[104] M.H. Ismail and M.M. Matalgah. Complete analytical framework for throughput calculation in wcdma downlink tdd mode. In *Wireless Communications and Networking Conference, 2005 IEEE*, volume 1, pages 212 – 217 Vol. 1, march 2005.

[105] Z. Dawy, S. Davidovic, and I. Oikonomidis. Coverage and capacity enhancement of cdma cellular systems via multihop transmission. In *Global Telecommunications Conference, 2003. GLOBECOM '03. IEEE*, volume 2, pages 1147 – 1151 Vol.2, dec. 2003.

[106] Andrea Goldsmith. *Wireless Communications*. Cambridge University Press, New York, NY, USA, 2005.

[107] V. Erceg, Zyray Wireless Inc, M. S. Smith, P. Soma, Iospan Wireless, S. Ghassemzadeh, T Labs, A. J. Rustako, R. S. Roman, K. P. Sheikh Sprint, J. M. Costa, C. Bushue Sprint, A. Sarajedini, R. Schwartz,

D. Branlund, T. Kaitz, and D. Trinkwon. IEEE 802.16.3c-01/29r4: Channel Models for Fixed Wireless Applications.

[108] J. Hakegard, B. Myhre, P. Lehne, T. Ormhaug, V. Bjugan, M. Mondin, M. Elkotob, and F. Steuer. Scenarios and Wireless Performance and Coverage., 2005.

[109] Antonio Forenza, David J. Love, and Robert W. Heath Jr. Wireless LANs 802.11 TGn "Channel Model Special Committee Simulation of the Spatial Covariance Matrix". October 30, 2003.

[110] International Telecommunication Union/ITU Radiocommunication Sector. Guidelines for Evaluation of Radio Transmission Technologies for IMT-2000, 1997.

[111] N. Nakagami. The *m*-distribution, a general formula for intensity distribution of rapid fading. In W. G. Hoffman, editor, *Statistical Methods in Radio Wave Propagation*. Oxford, England: Pergamon, 1960.

[112] H. Hashemi, M. McGuire, T. Vlasschaert, and D. Tholl. Measurements and modeling of temporal variations of the indoor radio propagation channel. *Vehicular Technology, IEEE Transactions on*, 43(3):733 –737, aug. 1994.

[113] K.S. Gilhousen, I.M. Jacobs, R. Padovani, A.J. Viterbi, Jr. Weaver, L.A., and III Wheatley, C.E. On the capacity of a cellular cdma system. *Vehicular Technology, IEEE Transactions on*, 40(2):303 –312, may 1991.

[114] Yongmin Choi, Hyun Wook Ji, Jae yoon Park, Hyun chul Kim, and J.A. Silvester. A 3w network strategy for mobile data traffic offloading. *Communications Magazine, IEEE*, 49(10):118 –123, oct. 2011.

[115] C.B. Sankaran. Data offloading techniques in 3gpp rel-10 networks: A tutorial. *Communications Magazine, IEEE*, 50(6):46 –53, june 2012.

[116] K. Samdanis, T. Taleb, and S. Schmid. Traffic offload enhancements for eutran. *Communications Surveys Tutorials, IEEE*, 14(3):884 –896, quarter 2012.

[117] 3GPP. TS 23.401, General Packet Radio Service (GPRS) enhancements for Evolved Universal Terrestrial Radio Access Network (E-UTRAN) access, Release 11. Technical report, June 2012.

[118] Ofcom. The Communications Market 2010, Annual Communications Market Report. Technical report, United Kingdom, Office of Communications (Ofcom) <http://www.ofcom.org.uk/research/cm/cmr09/>, Aug.2009.

[119] Erik Dahlman, Stefan Parkvall, Johan Skold, and Per Beming. *3G Evolution, Second Edition: HSPA and LTE for Mobile Broadband.* Academic Press, 2008.